

The Development of a Porcine Model to Evaluate Wound
Healing and Infection of Transcutaneous Osseointegrated
Weight-Bearing Prostheses

BY

Kevin James Colbert

©2013

Submitted to the graduate degree program in Bioengineering and the graduate faculty of the University of Kansas in partial fulfillment of the requirements for the degree of Master of Science.

Committee:

Dr. Terence E. McIff (Chairperson): _____

Dr. Kenneth J. Fischer: _____

Dr. Lorin P. Maletsky: _____

Date Defended: May 15, 2013

The Thesis Committee for Kevin J. Colbert certifies that this is the approved version of the following thesis:

The Development of a Porcine Model to Evaluate Wound Healing and Infection of Transcutaneous Osseointegrated Weight-Bearing Prostheses

Dr. Terence E. McIff (Chairperson): _____

Date Approved: _____

Abstract

Clinical studies have shown that up to 73.9% of the 1.04 million US lower limb amputees report skin problems such as sweating, irritation, and sores associated with their conventional prosthesis. An alternative option redirects ambulatory forces back to the skeleton using an implant that permanently protrudes through the skin (transcutaneous) to enable direct bone anchorage (osseointegration) of a prosthesis. Transcutaneous osseointegrated prostheses show a marked improvement in amputee acceptance over conventional prostheses. Advantages include limited tissue breakdown, a non-restricted range of motion, and enhanced functionality. However this prosthetic option has not been clinically implemented in the United States because of infection concerns and an incomplete understanding of transcutaneous wound healing. Being a potential state-of-the-art altering surgical option for trauma-induced amputees, transcutaneous osseointegration will require preliminary animal studies.

To evaluate the efficacy of the transcutaneous osseointegrated option, a physiologically-similar, axially-loaded, weight bearing animal model was developed. Two pigs were fit with transcutaneous osseointegrated prostheses in a single-stage amputation and implantation surgical procedure. Clinical, microbiological, and histological data were examined to assess wound healing and infection at the skin-bone-implant interface. The animals achieved 70% and 67% pre-operative weight-bearing. Bacterial cultures indicated a likely deep tissue infection in one of the two animals. The transcutaneous wounds were in the proliferative phase of wound healing by the end of the 35 and 56 day studies. The epithelial skin layer was migrating towards the implant in one animal.

Results obtained from the animal model will be used to implement future topographical and material changes at the transcutaneous site. The porcine model should become the standard for implementing and testing future iterations of weight-bearing transcutaneous osseointegrated prosthetic devices.

Acknowledgements

I would like to thank the Elise A. Borck Orthotics Research Fund and the Marc A. and Elinor J. Asher Orthopedic Research Endowment Fund for financial support of this research. I would also like to recognize Dr. Dhaval Bhavsar and Dr. Kurt Schropp for their insight regarding wound healing and stoma care, Marsha Danley for her histological preparation and staining, Dr. Garth Fraga for his histopathological expertise, Sinclair Farms for their help with animal procurement, and the entire LAR staff, especially Dr. Travis Hagedorn and Erin Hood, for their support with the animal care.

Further, this research could not have taken place without my advisory board. Dr. Fischer, Dr. Maletsky and Dr. Friis were instrumental in developing my engineering skills throughout my time as an undergraduate student in Lawrence, KS. As a graduate student, I chose to pursue research at the KU Medical Center to gain a firsthand interaction with the health care system. My experiences here reiterated my belief in a bedside to bench to bedside approach to clinical needs finding and solution development.

The campus move also allowed me to work in Dr. McCliff's Orthopedic Research Lab. This was the single best decision I made as a graduate student. I have been rewarded with not only personal interaction with surgeons, residents, nurses, medical sales teams, anesthesiologists, histologists, and prosthetic specialists, but also the opportunity to work in a quickly evolving, cutting edge research lab. Dr. McCliff has proven to be a superb mentor and was instrumental in all parts of this research. I would also like to thank the staff that has been involved in the lab while I've been here, in order of gratitude specifically to this project: Damon Mar, Aly Boyer, Dr. Adam Goodyear, Michelle Settle, Dr. Rick Seagrave, Jeff Lamping, Aaron Heller, Dr. Nick Barnthouse, and Jessica Witherspoon.

The support of my mom, dad, and brother were also instrumental. It was nice to be kept grounded through the ups and downs of research. Thanks to all for making this experience memorable!

Kevin

"The fight is won or lost far away from witnesses – behind the lines, in the gym, and out there on the road, long before you dance under those lights." - Ali

Table of Contents

Abstract	iii
Acknowledgements	iv
Table of Contents.....	v
List of Figures	viii
List of Tables	viii
List of Equations.....	ix
List of Appendices.....	ix
Notations and Conventions	x

Chapter 1: Introduction and Review of the Literature

1.1 Overview	2
1.1.1 By the Numbers.....	2
1.1.2 Project Motivation	2
1.2 Conventional Prosthetic Suspension	3
1.2.1 Introduction to Conventional Prosthetic Suspension	3
1.2.2 Problems with Conventional Suspension	3
1.3 Transcutaneous Osseointegration (OI) Method	6
1.3.1 Introduction to the Transcutaneous OI Method	6
1.3.2 Advantages of Transcutaneous OI	8
1.3.3 Problems with Transcutaneous OI	8
1.3.4 Human Transcutaneous OI Devices.....	9
1.3.5 Human Clinical Trials	11
1.3.6 Translational Animal Models.....	14
1.3.7 Relevant Transcutaneous Wound Healing Studies	16
1.3.8 Comparing Treatment Costs.....	20

Chapter 2: Specific Aims

2.1 Specific Aim #1: Animal Model.....	22
2.2 Specific Aim #2: Infection	23
2.3 Specific Aim #3: Wound Healing	23

Chapter 3: Materials and Methods

3.1 Specific Aim #1: Pig Model	25
3.1.1 Animal Study Design.....	25

3.1.2 Endo-prosthesis Design Process	25
3.1.3 Final Endo-prosthesis Design.....	28
3.1.4 Endo-prosthesis Manufacturing Process	30
3.1.5 Exo-prosthesis Design Process	31
3.1.6 Surgical Technique	38
3.1.7 Post-operative Recovery	40
3.1.8 Post-operative Care.....	42
3.1.9 Force Plate Data Collection	43
3.2 Specific Aim #2: Infection	43
3.2.1 Microbiological Evaluation	43
3.2.2 Soft Tissue Biopsy Evaluation	43
3.3 Specific Aim #3: Wound Healing	44
3.3.1 Gross Observation.....	44
3.3.2 Histological Evaluation	44
Chapter 4: Results	
4.1 Specific Aim #1: Pig Model	46
4.1.1 Animal Observation.....	46
4.1.2 Assessment of Hypothesis.....	48
4.2 Specific Aim #2: Infection	49
4.2.1 Microbiological.....	49
4.2.2 Soft Tissue Biopsy.....	50
4.2.3 Assessment of Hypothesis.....	51
4.3 Specific Aim #3: Wound Healing	51
4.3.1 Gross Observation.....	51
4.3.2 Histological Evaluation	53
4.3.3 Assessment of Hypothesis.....	55
Chapter 5: Discussion	
5.1 Specific Aim #1: Pig Model	57
5.2 Specific Aim #2: Infection.....	58
5.3 Specific Aim #3: Wound Healing	59
5.4 Statistical Limitations	62
5.5 Future Directions	63
5.5.1 Future Endo-prosthesis Design.....	63
5.5.2 Future Exo-prosthesis Design.....	66

5.5.2 Study Execution.....	68
5.5.3 Direction of Porcine Model	68
Chapter 6: Development of a Computational Model	
6.1 Introduction	72
6.2 Methods.....	72
6.3 Preliminary Results	74
Chapter 7: Conclusions	
7.1 Conclusions	77
References	78
Appendices	84

List of Figures

Figure 1.1: Problems with conventional suspension.....	5
Figure 1.2: Transcutaneous OI schematic	6
Figure 1.3: Human transcutaneous OI patients	7
Figure 1.4: Existing transcutaneous OI implant systems	11
Figure 3.1: Iterative endo-prosthesis design process.....	28
Figure 3.2: Final endo-prosthesis design.....	29
Figure 3.3: Important steps in the manufacturing process for the endo-prosthesis.....	30
Figure 3.4: Initial exo-prosthetic design.....	31
Figure 3.5: Mechanical test set-up.....	32
Figure 3.6: Results from the mechanical test for the two-legged bracket	33
Figure 3.7: Results from the mechanical test for the one-legged bracket	34
Figure 3.8: Iterations of the bracket for the endo-exo prosthetic attachment	35
Figure 3.9: Iterative exo-prosthesis design process	36
Figure 3.10: Animal surgery	39
Figure 3.11: Post-operative radiographs.....	40
Figure 3.12: Post-operative recovery.....	42
Figure 4.1: Porcine model	48
Figure 4.2: Animal bacterial colonies	50
Figure 4.3: Transcutaneous wound healing	52
Figure 4.4: Transcutaneous wound site at necropsy after implant removal	52
Figure 4.5: Histological evaluation of transcutaneous wound	54
Figure 5.1: Post-mortem radiograph.....	63
Figure 5.2: Post-mortem radiograph, close-up of the bone-implant interface	65
Figure 5.3: Future exo-prosthetic design	67
Figure 6.1: Strain surrounding the transcutaneous OI implant	75

List of Tables

Table 1.1: Skin problems associated with conventional prosthetic suspension.....	5
Table 1.2: Results from European transfemoral human clinical trials.....	12
Table 4.1: Percentage animal weight-bearing.....	47
Table 6.1: Material properties for computational model	73

List of Equations

Equation 3.1: Determining the implant shaft diameter	29
------------------------------------------------------------	----

List of Appendices

Appendix 1: Engineering Drawing for Transcutaneous OI Implant	84
Appendix 2: List of Medication	85
Appendix 3: List of Surgical Supplies.....	87
Appendix 4: Surgical Protocol	88
Appendix 5: Wound Cleaning Protocol	89
Appendix 6: Force Plate Analysis	90
Appendix 7: Histology Preparation Protocol	91
Appendix 8: Histology Processing and Embedding Protocol	94
Appendix 9: Histology Cutting and Staining Protocol.....	95
Appendix 10: Gait Progress and Monitoring	96
Appendix 11: Modified house of quality for endo-prosthesis.....	99
Appendix 12: Modified house of quality for exo-prosthesis	100

Notations and Conventions (Alphabetical)

AK – Above-knee

BK – Below-knee

DLC – Diamond-like carbon

EEFP – Endo-exo femur prosthesis

ESKA – Eska Orthodynamics

HA – Hydroxyapatite

H&E – Hematoxylin and Eosin

HO – Heterotopic ossification

IACUC – Institutional Animal Care and Use Committee

ILP – Integral Leg Prosthesis

ITAP – Intraosseous Transcutaneous Amputation Prostheses

KUMC – University of Kansas Medical Center

MSC – Mesenchymal Stem Cell

NPWT – Negative Pressure Wound Therapy

OEF – Operation Enduring Freedom

OIF – Operation Iraqi Freedom

OI – Osseointegration

OPRA – Osseointegrated Prostheses for the Rehabilitation of Amputees

PLSE – Percutaneous Load-Bearing Skeletal Extension

PMMA – Polymethyl methacrylate

POP – Percutaneous Osseointegrated Prosthesis

S1 – First surgery

S2 – Second surgery

SA – Specific Aim

SiFn – Silanized fibronectin

Tpi – Threads per inch

US – United States

USDA – United States Department of Agriculture

Chapter 1: Introduction and Review of the Literature

1.1 Overview

1.1.1 By the Numbers

It is estimated that 1.6 million people in the USA, or one out of every 195 citizens, have had an amputation resulting in limb loss [1]. The lower extremities are at greater risk, constituting 1.04 million (65%) of all amputees. Vascular disease is the cause of 54% of lower limb amputations, trauma 45%, and cancer 1%. US amputations occur most often in an aging population as 42% of amputees are 65 years or older. Sixty-five percent (65%) of amputees are men and 42% of amputees are nonwhite. Of all lower limb amputations, 60% are categorized as major (i.e., excluding only toes). Of all amputations at the level of the knee, above-knee (AK) accounted for 48.3% and below-knee (BK) constituted 51.7%. There is an increasing trend in the number of amputations. By the year 2050, there will be a projected 3.6 million American amputees [2]. Sufficient data is not available to estimate the number of worldwide amputees.

The United States Armed Forces compiles detailed injury statistics for service members. During the years 2000 to 2011, there were 6,144 amputations among soldiers engaged in ground combat operations while on deployment or in other settings [3]. Of these, 2,037 (33%) were major limb amputations. As of December 2012, 1,715 service members had an amputation during Operation Iraqi Freedom (OIF) and Operation Enduring Freedom (OEF). Eighty-seven percent (87%) of these amputations were major limb [4].

1.1.2 Project Motivation

Clinical studies have shown that up to 73.9% of the 1.04 million US lower limb amputees report skin problems such as sweating, irritation, and sores associated with their conventional prosthesis. Transcutaneous osseointegration prosthetic devices, which permanently protrude through the skin (transcutaneous) to enable direct bone anchorage (osseointegration) of a prosthetic limb, offer an alternative option for connection of a prosthetic to the body. Transcutaneous osseointegration prosthesis, which will be further discussed in the following thesis chapters, have yet to receive FDA approval for clinical use in the United States. Although over 250 of these procedures have been performed on humans, primarily in Europe, the US health care system is hesitant to implement the amputation and implantation technique largely

because of concerns about potential bacterial complications around the implant and mechanical failure of the bone/implant interface (i.e., fixation) [2]. Before transcutaneous osseointegration techniques are introduced in the US, these complications will need to be sufficiently resolved via computational models, animal studies, and human clinical trials. This pilot study is the initial investigation into the establishment of an appropriate *in vivo* large animal model for transcutaneous osseointegrated prostheses.

1.2 Conventional Prosthetic Suspension

1.2.1 Introduction to Conventional Prosthetic Suspension

The earliest of rehabilitative lower limb prostheses date back to the Greek and Roman civilizations of 300 BC [5]. These were weight-bearing prosthetic legs made of wood and secured to the body with leather straps. While advancements in material science and robotics have made the lower limb prosthesis lighter, stronger and more functional, the prosthetic limb attachment has remained largely unchanged for the last 2,000 years. Straps, belts, sleeves, or suction remain the primary attachment options for today's amputees [6].

1.2.2 Problems with Conventional Suspension

Modern lower limb amputation techniques have progressed to improve patient satisfaction. They attempt to achieve the following: a skin incision away from a potential rub site of a prosthetic limb, smoothed bone edges, remaining muscle shaped to provide sufficient padding around the residual bone, and nerves cut proximally to minimize pain. Even with these adaptations, the soft tissues of the residual stump still encounter all of the force and wear that is normally associated with ambulation. It has been shown that repeated loading of soft tissue may hinder the local blood supply and lymphatic system [7]. High-frequency and long-term use of a socket prosthesis can lead to local cell necrosis, tissue breakdown and eventual skin sores (Figure 1.1). Beyond skin problems, some amputees are left with a residual limb too short to enable adequate mechanical fixation with conventional suspension [8]. This is often the case in trauma-induced amputations.

Table 1.1 at the end of this section summarizes the reports of skin problems associated with conventional prosthetic suspension. In a study of 261 prosthetic-wearing amputees, 30

patients (11%) encountered skin problems requiring treatment from a health center [9]. The most commonly diagnosed skin problems were pressure sores, irritant contact dermatitis, negative pressure hyperemia, intertrigo, and xerosis. A survey of ninety-seven amputees with unilateral trans-femoral amputations reported common troubles associated with the conventional prosthetic suspension [10]. One quarter of those amputees surveyed considered their quality of life to be poor to extremely poor because of problems associated with their prosthesis. Problems included sweating (72%), skin irritation (62%), limited mobility (61%), and stump pain (51%). In a questionnaire-based study of 210 amputees, 71 (34%) reported a skin problem. Problems included lesions and contact dermatitis [11]. A clinical study of 124 amputees estimated a 36% prevalence of skin problems of the stump due to the prosthesis [12]. The most commonly reported problems were pressure ulcers (39%) and infection (25%). Of those participants with prosthesis-induced skin problems, 50% reported a reduction in prosthesis use and 54% reported a reduction in walking distance without taking a break. In a six-year retrospective chart review of 828 lower-limb amputees, 337 (41%) had at least one skin problem [13]. Commonly reported skin problems were ulcers (27%), irritation (18%), inclusion cysts (15%) and callus (11%). Amputation level, type of employment, type of walking aid, and peripheral vascular disease were all statistically correlated with the incidence of a skin problem. In a survey of 581 veterans and service members of Vietnam and OIF/OEF, 58% reported that they were bothered by skin problems associated with their prosthesis [14]. Commonly reported problems included pain, sweating, skin irritation, and socket fit. A clinical study of 142 amputees reported skin problems in 105 (73.9%) of them [15]. Of those patients reporting skin problems, contact dermatitis was the leading cause (54.3%).

Differences in inclusion criteria between the studies led to a considerable range (11%-73.9%) of patients reporting “skin problems” (Table 1.1). Nevertheless, the clinical studies demonstrate that the conventional prosthetic suspension leaves amputees with pain, infection, and an uneven pressure distribution on the residual stump. These skin problems culminate in limited mobility and demonstrate the clinical need for improved methods of prosthetic attachment.



Figure 1.1: Problems with conventional suspension. a) An amputee with pressure sores, b) Contact dermatitis on the proximal edge of the prosthesis' contact surface. *Images reproduced from Highsmith et al. (2007) [9].*

Table 1.1: Skin problems associated with conventional prosthetic suspension

Type of Study (Publication Year)	Skin Problems	Common Problems
Clinical assessment (Highsmith et al., 2007)	30/261 (11%)	Pressure sores, irritant contact dermatitis, negative pressure hyperemia, intertrigo, xerosis
Questionnaire-based (Hagberg et al., 2001)	24/97 (25%)	Sweating, skin irritation, limited mobility, stump pain
Questionnaire-based (Lyon et al., 2000)	71/210 (34%)	Lesions, contact dermatitis
Questionnaire-based and clinical assessment (Meulenbelt et al., 2011)	45/124 (36%)	Pressure ulcers, infection
Retrospective chart review (Dudek et al., 2005)	337/828 (41%)	Ulcers, irritation, inclusion cysts, callus
Veteran survey (Berke et al., 2010)	337/581 (58%)	Pain, sweating, skin irritation, socket fit
Clinical assessment (Koc et al., 2008)	105/142 (73.9%)	Contact dermatitis

1.3 Transcutaneous Osseointegration (OI) Method

1.3.1 Introduction to Transcutaneous OI

An alternative option to socket-stump artificial limb attachment, known as transcutaneous osseointegration, redirects the forces of loading entirely back to the skeleton, bypassing the soft tissue, and thus circumventing many of the soft tissue problems associated with conventional prosthetic suspension. This technique uses a transcutaneous prosthesis to enable direct bone anchorage of an implant (Figure 1.2).

“Osseointegration” was a term coined in the 1950’s by Per-Ingvar Branemark to describe permanent fixation and integration of titanium and bone. Initially, Branemark’s work focused on the circulation of bone marrow using a channeled titanium implant within the ear chamber of a rabbit [16]. After some time, Branemark was unable to remove the titanium screws from the bone because the interface had become completely fused. Bone and vessels had grown into the titanium chamber and could not be separated without fracture. Inadvertently, Branemark showed that titanium has properties capable of permanent fixation with bone. Branemark originally defined osseointegration as a direct structural and functional connection between ordered living bone and the surface of a load-carrying implant [17]. The current definition defines osseointegration as a non-progressive relative movement between the directly contacted implant and bone while subjecting the interface to all normal conditions of loading [16].

Osseointegration was first established as a reliable and effective treatment in the field of dental reconstruction. Since 1965, it has been used clinically to replace single teeth, bridges, and overdentures supported by implants in more than 2 million patients [18]. A retrospective dental study reported a 90% implant survival rate at 15 years post-implantation [19]. Research momentum has more recently shifted to studies focused on facial prosthesis, bone-anchored

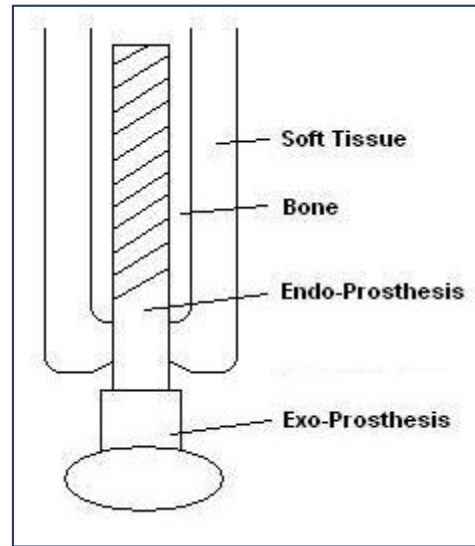


Figure 1.2: Transcutaneous OI schematic

hearing aids, finger joint prosthesis, and most notably for this thesis, lower limb amputations [16].

Lower limb transcutaneous OI procedures currently require two surgeries and an extensive rehabilitation treatment. At the first surgery (S1), a titanium insert is implanted into the medullary cavity and the site closed for a period of unloaded healing. This healing period ranges from six weeks to six months depending on the healthcare provider's recommendation. The second surgery (S2) reopens the residual limb to expose the distal end of the insert. A transcutaneous abutment is then permanently fixated into the insert with its distal end protruding through the skin (Figure 1.3a). The Osseointegrated Prostheses for the Rehabilitation of Amputees (OPRA) protocol details an additional six month rehabilitation period with incrementally increasing loads and weight bearing activity [20]. Introduced in 1999, the OPRA protocol has limited the frequency of failure by standardizing the treatment [21]. The external prosthetic attachment is then connected to the abutment allowing for patient ambulation (Figure 1.3b). This transcutaneous OI option has shown promise in enabling amputees a statistically significant better Health Related Quality of Life [22].

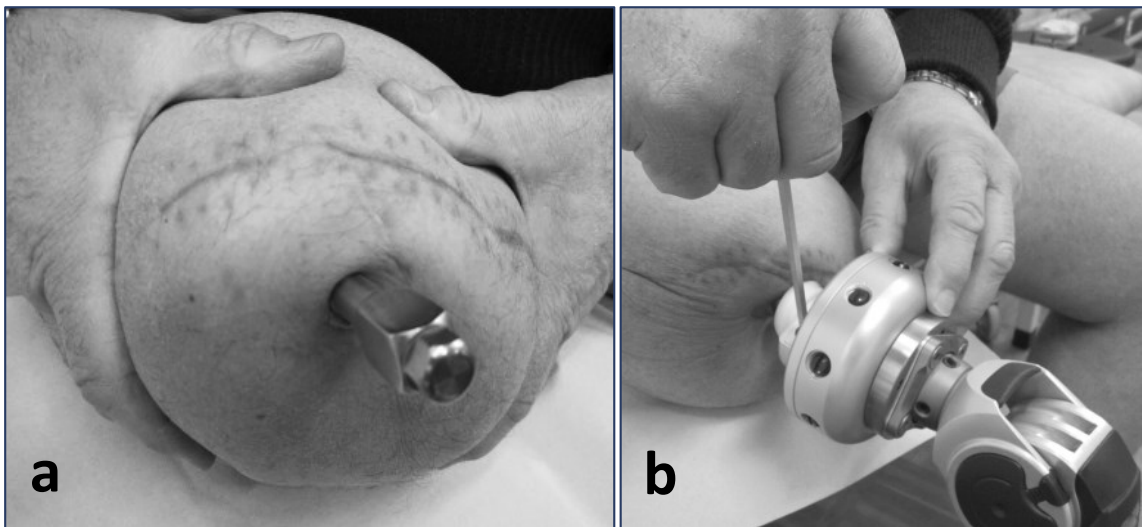


Figure 1.3: Human transcutaneous OI patients. a) Patient with transcutaneous OI endo-prosthesis implanted into femur, b) Patient securing exo-prosthesis to the endo-prosthesis. *Images reproduced from Hagberg et al. (2005) [23].*

1.3.2 Advantages of Transcutaneous OI

Advantages of transcutaneous OI prosthetics include less pain [18], limited tissue breakdown [18], easier donning and doffing [18], proper prosthetic fit [18], non-restricted range of motion [18, 23], and enhanced control of the residual limb [18]. As an extension of the bony skeleton, OI prosthetic limbs also have amputees reporting improved sensations of proprioception, i.e., the sensory feedback transmitted through the prosthesis [18, 24]. In a retrospective study, the 100 patients treated at Sahlgrenska University Hospital in Sweden reported improved prosthetic use and mobility scores with decreased problem scores after switching from conventional to OI prosthetics [21]. Twelve amputees from this group participated in a temporal gait study to demonstrate the functional advantages of the prosthesis. The transcutaneous OI amputees performed cadence, gait cycle duration, stance and swing phases that were 2% quicker, 3% shorter, 6% shorter, and 1% longer than socket amputees and 11% slower, 9% longer, 6% longer, and 13% longer than able-bodied participants, respectively [25]. These results demonstrate the functional improvement over conventional suspension.

1.3.3 Problems with Transcutaneous OI

Attachment of lower limb prostheses by means of transcutaneous OI implants offers the potential for vast improvements over conventional lower limb socket-secured prostheses. Complicating the comparison, however, is the nature of the transcutaneous implant. Marsupialization, permigration, avulsion, and most notably infection are all modes of failure which must be addressed in the presence of a foreign, metal implant permanently breaching the skin barrier [26]. Marsupialization, or epidermal downgrowth, occurs when the epidermis grows internally along the percutaneous post creating a sinus tract surrounding the implant. Permigration refers to marsupialization with a porous percutaneous post. Over time, the implant extrudes as the post fills with cell debris. Avulsion refers to a tearing away of the implant from the soft tissue due to externally applied mechanical forces. Infection is the most concerning mode of failure for clinical implications. The permanence of the surgical insult created in the skin by a transcutaneous implant undermines the protection function of the

natural human skin barrier. In healthy skin, the outermost layer of the skin's epidermis, known as the stratum corneum, functions as the body's first barrier to infection. With this skin layer compromised, the body is susceptible to bacterial and viral infiltration, thus dramatically increasing the rates of deep tissue infection [27]. Infected tissue around the implant can ultimately precipitate implant removal; thus eradicating the advantages of transcutaneous, OI implants [27-29].

Mechanical failure of fixation and subsequent loosening of the OI implant, previously considered problematic, have been addressed through numerous dental and orthopedic studies [19, 30, 31]. Threaded and porous in-growth implant surfaces have both been successfully used as the method of fixation to the bone. A radiostereometric analysis (RSA) of 51 transfemoral patients indicated a stable fixation in all threaded implants [31]. There do remain some unanswered questions such as how the bone surrounding the implant remodels. Xu et al. used clinical x-rays and finite element (FE) modeling to correlate bone remodeling in the femur to the stress/strain distribution induced by ambulation [32]. Clinical x-rays of 11 transcutaneous OI patients showed bone absorption at the distal end of the implant and bone formation at the proximal end. The authors concluded that this type of bone remodeling could not be described by only the stress/strain adaptive bone remodeling theory or the fluid flow base stress gradient theory. Instead, the observed bone remodeling was a function of both overall stress/strain level and stress gradient.

Frossard et al. analyzed patient gait to determine that the maximum load applied to the implant along its long axis constitutes 120% of the amputee's body weight [33]. High subject to subject variability of applied loading indicated that the mechanical design of the implant should be customized per amputee [34]. The personalized nature of an implant could lead to increased patient costs for amputees that choose a transcutaneous OI prosthetic.

1.3.4 Human Transcutaneous OI Devices

Three distinct transcutaneous OI implant designs have been used in European human clinical applications: 1) OPRA system (Integrum AB, Göteborg, Sweden), 2) Integral Leg Endo/Exo Prosthesis (ESKA Implants AG, Lübeck, Germany), 3) ITAP system (Royal National

Orthopaedic Hospital, Stanmore, Middlesex, UK). All three of the implant systems attempt to use a soft tissue seal around the implant as the primary barrier to bacterial infection.

Developed in the 1990's, the OPRA system is a two part implant consisting of a threaded titanium, bone-anchoring fixture and a skin penetrating abutment (Figure 1.4a). The associated surgical technique removes excess soft tissue from the residual limb in an attempt to stabilize the healing wound. Reducing relative motion near the implant is thought to improve the skin seal at the bone [35].

Developed in 1999, the Integral Leg Prosthesis (ILP) Endo/Exo system is a three piece implant consisting of a cobalt-chromium-molybdenum stem coated with a porous Spongiosa Metal II, a stability piece, and a transcutaneous adapter (Figure 1.4b). The associated surgical technique leaves as much soft tissue on the residual limb as possible in order to create a healthy stoma. The desired wound healing response is skin closure into the wound creating a permanent seal at the level of the bone. This protocol requires a much shorter 6 week osseointegration unloaded healing period which has received a positive patient response.

Developed in the 2000's, the ITAP system is a one piece implant consisting of a smooth intraosseous titanium stem with a perforated, umbrella-shaped, hydroxyapatite (HA) coated flange (Figure 1.4c). The associated surgical technique lays the skin over the top of the flange in an attempt to minimize downgrowth and encourage epithelial soft tissue adhesion. The subcutaneous flange reduces relative interfacial movement between the epithelium and the implant [36]. This technique was developed as a biomimetic model of deer antlers [37].

Verkerke et al. used FE analysis to assess bone failure and the bone-implant interface [38]. The study compared the OPRA system and the ILP Endo/Exo prosthesis. Results indicated that the porous ILP implant generated favorable bone strain energy density levels while the threaded OPRA implant generated lower peak bone stress levels.

Both the OPRA and ILP systems are being marketed in Europe. A fourth implant, the Percutaneous Osseointegrated Prosthesis (POP) system is being developed at the University of Utah. It consists of a conical, ribbed bone implant region and a titanium P² porous coated transcutaneous section (Figure 1.4d). Similar to the ITAP implant, the POP uses a subcutaneous

collar in an attempt to reduce interfacial movement. Clinical trials using the POP system have been set to begin within two years at the University of Utah.

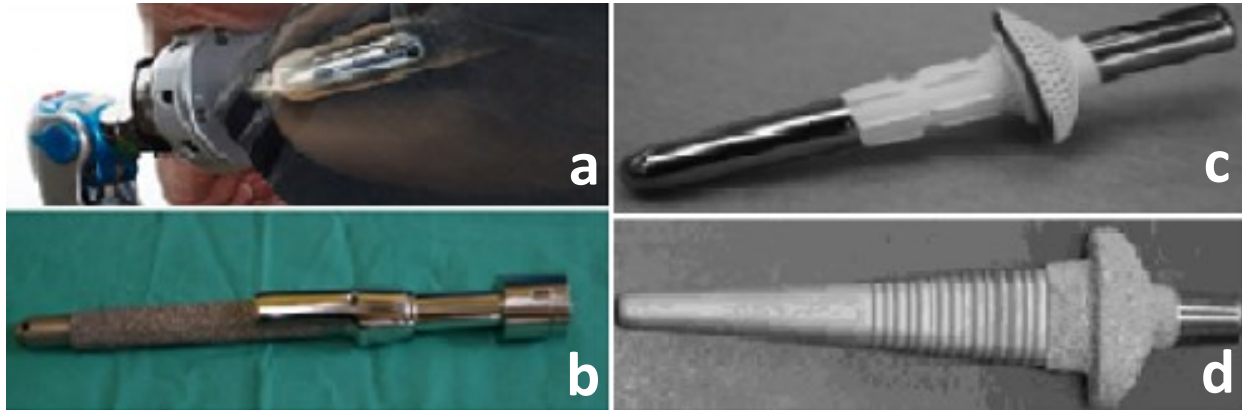


Figure 1.4: Existing transcutaneous OI implant systems: a) OPRA implant, b) ILP implant, c) ITAP implant, d) POP implant. *Images reproduced from: a) Sahlgrenska Website [39], b) Endo-Exo Prosthesis DVD [40], c) Fitzpatrick et al. (2011) [41], d) Bloebaum et al. (2012) [42].*

1.3.5 Human Clinical Trials

Over the last two decades, transfemoral surgical implantations have been performed on over 250 European amputees in a clinical environment [27, 28, 43]. A three-year follow-up of the initial 16 transfemoral patients treated with the OPRA system beginning in 1990 reported fourteen superficial infections and seven deep infections necessitating three (19%) implant removals [29]. A one-year follow-up of the initial 11 candidates treated in the United Kingdom (following the Swedish protocol) from 1997 to 2003 reported two (18%) implant removals secondary to infection [28]. A three year prospective study followed 39 patients treated in Sweden from 2005 to 2008. Implant infection was reported in 5% of cases at inclusion and 18% at follow-up [27]. From 1999 to 2009, 39 ILP systems were implanted in Lubeck, Germany [43]. Three implants (8%) were explanted due to deep bone and superficial soft tissue infections. Interestingly, in this study 37 of the 39 patients said they would undergo the implantation again. Summarizing the clinical trials, transcutaneous OI implants have reported 8-19% infection rates (Table 1.2). This is consistent with other permanent transcutaneous devices;

venous catheters, dental implants, and bone anchored hearing aids have shown an infection rate of 3-8%, 5-10%, and 23.9%, respectively [44, 45].

Table 1.2: Results from European transfemoral human clinical trials

Clinical Trial	Approximate Dates (Follow-up)	Cases of Infection	Explanation
OPRA system	1990 (3 year)	14 superficial, 7 deep	3/16 (19%)
OPRA system	1997-2003 (1 year)	2 total	2/11 (18%)
OPRA system	2005-2008 (3 year)	2 at inclusion, 7 at follow-up	Did not report
ILP system	1999-2009	2 superficial, 1 deep	3/39 (8%)

In 1999, an OPRA (Osseointegrated Protheses for the Rehabilitation of Amputees) protocol was established to standardize rehabilitation treatments [22]. The study used the Questionnaire for Persons with a Transfemoral Amputation (Q-TFA) to report prosthetic use scores on a scale of 0 to 100. They found pre-OI scores to be wide-ranging with a mean score of 51. A two year post-OI follow up of 18 subjects reported a mean use score of 83, a 32 point improvement in functionality.

Webster et al. reported the perceptions of the transcutaneous OI procedure for 73 current lower limb amputees [46]. One-third said they would consider the prosthetic option citing anticipations of prosthetic function (92%), improved walking ability (88%), prosthetic attachment (83%), and improved activity level (79%). Interestingly, only 50% of the amputees report decreased skin breakdown as a perceived advantage. Forty-two percent (42%) said they would not consider the option because of perceived disadvantages including infection (75%), potential for limited activity due to failure (65%), lengthy rehabilitation period (65%), and risk of bone fracture (63%). Significant lifestyle differences between individuals willing to consider osseointegration and those unwilling included living in a rural community, pain inhibiting daily activity, and detachment of their current prosthesis. The study concluded that infection prevention and rehabilitation efficiency need to be addressed in order to improve amputee perception of the transcutaneous OI method.

The transcutaneous OI prosthetic option is best suited for lower limb, AK, traumatic amputees with ample soft tissue coverage. Below knee amputees exhibit greater success with conventional prostheses and therefore would likely not prefer the higher risk transcutaneous option. A survey of 59 amputees reported daily prosthetic use in 96% of the BK compared to 50% of the AK [47]. Further, a survey of 134 lower extremity amputees reported that BK amputees were significantly more independent than AKs [48]. Lower limb, AK, traumatic amputees account for roughly 300,000 Americans, or approximately 19% of the US amputee population.

An interview with thirteen Swedish patients explored first-hand transcutaneous OI patient accounts [49]. Almost all patients responded favorably to the procedure describing the new method of attachment as “revolutionary” and “radical”. The authors grouped the patients into three classes of prosthetic acceptance: 1) Practical prosthesis, 2) Pretend limb, 3) A part of me. The practical prosthetic group felt it was a better tool than their previous prosthetic, but a tool nonetheless. One subject from this group stated, “This is perhaps 70 percent as compared to a real leg...being 100 percent and an old prosthesis is perhaps 25 percent.” The pretend limb group valued their new prosthetic as more than a tool, but still carried a burden of loss. The third group of patients seemed to accept their osseointegrated leg as an extension of their body. A subject stated, “I can feel when I put the foot down, so that I can feel the shock throughout the body – not in an unpleasant way but I feel it, and it gives me a positive experience of my body as a whole.”

The internet has allowed further communication of inspirational personal accounts of the lifestyle that the procedure has returned to amputees. In 1993, a motorbike accident caused a man to lose his right leg [50]. For 15 years he used conventional prostheses and experienced a range of problems including stump soreness and soft tissue pain. He writes, “Living with this restriction became the norm and soon the changes to my daily life required to compensate for my disability became routine – the life of an amputee...” In 2008, he became the second recipient of the ITAP transcutaneous OI prosthetic. He was discharged from the hospital one week after surgery and trained with varying prosthetics for 18 months. In 2010, he climbed Mount Kilimanjaro, the largest mountain in Africa, with his ITAP prosthesis. He blogs

about his very active lifestyle and wrote, “In essence this procedure has given me my leg back!” Retrospective studies have previously shown that amputees using transcutaneous OI prostheses report an improved Health Related Quality of Life when compared to those using conventional prosthetics [21]. This type of first-hand account drives home the potential lifestyle overhaul that the transcutaneous OI option offers to amputees.

1.3.6 Translational Animal Models

While it is well documented via human clinical trials that transcutaneous OI implants have an 8-19% risk of infection in clinical application, there is an incomplete understanding of the human wound healing process. The lack of understanding is twofold: 1) the procedure was developed in a clinical setting geared towards an end product. This effort leads to retrospective clinical studies as opposed to hypothesis driven research questions. 2) The transcutaneous wound healing is a complicated process that requires a thorough evaluation of culture swabs, biopsies, and histology which is unfeasible to accomplish in a human clinical study. Translational animal models provide an opportunity to answer relevant questions about wound healing and infection around weight-bearing prosthetics. Over the last four decades, such models have attempted to improve the skin-implant seal around transcutaneous OI implants.

The first weight-bearing translational animal model was introduced in 1977. Lobb et al. investigated tissue integration into percutaneous prosthetics using a porcine model [51]. The group of 14 pigs was split into two, seven with nylon velour covering the transcutaneous section and seven with a double-velour Dacron fabric. They reported dry wounds with good subcutaneous adhesion and some skin adhesion over the first two weeks. By week three they observed soft tissue retraction resulting in minimal tissue adhesion by week five. By week ten, there was complete tissue retraction around the transcutaneous implants in all fourteen pigs. The study concluded that Dacron and nylon velours are not suitable for transcutaneous, weight-bearing applications. In 1985, Hall et al. evaluated a Percutaneous Load-Bearing Skeletal Extension (PLSE) device using a weight-bearing caprine model [24]. This device anchored into the amputee using a large pin perpendicular to the residual bone leaving two transcutaneous holes. An external yoke was then attached to the pin. The authors hypothesized that the

interfacial bonds would not tear at the exit sites because there is greatly reduced stress away from the end of the limb. Goats with the PLSE devices survived without complications for up to 14 months in the pasture until they “inevitably” became infected due to trauma or exposure to the elements.

Throughout the 1990’s and early 2000’s little work was published on the development of a translatable large animal model for transcutaneous OI prosthetics. The field has since seen a resurgence as a result of the progress demonstrated in the European human clinics. The FDA has stricter guidelines for device clearance, thus efficacy is usually first shown in an animal model. In 2008, Drygas et al. reported the successful implantation of a tapered, threaded titanium stem with a porous tantalum transcutaneous section into a dog model [52]. At a two-year follow-up, the implant was infection free allowing the dog to run on the OI prosthetic leg. In 2011, Blunn and colleagues implanted the flanged ITAP prosthetic device in four dogs for limb salvage purposes [41]. They reported favorable bone and soft tissue integration with the animals returning to their pre-operative levels of ambulation. The sites were infection free from three weeks until approximately one year when the dogs died of unrelated circumstances. In 2011, Bloebaum, Bachus and colleagues at the University of Utah investigated the use of the POP device in a 12 month ovine model [53]. The group concluded that an ovine model was feasible. Results indicated weight-bearing peaked at a maximum of 80% pre-operative levels over a 12 month time period. The group has since used the ovine model to investigate porous subcutaneous components, skin immobilization, and cortical bone response. In an evaluation of 86 sheep, they compared porous and smooth subcutaneous surfaces [42]. Results showed zero of the 77 sheep with porous ingrowth surfaces and two of the eight sheep with smooth surfaces were infected at the nine month endpoint. They concluded that a porous subdermal barrier is advantageous for infection prevention. In an overlapping study using 37 sheep, Bloebaum’s team measured skin regression on a porous subdermal coating at six, nine and 12 month time points [35]. The percent of sub-epithelial attachment was shown to decrease over the course of the study. The tissue regression was attributed to the high contact area of the porous surface. Results confirmed that micro-motion hinders soft-tissue implant fixation. Using

the ovine model as preliminary data, human feasibility trials for the POP device have been approved and are expected to begin in 2014 at the University of Utah.

1.3.7 Relevant Transcutaneous Wound Healing Studies

While relatively few attempts have been made at the development of a large weight-bearing animal model for transcutaneous OI prosthetics, other permanent transcutaneous devices (e.g., venous catheters and bone anchored hearing aids) have been more thoroughly investigated in animal models. Much like transcutaneous weight-bearing prosthetic devices, catheters and hearing aids require an infection resistant seal at the protrusion of the transcutaneous device. The following describes relevant research literature investigating material, topography, treatments, biological coatings and surgical technique alterations.

Researchers acknowledge that the success of transcutaneous implants is partially dependent on the material selection of the transcutaneous portion of the device. In 1974, Hall et al. used a caprine model to assess a nylon velour as a transcutaneous implant surface [54]. The team hypothesized that the material would eliminate the problems associated with marsupialization. The method was successful in creating a bacteriostatic seal but a “growth phenomenon” slowly extruded the implant. The study concluded that nylon or Dacron velour showed excellent results and eliminated the problems at the skin-implant interface. In 1977, von Recum et al. studied Dacron velour transcutaneous components in dogs, goats, and rabbits [55]. Results indicated that epidermal migration rate and connective tissue maturation differed among species. Further, the authors noted that percutaneous healing is a product of implant material histocompatibility, mechanical interfacial forces, and epidermal proliferative patterns. In 1990, Jansen et al. compared hydroxyapatite, titanium and carbon implants in a rabbit model [56]. It was importantly concluded that direct attachment to bone aids the longevity of transcutaneous devices. Further, no difference in tissue reaction as a result of the material selection was found at four or eight month endpoints. Notably, this was inconsistent with a 1977 human case study by Mooney et al. In this study, a skin-implant seal failed to develop with a smooth carbon surface at the transcutaneous interface after implantation in three amputees [57]. The devices were retrieved due to poor vascularization, mechanical factors, and

ultimately infection. In 1998, Kormos et al. hypothesized the use of a fine trabecularized carbon as the transcutaneous catheter material in a bovine model [58]. At the 30 day endpoint, epidermal downgrowth was minimized while connective tissue and neovascularization proliferated around the implant. The study concluded that the fine trabecularized carbon material is suitable for percutaneous devices. In 2009, Chou et al. compared porous tantalum and porous titanium as the material selection for the transcutaneous section [59]. There was no difference in rates of pin track infection between material groups.

Studies have shown that infection rates also correlate to the surface topography and characteristics where the implant breaches the skin. In 1974, Winter et al. compared porous and nonporous titanium surfaces for the transcutaneous region of an implant [60]. His team concluded that at the 10-week post-implantation time point, the nonporous implants created an unstable, infection prone site while the porous implants allowed fibrous tissue ingrowth resulting in a stable junction. In 1981, Squier and Collins attempted to characterize the relationship between soft tissue attachment, epithelial downgrowth and surface porosity [61]. The team concluded that larger pores (up to 8.0 μm) induced greater soft tissue ingrowth. In 1984, Grosse-Siestrup and Affeld reviewed natural percutaneous devices such as horns, hair, feathers, fingernails, hoofs, teeth, and antlers [62]. The group emphasized the importance of shifting mechanical stresses away from the skin attachment interface. They proposed the use of a subcutaneous flange to distribute the stresses induced by loading. In 1991, Chehroudi et al. investigated the effects of micromachined grooved surfaces on the epithelial downgrowth and tissue-implant seal at a microscopic level [63]. Electron microscopic analysis concluded that micro grooves can improve epithelial cell attachment. In 2002, Chehroudi et al. evaluated the effect of subcutaneous and percutaneous surface topographies on tissue integration in a rat model [64]. Results indicated that subcutaneous grooved surfaces improved tissue adhesion. In 2005, Jansen et al. compared smooth and microtextured transcutaneous section of silicone catheters using a rat model [65]. They found epithelial downgrowth in all animals regardless of texturing, but concluded that the direction of the grooves can dictate ingrowth patterns. In 2007, Pendegrass et al. reported that smooth polished surfaces show significantly reduced infection rates by optimizing epithelial layer attachment in an in-vitro study [66].

Contradictorily, in 2011, Bachus et al. showed that porous coated implants displayed tissue ingrown whereas the smooth implants were surrounded by a fibrotic capsule inhibiting a long-term seal in a rabbit model [67]. The imperfect skin seal around the smooth implant induced an infection tract for the migration of infecting microorganisms; prompting a seven-fold increase in infection risk when compared to porous coated surfaces. Epithelial downgrowth was not correlated with implant type. In 2011, Blunn et al. assessed the use of silanized fibronectin (SiFn) on titanium surfaces to improve *in vivo* soft tissue attachment in an ovine model [68]. They concluded that SiFn surfaces resulted in better cell alignment and thus improved dermal attachment. Affeld et al. have recently developed a novel active skin-penetrating device for use in catheters [69]. Using a protective sleeve and active traction device, a permanent and stable ingrowth of skin cells is possible. The technique was shown effective at maintaining an infection-free skin barrier for 420 days in 10 goats.

Animal studies have also considered surface treatments and coatings to combat bacterial isolates and promote soft tissue adhesion. In 1988, Jansen et al. implanted HA coated transcutaneous devices in the tibia and dorsum of guinea pigs and the tibia and cranium of rabbits [70]. Results indicated stable epidermal junction at the tibia and cranial implant sites but epidermal migration at the dorsal implant site. This was likely due to the amount of interfacial movement at the dorsal site compared to the other sites as numerous research groups have shown interfacial movement to be detrimental to seal formation. In 2006, Blunn et al. evaluated HA as a coating for the transcutaneous section in a non-weight bearing caprine model [37]. HA was applied to increase the surface porosity in an effort to tighten the seal between the implant and the dermal tissues. Results indicated that the treatment reduced soft tissue attachment and supported the ingrowth of fibroblastic and soft tissues. The coating demonstrated reduced epithelial layer downgrowth and thus decreased rates of infection. That same year, Blunn and colleagues evaluated diamond-like carbon (DLC) and HA coatings in an ovine model [71]. At the 10-week endpoint, results indicated decreased bacterial colonies and biofilm formation with DLC implants and improved dermal and bone adhesion with HA implants. In 2009, Chou et al. assessed pexiganan acetate as a topical antimicrobial to prevent pin tract infection using a rabbit model [59]. They concluded that daily application of pexiganan

acetate correlated to a 75 percent reduction in infection rates. In 2010, Bloebaum et al. determined CSA-13, a broad spectrum antimicrobial, to be ineffective in preventing pin tract infections in a percutaneous pin wound site in a sheep model [72, 73]. The model was deemed overly aggressive, allowing for too much interfacial motion at the skin-implant interface. This work proposed that antimicrobials may be used as secondary barriers to infection, but ultimately skin attachment to the implants surface is most essential. In 2011, Bachus et al. showed Mesenchymal Stem Cell (MSC) treatments effective in improving skin attachment and early tissue integration on a porous metal percutaneous implant in a rat model [74]. Treated implants showed an early influx of cellular inflammatory infiltrates compared to the untreated implants. Epidermal downgrowth was observed in all implants and therefore uncorrelated to MSC treatment. That same year Bachus et al. showed MSC treated implants to be at lesser risk of infection compared to untreated implants in a bacterially challenged rat model [75]. Further, the group showed that MSC treatments stimulated tissue infiltration into the porous coatings and prompted a fortified seal from microbial infection.

Finally, surgical techniques have been compared in animal models. In 1993, Jansen et al. evaluated a two-stage OI implantation procedure in a rabbit model [76]. At S1, HA coated titanium implants were implanted in the bone and the wound closed. At S2, three months later, a dense HA percutaneous portion was connected with the enossal part. At five months post-S2, there existed an effective percutaneous seal. However, the study was unable to irrefutably conclude that two-stage surgical procedures enabled greater success for transcutaneous bone-anchored prosthetics than one-stage procedures. In 1996, the same team again evaluated one-stage versus two-stage surgical techniques using titanium fiber mesh implants in twelve goats [77]. In each goat, they inserted a one-stage and a two-stage implant. A three month healing time was allotted for the two-stage implants. At four months post-S2, all implants were removed. While there was no difference in epidermal downgrowth between surgical groups, there was an enhanced inflammatory response found in the tissue inside the titanium mesh for one stage implants. The study concluded that the two-stage surgical procedure was advantageous for the incorporation of host tissues and transcutaneous devices. Jansen's team realized the required three month healing time between surgeries was inhibitive from a clinical

standpoint. They further investigated the possibility of reducing the time interval without compromising the tissue response [78]. They implanted one transcutaneous device a week for six consecutive weeks into the back of nine goats. Histological analysis indicated that an inflammatory response was active for two weeks, after which no difference was found. They concluded that a three week healing period between surgeries is sufficient for titanium mesh percutaneous devices.

As outlined above, material selection, surface topography, biological treatments, and alterations to surgical techniques have shown varying degrees of success at promoting wound healing and preventing infection. One conclusion that has been consistent throughout experimentation is that interfacial movement is detrimental to the formation of an effective tissue-implant seal. Further overarching conclusions are difficult to draw because of the variety of animal models and study designs. A widely-accepted, translatable animal model would be beneficial in making the permanently attached endo-prosthetic more than a nearly-achievable orthopedic dream.

1.3.8 Comparing Treatment Costs

As a potential barrier to market, cost needs to be compared between traditional socket stump attachment and the transcutaneous OI method. In a study of 601 US amputees using traditional suction attachment, average initial hospitalization costs plus two years of health care costs, including prosthetics, for AKs were estimated at \$110,039 [79]. The average lifetime health-care cost for amputees was \$509,275. The personalized nature of the transcutaneous OI treatment, coupled with the increased surgical and recovery time will likely result in a more expensive treatment option. However, transcutaneous OI patients have shown increased levels of functionality. Their improved mobility could allow for a more complete return to work, thus improving their overall return on treatment investment. A more thorough understanding of cost will be important to evaluate the prospect of widespread clinical implementation for the transcutaneous OI prosthetic option.

Chapter 2: Specific Aims

This pilot study was designed around the execution of three specific aims: 1) animal model, 2) infection, 3) wound healing. Specific Aim #1 evaluated the use of a porcine (pig) model in the assessment of transcutaneous OI prostheses. Specific Aim #2 assessed superficial and deep soft tissue infection around the transcutaneous OI implant. As discussed in chapter 1, infection rates of 8 to 19% have been reported in human clinical trials. Lowering the incidence of infection continues to be the primary goal of transcutaneous OI prosthetic research. Specific Aim #3 evaluated wound healing around the transcutaneous implant. The animal model allows assessment techniques of wound healing that are not possible in a human clinical studies. Unless stated otherwise, this study was designed and executed by the author of this thesis.

2.1 Specific Aim #1: Animal Model

Specific Aim #1 evaluated the use of a porcine model to simulate the human transcutaneous OI condition. Previous non weight-bearing and weight-bearing caprine, canine, and ovine models have considered material, topography, treatments, and surgical alterations in an attempt to expedite wound healing and ensure a skin-implant seal around transcutaneous OI implants. The following important considerations regarding wound healing and infection have been overlooked when simulating the human transcutaneous OI condition in these previous animal models; 1) mimicking the physiological tissue response of a human, and, 2) creating a transcutaneous site with comparative soft tissue coverage.

It is to be noted that no studies have successfully tested a weight-bearing transcutaneous OI prosthetic device in a porcine model. Pig skin, like human, is relatively hairless, tightly attached to the subcutaneous tissue, vascularized by a cutaneous blood supply, and healed by means of epithelialization [80, 81]. The pig has been extensively utilized for superficial and deep wound healing studies and allows for ample soft tissue coverage following a lower limb amputation [82-84]. Sullivan et al. compared the translatability of different models in drawing conclusions about human clinical wound healing [80]. They found that porcine, small animal, and *in vitro* models are in agreement 78%, 53% and 57% of the time. Therefore, a porcine model appears to be the best tool for studying the wound healing of the transcutaneous OI

prosthesis. The work being presented is the first known *in vivo* large animal model physiologically similar to the human condition in which an axially-loaded, weight-bearing implant is currently being used. It was hypothesized that the pig will be capable of ambulation with a prosthetic leg within one week of surgery. Further, the pigs would achieve 80% pre-operative weight-bearing on the operative limb by the end of the study.

2.2 Specific Aim #2: Infection

Specific Aim #2 assessed the presence of superficial and deep tissue infection surrounding a smooth transcutaneous implant. While superficial skin swabs can be obtained from human amputees, deep tissue evaluation is unfeasible in a human clinical study. The porcine model allowed for superficial bacterial swabs to be collected throughout the study and deep tissue samples to be collected at necropsy. Topical antibiotics were used throughout the study but oral antibiotics were only to be given after an infection was suspected. It was hypothesized that neither pig would develop an infection by the end of the study.

2.3 Specific Aim #3: Wound Healing

Specific Aim #3 evaluated the wound healing around a transcutaneous implant by assessing adherence of skin to implant, extent of epidermal down growth, and the types of cells present at the bone-skin-implant interface. Previous animal studies have assessed wound healing using similar measures but never on a pig model. It was hypothesized that the skin would not adhere to the smooth transcutaneous portion of the implant and that there would be a fully developed epidermal layer by the end of the study.

Chapter 3: Materials and Methods

3.1 Specific Aim #1: Pig Model

3.1.1 Animal Study Design

Primary considerations when selecting the breed for the porcine model were availability, gender, age, weight, soft tissue coverage, and amount of hair on the skin. Male, nine months old, 80 pound Yucatan pigs were selected. Males were chosen to keep urine away from future wound wrapping sites. Animals needed to be at least nine months of age at the time of the surgery as this is when they are considered to be nearing skeletal maturity. This was important so as to limit growth-related cortical bone remodeling that could disrupt the integrity of the bone at the bone-implant interface. Eighty pounds was considered a manageable weight for handling. The Yucatan species also offered a minimal hair coating and substantial soft tissue coverage around the hind tibia that was comparable to the human amputee.

Regulatory compliance, risk, and cost were the primary considerations for selecting the number of animals for the initial pilot study. Two animals were selected. The United States Department of Agriculture (USDA) and the Institutional Animal Care and Use Committee (IACUC) govern animal care policies. Regulatory standards advise that pigs be dual-housed, meaning that the animals had to be kept in the same room at the same time. IACUC regulations required a week long acclimation period for the animals. The surgery on the first animal was performed at the end of this initial acclimation period. The animal's recovery was closely monitored for three weeks as detailed in section 3.1.4 'Post-operative Recovery.' At post-operative day 21 for the first animal, the surgery was performed on the second animal. The study continued for 35 additional days. The animals were sacrificed on the same day which corresponded to post-operative day 56 and day 35, respectively. These time points were chosen to give insight into wound healing and infection over the course of the healing process.

3.1.2 Endo-prosthesis Design Process

The endo-prosthesis (i.e., implant) is defined as the portion of the prosthetic which is permanently attached to the host body. The endo-prosthesis design process was iterative as there has been no previous successful transcutaneous OI implant design for a porcine model. Implants were designed with four primary considerations: 1) bone fixation, 2) shape, 3) ease of implantation, and 4) transcutaneous design. The implant used in this study was designed

specifically for use in a 56 day porcine model. The final design is not meant to be directly applied or translated to a human model at this time.

Immediate bone-implant fixation upon implantation was an important requirement because the pig would be trying to ambulate within minutes of waking up from surgical anesthesia. Threaded, porous bone ingrowth surface, and press fit were all considered as methods of mechanical fixation. Because the animal model required a single surgery, there would not be an unloaded healing period, and therefore porous bone ingrowth could not be effectively used as the method of bone-implant fixation. The Yucatan pigs had thick cortical bone in the distal tibia. To leverage this anatomical feature, threading was chosen over a press fit design.

The shape of the implant determined how loads were distributed from the implant to the bone. Cylindrical, conical, and curved shapes were all considered as potential designs. A curved shape could ensure bone-implant contact with less bone removal. However, a non-symmetric design would greatly increase the complexity and cost of the manufacturing process. A conical or tapered implant would allow better distribution of axial loads to the entire bone surface than a cylindrical implant. A taper was successfully applied to the early nylon and aluminum prototypes (Figure 3.1). However, the taper was felt to compromise the effectiveness of the thread engagement. Achieving threads over the full length of the tapered stem would require that the thread depth be at least as large as the taper depth. With a thread depth of only 0.78mm chosen for the implants, any functional taper prohibited full bone-implant engagement at the most proximal threads. A taper was considered again in the design of the implant for pig #2 but dismissed because of its constraint on the ability to put a flat at the proximal end of the implant. As discussed in section 3.1.3 'Final Endo-Prosthesis Design,' the flat increases the rotational stability of the implant. If the flat was included on a tapered implant, the flat would only be able to be as wide as the smallest portion of the taper. The flat provides necessary torsional stability that was considered more important than the conical shape and therefore a cylindrical implant was chosen. Further, the cylindrical shape simplified

the surgical procedure as a custom tapered reamer would have had to be manufactured if the conical shape had been chosen.

An unfluted implant was initially used in the cadaver practice surgeries. However, the torque required to screw in the implant was unachievable by hand. A single full-length flute was incorporated and tested in a subsequent cadaver surgery. The implant performed better at cutting through the bone. Cutting flute surface area was increased by replacing the one 100 percent-length cutting flutes with two 60 percent-length cutting flutes in the implants for pig #1 and pig #2. The flutes were successful in tapping the bone and easing insertion of the implant by hand. As discussed in section 5.5.1 'Future Endo-prosthetic Design,' an alternative cutting flute pattern should be incorporated to increase holding strength.

A porous coating and smooth surface were both considered as the potential surface for the transcutaneous section. As detailed in section 1.3.7 'Relevant Animal Studies,' much of the literature has shown that porous surfaces are advantageous for inducing skin-implant incorporation. However, the smooth transcutaneous surface has been better represented in human clinical trials as approximately 240 out of the 250 European amputees with transcutaneous OI weight-bearing prosthesis have either the OPRA or ILP implants. Despite the success of the human clinical trials, there has been very little translational animal research using a smooth transcutaneous portion. By preventing the skin from incorporating with the implant, it was theorized that the epidermal layer would migrate towards the bone to form a skin-seal at that location. Attempting to create a biological tissue interface with skin and bone is advantageous to the potential interface created with skin and implant. Therefore, the final implant design for the porcine studies used a smooth transcutaneous section of the implant in an attempt to create a relevant animal model for the most common of the European human implants.

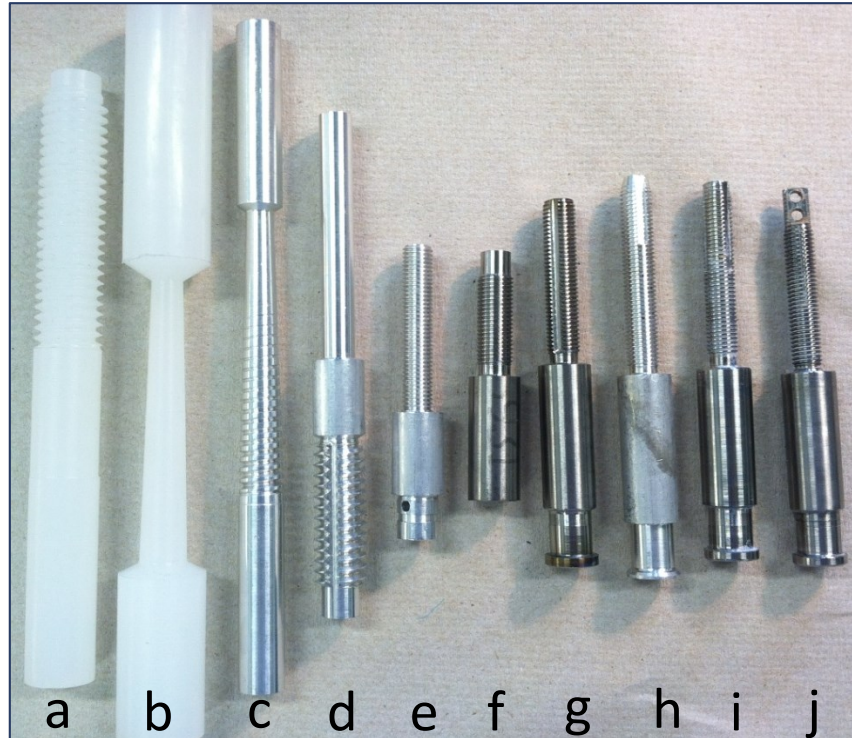


Figure 3.1: Iterative endo-prosthesis design process. a) Practice threading with nylon, b) Practice taper with nylon, c) Practice threading and taper with aluminum, d) Practice coarse thread pitch with aluminum, e) Practice exo-prosthesis attachment site with aluminum, attachment design pictured was not used again, f) Practice machining with titanium, g) Practice full implant with titanium, h) Full-length cutting flute with aluminum, i) Titanium implant used on pig #1 with two half-length cutting flutes on threads, j) Titanium implant used on pig #2 with two half-length cutting flutes on threads and flat with holes at proximal end.

3.1.3 Final Endo-prosthesis Design

The final endo-prosthesis was a one piece construct consisting of a shaft, transcutaneous collar, and exo-prosthetic attachment site. Pre-operative anterior-posterior and medial-lateral tibial radiographs were taken for each animal. Using the radiographs, the surgery was planned. The length of the implant was custom fit for each animal by first determining the amount of distal bone to remove. This equated to approximately 25% of the bone, with the intention of opening up the medullary canal for implant insertion. Shaft length was then determined from the radiograph. The most proximal tip of the shaft was positioned to extend just beyond the medullary canal, distal to the metaphysis. Endo-prostheses shaft diameters

and lengths were custom fit for each animal using their respective periosteal and endosteal diameters. Equation 3.1 was optimized after numerous cadaveric practice implantations.

Equation 3.1: Determining the implant shaft diameter.

$$\text{Implant shaft OD} = [(P-E) \times 0.53] + E$$

where OD = Outside Diameter, P = Periosteal diameter, E = Endosteal diameter

The implant for the first pig was cylindrical, threaded, and self-tapping to provide for secure immediate fixation and ease implantation (Figure 3.2a). A 7/20-20 thread was used for the final implants. The 7/20" nominal diameter was selected based upon the cortical diameter and thickness. The 20 tpi was chosen because finer thread pitches have been shown to increase the bone-implant contact area and primary stability of the implant [85]. An additional flat at the proximal end of the threads was incorporated into the implant for the second pig to resist rotation (Figure 3.2b). Two holes were drilled through the surface of the flat to incorporate bone cement as an additional method of rotational stability. The flats were oriented on the same sides of the implant as the cutting flutes. The transcutaneous collars, which permanently breach the natural skin barrier, were smooth to deter direct skin-implant adhesion. The distal end of the endo-prosthesis was fashioned to allow quick donning and doffing of the exo-prosthesis. A clamp secured the exo-prosthesis to the implant in the axial and radial directions. The implants were custom manufactured by the Orthopedic Research Lab at the University of Kansas Medical Center from a 5/8" diameter round bar of medical grade 5, Ti-6Al-4V alloy. A medical grade titanium alloy was chosen for biocompatibility. A detailed engineering drawing for the modified endo-prosthesis used on the second animal can be found in Appendix 1.



Figure 3.2: a) Endo-prosthesis for pig #1, b) Endo-prosthesis for pig #2. As pictured, the right threaded end of the implant is the side which goes into the bone. The smooth middle section is the transcutaneous piece. The left end with the smaller diameter is the portion onto which the exo-prosthesis is clamped.

3.1.4 Endo-prosthesis Manufacturing Process

The prototypes and final implants were designed so that they could be manufactured in the Orthopedic Research Laboratory at KUMC (Figure 3.3). This was considered necessary to minimize cost and manufacturing turnaround time. The initial prototypes were made from nylon to demonstrate and practice specific features. The material was then changed to aluminum to create functional prototypes for cadaveric surgeries. The final implants were made from titanium so they could be used in the *in-vivo* animal model.

The final implant was made from a 5/8" diameter rod of medical grade 5, Ti-6Al-4V alloy. The bar was cut using a horizontal bandsaw longer than the final implant length so it could be gripped in the vice of the lathe. The implant was placed in the lathe and a center hole was drilled on the proximal end for the lathe center support. Reference lines for the bone, skin, and exo-prosthetic attachment sections were touched off on the implant surface. The different sections were turned down to their respective diameters (Appendix 1). The portion to be threaded was taken to the nominal diameter of the threads. The implant was removed from the lathe and moved to a mill. Cutting flutes were made in the portion to be threaded using an end mill. The implant was moved back to the lathe and the threads were cut into the bone section using a 16ER20UN threading tool. The excess lengths from both ends of the implant were cut off using a bandsaw and the ends were faced off on the lathe. The implant was moved back to the end mill to put the flat and holes on the proximal end of the bone section.

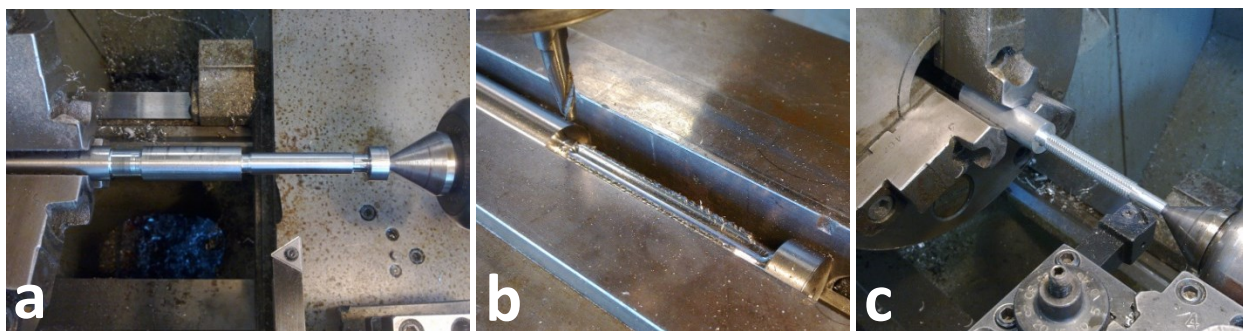


Figure 3.3: Important steps in the manufacturing process of the endo-prosthesis. a) Implant in the lathe after each section has been turned down to the respective outside diameters, b) Implant in the end mill after the cutting flutes have been made, c) Threading the bone section of the implant in the lathe.

3.1.5 Exo-prosthesis Design Process

The exo-prosthesis is defined as the portion of the prosthesis which is not permanently attached to the host body. Exo-prosthesis design was iterative as examples of previous swine prosthetic use were non-existent. Design attempts began by trying to make the exo-prosthesis closely resemble the shape of the natural leg. The amputation procedure included the removal of both the tibiocalcaneous joint and the metatarsal-tarsal joint. These joints are crucial to creating the forward motion of healthy gait. In order to simulate the joints post-amputation using a static prosthetic, it was thought that the foot positioning should remain the same relative to the tibia. To determine maximum strength requirements, a situation in which the animal was standing on its hind legs with half of the body weight transferred through the prosthetic was considered. Therefore, all components of the bracket construct would need to support half of the body weight of an animal weighing approximately 80 pounds. To achieve a factor of safety of 2.0, the construct would need to support 80 lbf or 356N. All prosthetic components and mechanical test fixtures were manufactured in the Orthopedic Research Laboratory.

Adjustability was thought to be essential so that the leg and foot positioning could be adjusted per animal size. This was a difficult task to accomplish because the exo-prostheses were being made before the delivery of the animals. Angles and lengths of the prosthetic components were initially selected based on cadaveric dissections and radiographs so that the

foot would strike the ground at the normal ground contact point relative to the animal's body. The weakest point of the prosthesis construct was assumed to be the hinge as it was the adjustable component. The initial exo-prosthetic bracket design used a two-legged housing that incorporated a set screw

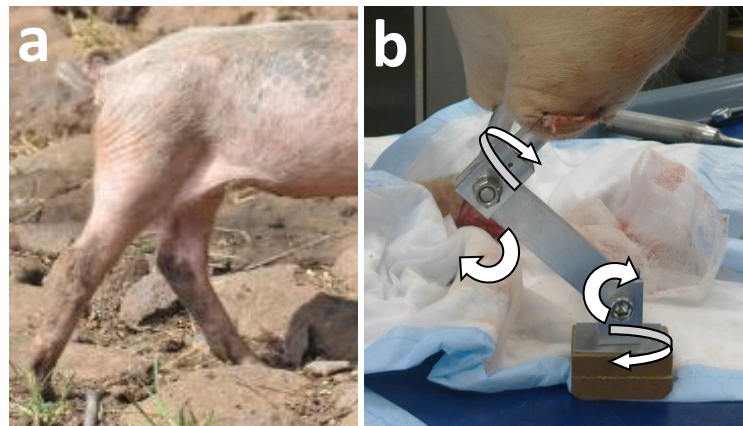


Figure 3.4: a) Healthy porcine stance, b) Initial rigid exo-prosthetic design with adjustable angles (as indicated by arrows) and length (by replacing the metal bar in between the brackets).

attachment to the implant and a hinge joint that connected to the aluminum member that comprised the length of the leg (Figure 3.8a). The joints could be fixed at any angle in two planes by tightening the nuts and set screws (Figure 3.4). The length could be adjusted by exchanging the rectangular bar or 'metatarsal' in between the joints. The prosthetic foot was attached by a second similar bracket. The adjustability in angulation was the design factor that largely drove this initial design.

Mechanical testing was used to determine the strength of the initial exo-prosthetic joint construct. An axial pull test was used to determine the point of failure for the hinge construct (Figure 3.5). The tests were run in displacement control at a rate of 1mm/sec over a distance of 10mm. Data was captured at 100 Hz. The joints were tightened by hand to approximately 80 N-m using a torque wrench. Data is presented as a force versus displacement curve. A reference slope was calculated from the initial linear section of the curve for each trial. The point of failure for the bracket construct was calculated by comparing a moving window of slopes to the reference slope. Failure was defined as a 50% change in slope between the moving window and the reference slope. This method was useful to determine the point at which the static friction of the bracket-member construct was compromised. This was considered the point of failure because if the construct loosened on the animals, they would no longer be able to walk. Every fifth data point was used in the calculations to increase the sample range and decrease the effect of noise. The point of failure was averaged over five trials to determine a mean point of failure for the bracket. Results indicated that the average point of failure for the two-leg hinge construct was 94.0N (Figure 3.6). This was only 26% of the predicted 356N that was required to support half the weight of the animal with a safety factor of 2.0.



Figure 3.5: Mechanical test set-up for the two-leg hinge joint mechanical test. Tests were run in displacement control at a rate of 1mm/sec over a distance of 10mm.

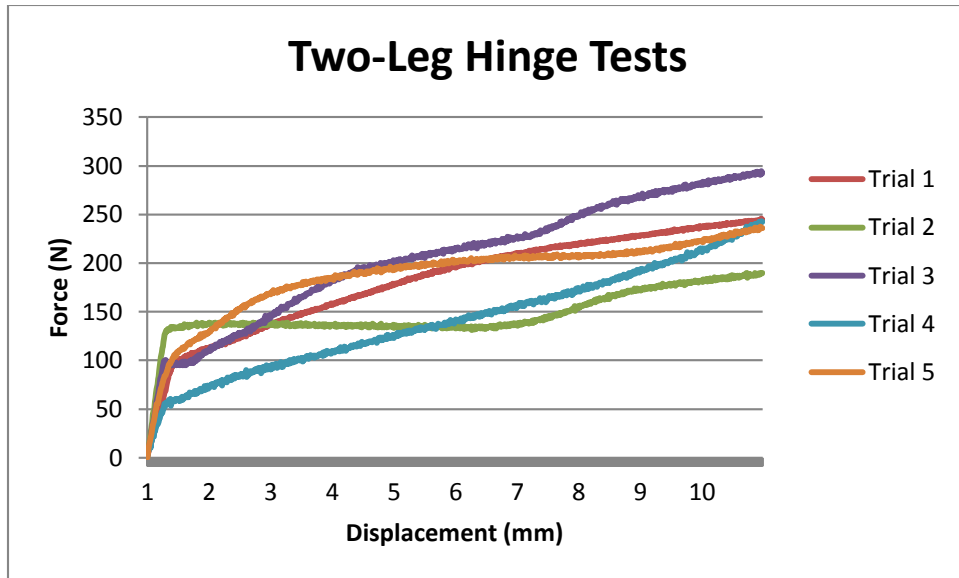


Figure 3.6: Results from the mechanical test for the two-legged bracket. The average point of failure over the five trials was 94.0N.

It was theorized that the two-legs of the housing were hindering the initial static friction effect of the slip washers. Therefore, a leg of the hinge was removed to increase the compressive strength of the slip washer, bolt, and nut combination and thereby increase the point of failure for the prosthetic joint (Figure 3.8b). A one-leg hinge was evaluated with the same axial pull test. The hinges were again tightened prior to testing to approximately 80 N-m using a torque wrench. Results indicated that the average point of failure over the five trials for the one-leg hinge construct was 125N (Figure 3.7). Again this was insufficient as it corresponds to 35% of the predicted 356N that was required to support half the weight of the animal with a safety factor of 2.0.

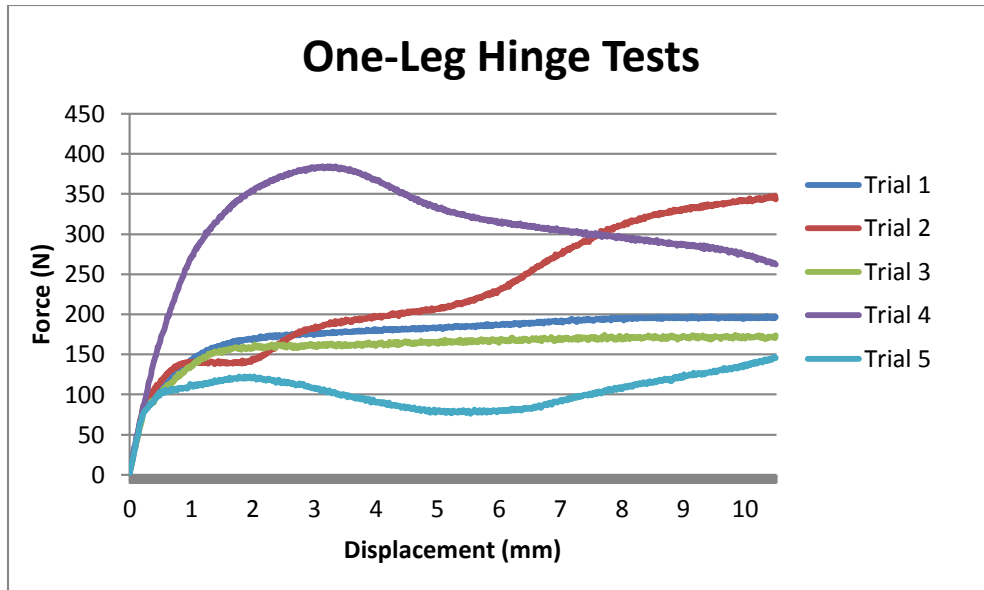


Figure 3.7: Results from the mechanical test for the two-legged bracket. The average point of failure over the five trials was 125N.

Removing a leg of the hinge only slightly increased the force required to overcome the initial static friction of the washer, bolt, and nut construct. The hinge performed better in Trial 4 because the bolt, nut, and slip washers were replaced with new ones before the test. On this trial, the initial slip occurred at about 278N compared to an average of 87N for the other four trials. New hardware was to be used on the final prosthesis but accounting for wear over time in the animal model, this performance could not be relied on and a new bracket design was necessary. At this time, the set screws were also reevaluated because they took too long to tighten and release and required a separate hex key to operate.

The third iteration of the bracket replaced the set screws with a clamp (Figure 3.8c). The clamp was quicker and easier to fix and unfix. Further, it provided much greater initial static friction because of the larger contact area between the bracket and implant. The slot beneath the clamp bolts was used to constrain the implant from pulling out axially. The slot was chamfered so that the implant could be marked and its radial position could be checked at dressing changes. This allowed the observer to check whether the implant was unthreading from the bone or the implant was spinning within the bracket. The adjustable hinge joint in the first designs was replaced with a fixed bolt design. The fixed bolt greatly exceeded the 356N

necessary to achieve the 2.0 factor of safety as it would require the bolt breaking. The holes for the bolts could be drilled at any angle in the bracket but the construct was no longer adjustable after the bracket was manufactured. Limiting adjustability to increase strength was considered a necessary tradeoff. The implant diameter was increased, causing the size of the bracket to be increased (Figure 3.8d). An additional hole was also drilled to enable two attempts at aligning the prosthetic foot. This prosthetic bracket was used as part of the rigid exo-prosthetic on the first animal but the angles were too extreme for correct foot positioning (Figure 3.9a). As a result, the first animal improperly loaded the prosthetic limb, nearly fracturing its operative limb. The bracket was replaced with the one pictured in Figure 3.8e. This bracket used clamps at both the top and bottom. A cylindrical aluminum 'metatarsal' was clamped into the bottom replacing the bolts and imperfect hole alignment.

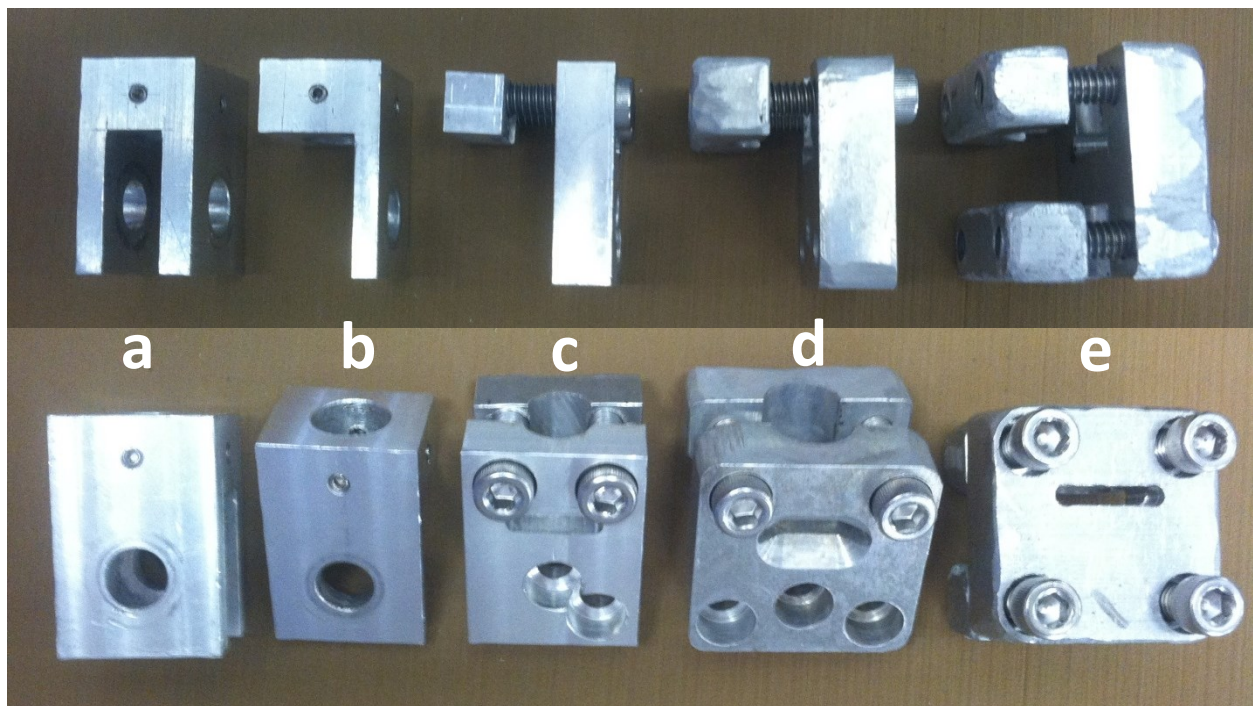


Figure 3.8: Iterations of the bracket for the endo-exo prosthetic attachment: a) Two-leg hinge, b) One-leg hinge, c) Small clamp with fixed bolts, d) Large clamp with fixed bolts, e) Two sided clamp. The large clamp with fixed bolts was attempted but the angles determined to be too extreme. The two sided clamp was used for the first animal throughout the later stages of the *in-vivo* animal model.

The bracket pictured in Figure 3.8e was used in conjunction with a peg after the training prosthesis was removed for the first animal as can be seen in Figure 3.9d/e. The straight peg aligned the prosthetic foot slightly behind the natural foot position for the animal. The bracket was not modified for this animal because it shortened the moment arm that was responsible for the implant unthreading as is discussed in section 4.1.1 'Animal Observation.' The implant was modified for the second animal as described in section 3.1.3 'Final Endo-prosthesis Design' so that unthreading was not a concern. The bracket could then be angled for the second animal so that the alignment of the foot could be corrected. The bracket was also modified to incorporate a threaded insert at the bottom (Figure 3.9d/e). The clamp at the top still allowed radial alignment and the threaded insert allowed connection of a fiberglass all-thread to secure the foot. A nut was tightened to the underside of the bracket to secure the construct.

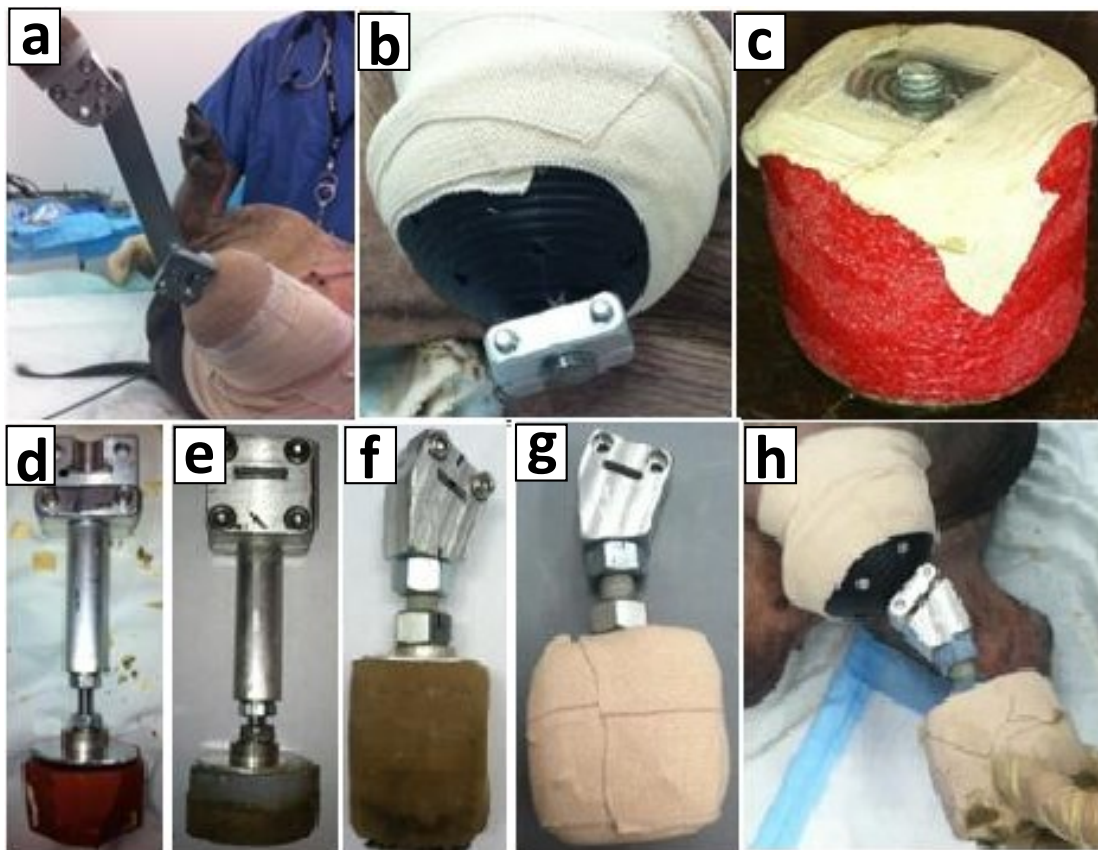


Figure 3.9: Exo-prosthesis design. a) Initial rigid exo-prosthetic, b) Retention cup, c) Foam training prosthesis, d) Peg with silicone foot, e) Peg with polyethylene/foam foot, f) Angled bracket with hard foam foot, g) Exo-prosthetic pictured in 'f' wrapped in medical tape, h) Exo-prosthetic pictured in 'g' on animal #2, also notice retention cup protecting the wound site.

The prosthetic foot was also adjusted throughout the design process to meet the needs of the animals. Immediately after surgery, a rigid exo-prosthesis and foot was attached to the first animal (Figure 3.9a). The prosthesis was quickly determined unsuitable for the animal model and replaced with only a retention cup that was used to protect the wound site. The retention cup was packed with gauze and secured directly to the implant for the initial non-weight bearing healing period (Figure 3.9b). It was made of a hard plastic and perforated to allow the wound to be exposed to air. The top of the retention cup was secured to the residual limb with medical tape and held from below by the exo-prosthetic clamp. The retention cup was cleaned and the gauze replaced at dressing changes. The cup was left to protect the wound on both animals for the entirety of the study. The training prosthetic was attached at day six for the first animal and was not used on the second animal for reasons described in section 4.1.1 'Animal Observation' (Figure 3.9c). The training prosthetic was meant to provide support at the natural leg height while limiting the length of the moment arm to reduce torque on the implant. The foot attached to the peg for the first animal was initially made from silicone (Figure 3.9d). The repeated loading of the prosthetic caused the metal peg to pierce the silicone. The silicone foot was replaced with a composite polyethylene and foam meant to mimic the pliability of a natural foot while withstanding the potential deformation caused by numerous loading cycles (Figure 3.9e). The exo-prosthesis was designed so that the feet could be quickly replaced using a bolt on the underside of the foot that threaded into the prosthetic leg. The second animal used the angled bracket with a foam foot exo-prosthetic (Figure 3.9f/g). The bracket could be clamped to the implant at any rotational angle to align the prosthetic foot with the pig's natural foot-ground contact point. The prosthetic leg was made of aluminum and fiberglass to keep the leg lightweight while maintaining material strength. This was attached at day two for the second animal and used throughout the entirety of the study (Figure 3.9h). After the failure of the initial rigid exo-prosthesis, the overall trends in the remainder of the exo-prosthetic foot design were from larger to smaller contact areas and pliable to stiffer foams. The combination of these variables allowed the leg to adjust to the needs of the animal based on gait observation. The final exo-prosthetic design for both animals simulated the natural foot as much as possible. The exo-prosthesis incorporated interchangeable and

replaceable parts wherever possible to adjust angle and height while easing donning and doffing of the prosthesis.

3.1.6 Surgical Technique

The following describes the surgical procedure for the first pig. IM Ketamine (15-25mg/kg), IM Midazolam (100-500mg/kg), and transdermal Fentanyl (100µg/hr) were administered as pre-anesthetic medications, Bupivacaine (4.4mg/kg) was administered as an epidural, and anesthesia maintained with oxygen and isoflurane (1-2%) by house veterinarians. A complete list of medication used intraoperatively and during recovery can be found in Appendix 2. The pig was placed in dorsal recumbency to enable the surgical approach. A complete listing of surgical supplies can be found in Appendix 3 and detailed surgical protocol can be found in Appendix 4. The left hind limb was prepped using a chlorhexidine surgical scrub and the site was sterilely draped. A longitudinal fish mouth incision was made anteriorly, proximal to the ankle joint. Dissection was performed with electrocautery before and after the bone amputation (Figure 3.10a). Neurovascular bundles were clamped, divided and tied off with 3-0 silk sutures in standard fashion. Dissection was carried down to bone along the medial incision. The bone was cut 3cm proximal to the anterior skin incision. The fibula was cut and rasped proximal to the tibia. The tibia's medullary canal was reamed to 8mm, then 9mm. The implant was partially threaded into the canal to initiate the cutting flutes and then unthreaded. The muscle layer was closed with a 3-0 vicryl suture by pulling the muscles posterior to anterior over the end of the residual tibia and fibula. The skin was then closed with 3-0 nylon. A k-wire was sent through the skin to locate the medullary canal. A custom 2.2mm circular punch was used to pierce through the skin and muscle layer down to the level of the bone. Medium viscosity antibiotic bone cement (DePuy Orthopaedics, Inc., Warsaw, IN) was injected into the medullary canal and the implant threaded in (Figure 3.10b) Hemostasis was maintained throughout the entire procedure. The wound was sterilely dressed and immediate post-operative radiographs were taken to ensure initial fixation of the threads (Figure 3.11b/c). The implant was flush against the tibia's distal end as evidenced by the radiograph. The animal woke from general anesthesia uneventfully.

The same procedure was used for the second pig with three changes. First, the right hind limb was the operative leg as opposed to the left. The leg was changed because post-operative gait analysis from the first pig demonstrated that the implant was likely unthreading as a result of the pig's gait. With right hand threads, each step with the right leg rather than the left would theoretically tighten the screw rather than loosen it. Second, the medullary canal was only reamed to an 8mm diameter on the second pig because a smaller diameter implant was used. Finally, the implant design with the flat on the threads was used as opposed to the symmetric implant. This design feature was meant to engage the bone cement for increased rotational stability. The post-operative radiograph for the second pig showed that the implant was not completely flush against the tibia's distal end. There was soft tissue that was unable to be removed before implant insertion, leaving an approximate gap of 2mm between the implant and bone.

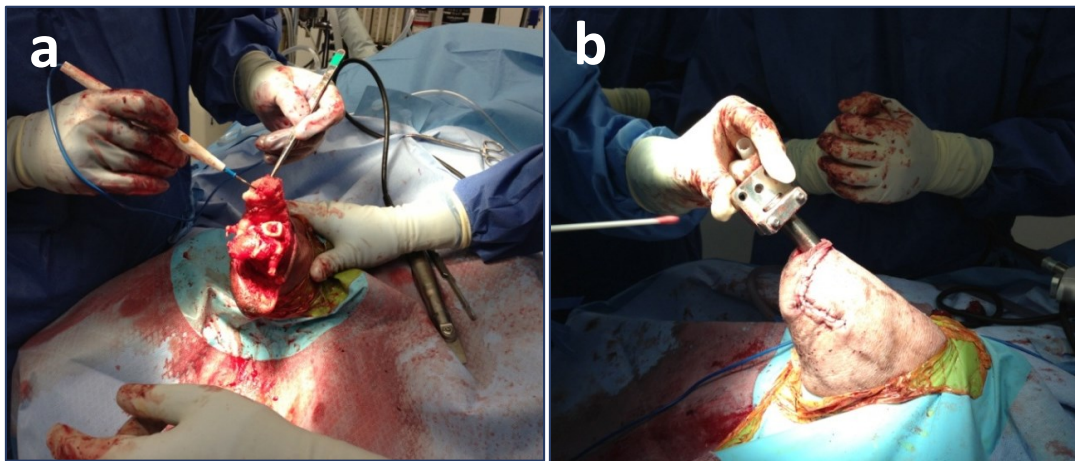


Figure 3.10: Animal surgery. a) Dissection with electrocautery after amputation. The amputated tibia can be seen as the white bone in the middle of the limb, b) Operative leg after skin closure and implant insertion.

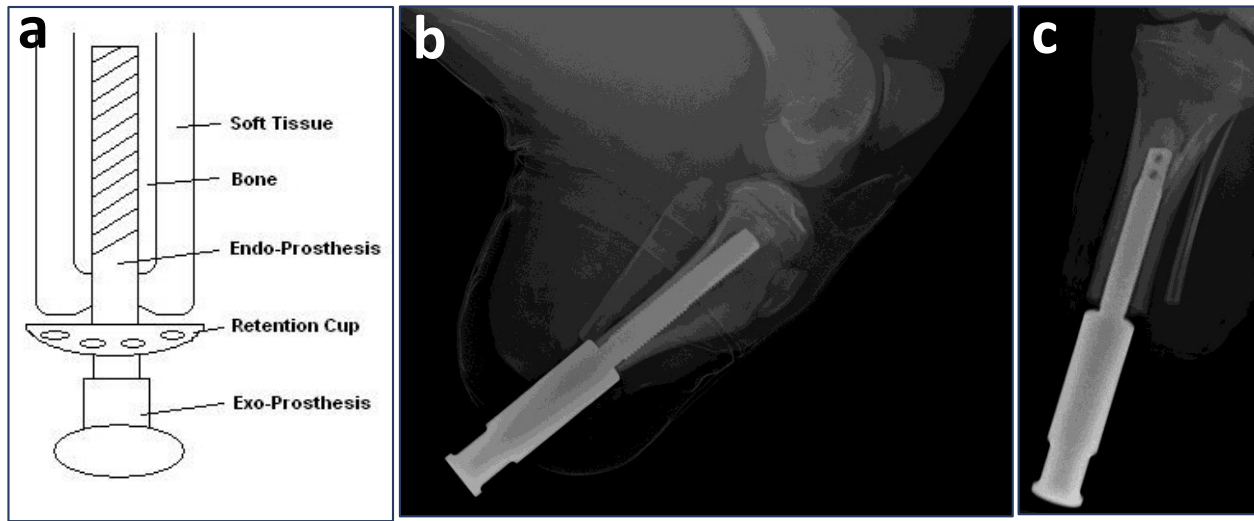


Figure 3.11: a) Post-operative dressing schematic, b) Pig #1 radiograph, c) Pig #2 radiograph. Notice the implant was not completely threaded in on the second animal due to soft-tissue interference while the bone cement dried during surgery.

3.1.7 Post-operative Recovery

The hours immediately following surgery were critical. Each animal was observed for clinical signs of distress including: hyperactivity, restlessness, nervousness, salivation, anxious facial expression, self-mutilation, hypo-activity, listlessness, reluctance to move or get up, altered gait, favored body part, excessive licking, aggressiveness when approached or touched, unprovoked vocalization, vocalization when touched, reduced intake of water and food, and dull, dirty or greasy changes in skin or hair coat. Clinical signs of a pig affected by ulcers include vomiting, rigid stance, melena, a loss of appetite and reduced growth rate.

Pig #1: The stoma was coated with a triple antibiotic and a rigid exo-prosthesis was attached to the distal implant immediately following surgery. As the pig awoke from surgical anesthesia, his weight was supported fully by a panepinto sling (Figure 3.12). The pig appeared agitated by the sling but ate and drank within 90 minutes of surgery. The pig was lowered to allow partial weight-bearing and then the sling was removed to allow full weight-bearing within 2.5 hours of surgery. The pig thrashed upon being initially lowered, resulting in high forces being applied to the long moment arm of the rigid prosthetic leg. The high torques experienced during immediate recovery were cause for concern but precautionary radiographs did not indicate fracture.

The rigid exo-prosthesis was removed and the stump wrapped securely to the animal's midsection using a compression wrap. From day one to three, the pig stayed fairly prone and then gradually transferred to standing and walking on three legs. At day four, the leg was released from the compression sling and a plastic retention cup fashioned in the Orthopedic Research Lab was packed with gauze and secured to the endo-prosthesis. It was thought that the animal would continue ambulation on three legs, but instead the pig immediately altered its gait so it could load the limb via the short exposure of the implant. The training prosthesis was then fashioned in the Orthopedic Research Lab and attached at day six restoring full length to the limb. As time progressed, the shape and material of the prosthetic was adapted due to changes in the behavior of the animal. The final design of the prosthetic is detailed in section 3.1.2 'Endo- and Exo-prosthesis Design'.

Pig #2: The stoma was coated with a triple antibiotic immediately following surgery. The operative leg was immediately wrapped in roll gauze for padding. As the pig awoke from surgical anesthesia, his weight was supported fully by a panepinto sling (Figure 3.12). The pig was lowered to allow partial weight-bearing and then the sling was removed to allow full weight-bearing within three hours of surgery. As the pig became more active, the bandaging fell off, compromising the sterility of the wound site. The wound was cleaned, layered with gauze pads, and secured with the placement of the retention cup seven hours after the initial surgery. The top of the retention cup was taped around the residual limb. The retention cup was held on axially by a clamp. The pig began loading the bone immediately, using the implant as a prosthesis. On day two, the final full-length exo-prosthesis was attached. Exo-prosthetic attachment occurred four days earlier than with the first animal because adjustments were made to the exo-prosthetic design. The training prosthesis was the first design attached instead of an unsuitable rigid exo-prosthesis as was the case with the first animal.

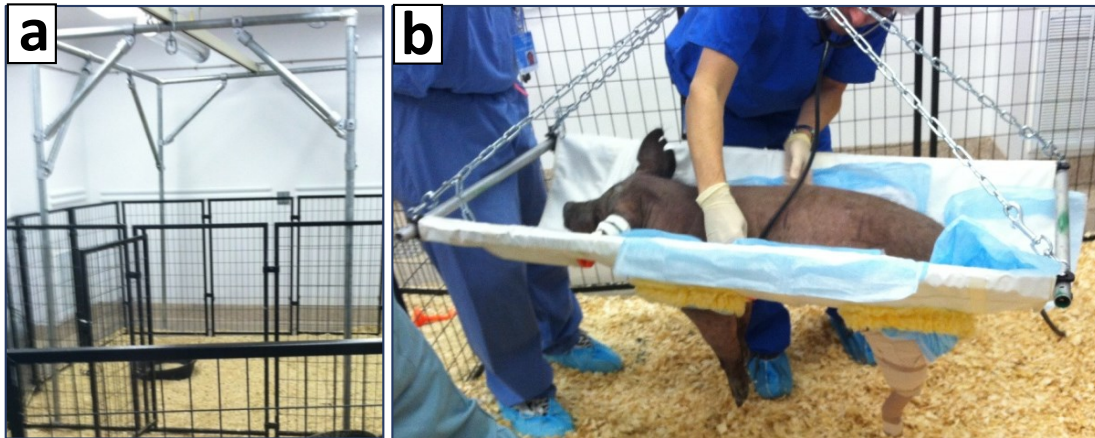


Figure 3.12: Post-operative recovery. a) Recovery cage setup, b) Panepinto sling with pig #1 immediately post-surgery. Pictured with rigid exo-prosthesis attached to the operative left hind limb. This was just before the pig thrashed, causing the rigid prosthesis to be removed. It was replaced with the retention cup and then the training prosthetic and eventually the full length peg as discussed in section 3.1.4.

3.1.8 Post-operative Care

Both animals were monitored daily. The stoma was coated with a triple antibiotic immediately following surgery. Every second day after surgery, the pigs were anesthetized using oxygen and isoflurine (2.0-2.5%) to allow for each dressing change. Daily dressing changes were not done because daily anesthesia would have been too much for the animal. At dressing changes, the superficial transcutaneous skin-implant interface was unwrapped, swabbed, cleaned with 1.5% hydrogen peroxide and saline, coated with triple antibiotic, rewrapped, and secured with the retention cup (Appendix 5). A hydrogen peroxide solution was used to decrease bacterial count and rid the wound of inhibitive agents such as dried blood. Infection was presumed to be the potential primary failure mechanism. Therefore, the intent was to keep the wound as clean as possible and thus minimize bacterial count [86]. It is to be noted that the 1.5% hydrogen peroxide solution killed both normal flora and pathogens without discrimination. This solution was replaced with a soap and water solution at 44 and 26 days, respectively. Skin sutures were removed on both animals at 14 days post-surgery. Pigs were sacrificed at 56 and 35 days after surgery, respectively. As explained in section 3.1.1 'Animal

Study Design,' the difference in sacrifice times was necessary to comply with IACUC regulations regarding the housing of multiple pigs.

3.1.9 Force Plate Data Collection

Force plate data collection and data analysis was primarily designed and executed by another student in the KUMC Orthopedic Research Laboratory. A 12' x 3' platform was built around a force plate (Bertec Corporation, Columbus, OH). The animals were guided on a leash at a steady walking state over the platform (Appendix 6). The force in the z direction was recorded on all trials in which the operative limb struck the force plate. The maximum force in the z direction was averaged across trials for each day and data analysis was reported as a percentage of animal body weight. This data is included in this thesis only to demonstrate that the animals were loading the operative limb throughout the study.

3.2 Specific Aim #2: Infection

3.2.1 Microbiological Evaluation

Bacterial swabs were taken prior to surgery to record baseline microbial flora on the lower limb. Swabs of the surgical incision site were taken every 48 hours until the incision healed at eight days post-surgery. Swabs of the transcutaneous skin-implant interface were taken every 48 hours for two weeks post-operation, and then every 72-96 hours for the remainder of the study. Swabs were preserved in Amies Transport medium and sent to St. Luke's Microbiology Laboratory (Kansas City, MO) for evaluation within 72 hours of collection. The swabs were only cultured to detect the presence of bacteria, unless *Pseudomonas aeruginosa* or *Staphylococcus aureus* were isolated in which case a sensitivity analysis was also done.

3.2.2 Soft Tissue Biopsy Evaluation

Soft tissue samples from the operative limb were collected at the bone-skin-implant interface just proximal to the transcutaneous site at necropsy. Samples were preserved in saline and sent to St. Luke's Microbiology Laboratory (Kansas City, MO) to assess the presence of a deep tissue infection.

3.3 Specific Aim #3: Wound Healing

3.3.1 Gross Observation

The wound site was visualized at each dressing change. Clinical signs of infection include smell, excessive and unusual discharge, inflammation at the surgical site, and increased temperature. Upon removal, gauze pad exudate was assessed with the assistance of the veterinary staff to determine whether it was excessive or unusual. Palpation allowed an assessment of inflammation. A thermometer allowed an assessment of body temperature and was taken daily if an infection was suspected. Pictures were taken every 48-96 hours to document the wound site.

3.3.2 Histological Evaluation

At necropsy, the operative hind limbs were harvested for fixation and further histological tissue evaluation (Appendix 7). The implant was unthreaded and removed. Tissue adhesion was evaluated during implant removal. The tissues of interest were fixed in 10% buffered formalin, processed and infiltrated with an automatic tissue processor in a routine manner (Tissue Tek VIP 2000, Sakura, Torrance, CA) and embedded in paraffin (Appendix 8). Specimens containing bone were decalcified with RBD decalcifying solution (American Master Tech Scientific, Lodi, CA). Tissue was sectioned to a thickness of 5 microns using a microtome (Shandon Finesse ME+, Thermo Fischer Scientific, Waltham, MA). Slices were stained with Hematoxylin and Eosin (H&E) and examined microscopically (Appendix 9). Histologic evaluation allowed assessment of epithelial migration patterns and evaluation of soft tissue-implant adherence.

Chapter 4: Results

4.1 Specific Aim #1: Pig Model

4.1.1 *Animal Observation*

Both pigs ambulated on three legs without substantial complications during the time their operative leg was wrapped in a compression sling. In both cases, the pigs immediately loaded a prosthetic when it was attached and quickly readjusted to a four limb ambulation pattern. By post-surgery day six and three respectively, both pigs were loading the operative limb while standing and walking with a minor limp. The first animal thrashed with the rigid prosthesis when the sling was initially lowered. After that rigid prosthesis was detached, none of the other clinical signs of distress were observed for either pig. The animals continued to load the transcutaneous OI prostheses throughout the entirety of the 56 and 35 day study, respectively (Figure 4.1). Detailed gait monitoring of both pigs can be found in Appendix 10.

Pig #1: The training prosthetic was attached at day six. The training prosthetic was replaced with a full length prosthetic at day eight. The pig demonstrated healthy ambulation patterns from day six to day 23. The implant was first noticed unthreading from the bone at day 21. The bone cement was compromised but the implant showed no degree of toggle and could not be threaded or unthreaded by hand. The implant unthreaded approximately one eighth turn, or 1/160 of an inch in the axial direction every day. At day 23, the animal began stretching the operative leg backwards on occasional steps. A gait study at day 29 suggested the pig was loading the operative leg at 46% of its total body weight (BW). At day 32, the angled bracket was replaced on the exo-prosthesis with a straight bracket. The change was meant to decrease the length of the moment arm and therefore limit the available torque to loosen the implant. This was successful as the pig seemed to load the peg normally and the endo-prosthesis stopped unthreading. A gait study at day 43 suggested the pig was loading the operative leg at 41% BW. A final gait study at day 55 suggested the pig was loading the operative leg at 39% BW. The slight decrease in weight-bearing was assumed to be due to the unthreading of the implant from the bone. The pig's weight fluctuated between 79 and 93 pounds over the duration of the study.

Pig #2: The pig demonstrated comfortable three-legged walking patterns from day one to day two. Occasionally the pig would alter its gait to load the implant, using the implant as a

very short prosthetic. The training prosthetic was deemed unnecessary because the pig was loading the implant at day one. A full length prosthetic was attached at day two. The pig gradually decreased its weight-bearing on the operative limb until the study's end at day 35. A gait study at day 13 suggested the pig was loading the operative limb at 48% of its total body weight. At day 14, the animal began stretching the operative leg backwards on occasional steps similar to the stretching movement described in pig #1. A gait study at day 34 suggested the pig was loading the operative leg at 42% BW. The implant for pig #2 demonstrated secure bone fixation without toggle or loosening throughout the entirety of the study. The slight decrease in weight-bearing followed the pattern seen in the first animal but the reason for the decrease is unexplained by the theory used in the first animal as the implant-bone interface was fixed throughout the study in the second animal. The pig's weight fluctuated between 79 and 87 pounds over the duration of the study. The percentage animal weight-bearing is summarized for both animals in Table 4.1.

Table 4.1: Percentage animal weight-bearing (%BW). The maximum Fz component of the pig gait was averaged over all successful trials. The percentage of body weight that the pig loads the operative limb is reported as percentage weight bearing. Notice pre-operative levels were below 100% as this is not reported as a percentage of pre-operative weight-bearing.

	Pre-op	Day 13	Day 29	Day 34	Day 43	Day 55
Pig #1	66%		46%		41%	39%
Pig #2	71%	48%		42%		

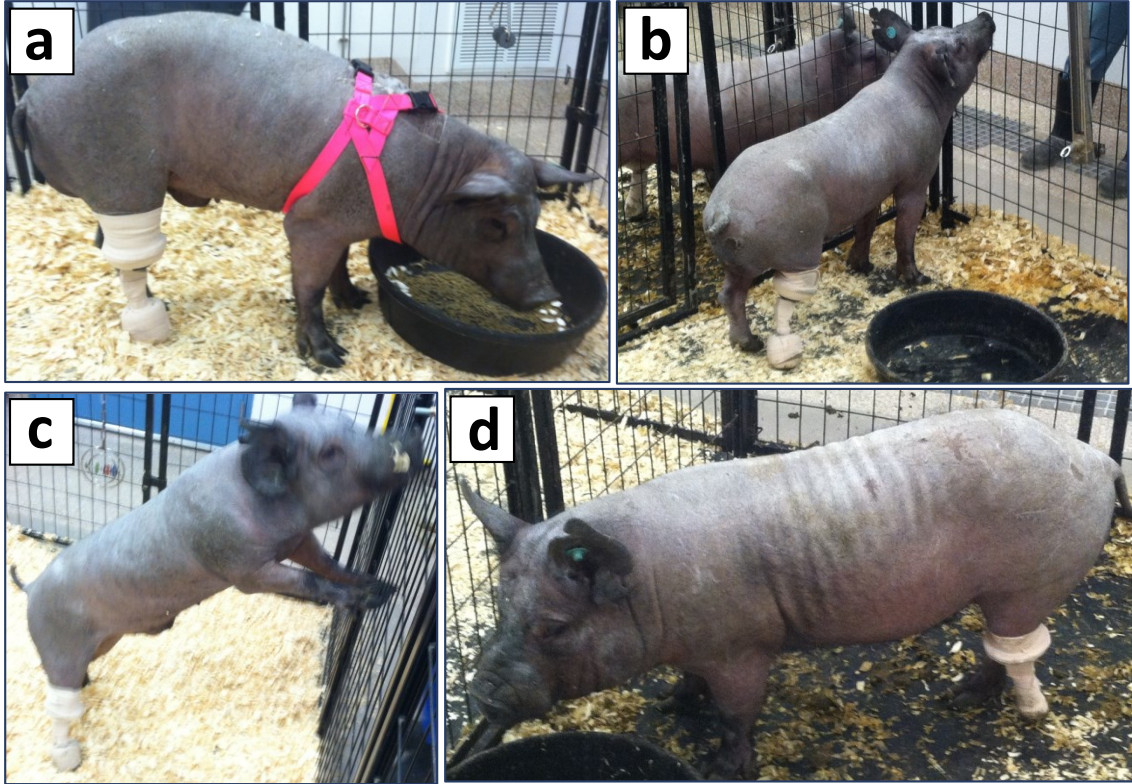


Figure 4.1: Porcine model. a) Pig #2 with a transcutaneous OI prosthesis at 2 days post-op, b) Pig #2 at 10 days, c) Pig #2 at 17 days, d) Pig #1 at 47 days.

4.1.2 Assessment of Hypothesis

It was hypothesized that the pig would be capable of ambulation with a prosthetic leg within one week of surgery. The results support this hypothesis as the pigs were walking at day six and two, respectively. It was further hypothesized that the pigs would be ambulating at 80% pre-operative weight-bearing on the operative limb by the 56 day endpoint. The highest percentage weight-bearing observed for pig one was 46% BW at day 29. This corresponds to 70% of the pre-operative weight-bearing. The highest percentage weight-bearing observed for pig two was 48% BW at day 13. This corresponds to 68% of the pre-operative weight-bearing. Thus this hypothesis was not supported by the pilot study's results.

4.2 Specific Aim #2: Infection

4.2.1 Microbiological

The wound sites for both pigs were sterile immediately following surgery as indicated by post-surgical swabs. Swabbing records specified the presence of bacterial types indicative of infection for both pigs over the length of the study (Figure 4.2). *Pseudomonas aeruginosa* and *Staphylococcus aureus* were of particular concern in the porcine model. Positive bacterial cultures do not necessarily indicate infection. Instead, cultured pathogens were coupled with clinical indications of infection to confirm whether an infection was truly present.

Pig #1: Yeast was the only species indicated by the bacterial swabs to be growing superficially around the transcutaneous implant for the first 44 days of wound healing. Superficial *Bacillus* species and *Pseudomonas aeruginosa* species were isolated at day 44 and 49, respectively. Neither of these species colonized successfully as neither were found at the following swabbing. At necropsy, a deep tissue bacterial swab indicated the presence of *Pseudomonas aeruginosa* species.

Pig #2: Yeast and *Enterococcus* species were indicated by superficial bacterial swabs throughout the majority of the study. There was a superficial *Staphylococcus aureus* species isolated at day four. The animal was given 400mg of Simplicef orally for three days. This antibiotic regimen effectively eliminated the *Staphylococcus aureus* species but did not reduce the prevalence of the *Enterococcus* species. Neither superficial *Staphylococcus aureus* nor *Pseudomonas aeruginosa* were isolated after day six. Unlike in pig #1, switching the cleaning solution from hydrogen peroxide to soap and water at day 26 did not cause a resurgence of bacteria cultures. The bacterial swabs taken post-mortem near the bone-implant interface were non-indicative of deep tissue infection.

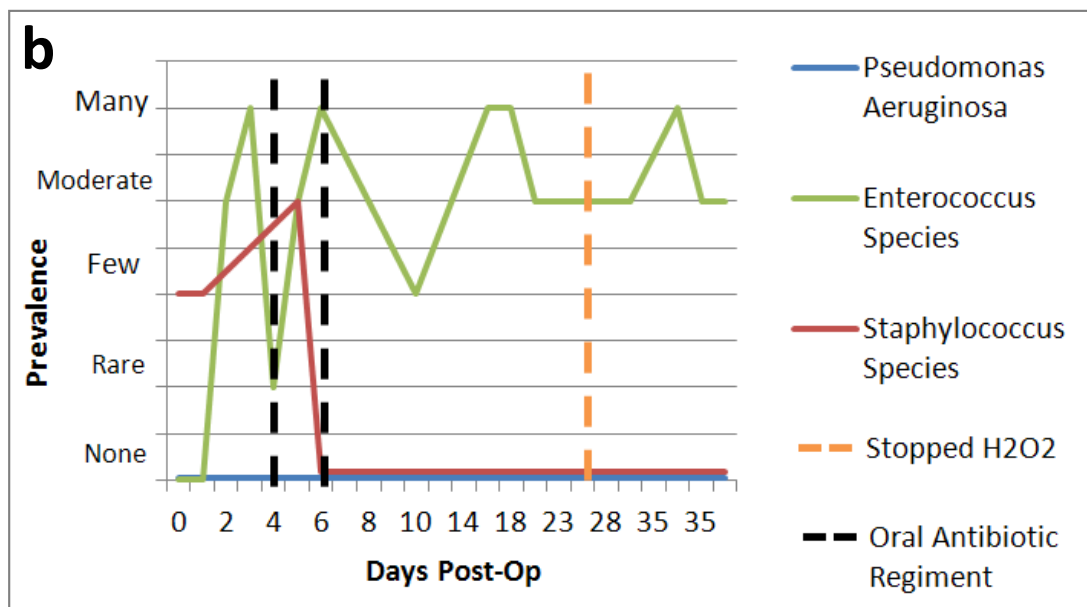
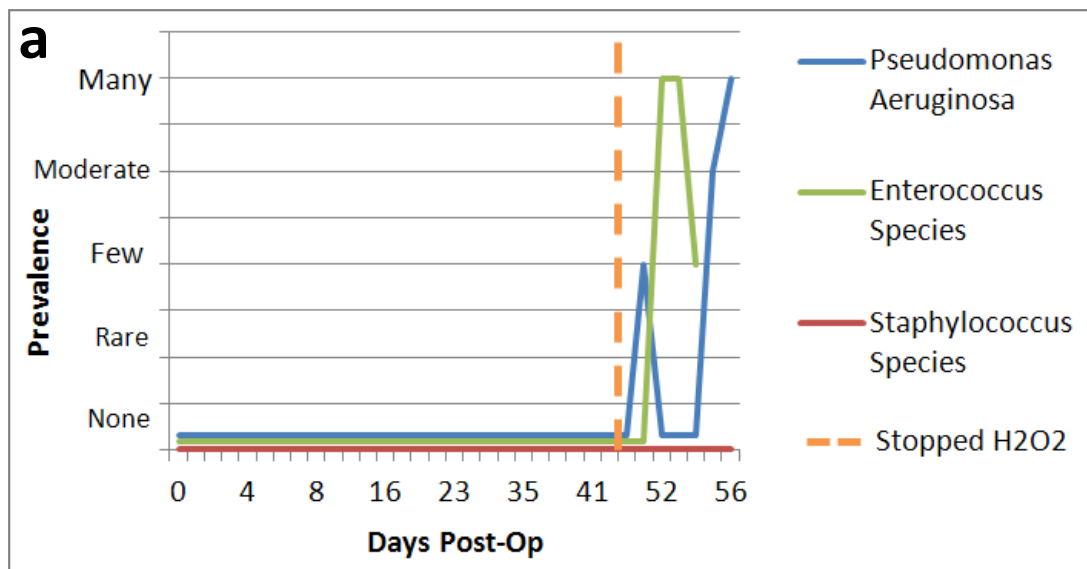


Figure 4.2: Animal bacterial colonies. a) Pig #1 Bacterial Colonies, b) Pig #2 Bacterial Colonies. The *Pseudomonas Aeruginosa* swabbed in the first animal was confirmed with a deep tissue sample.

4.2.2 Soft Tissue Biopsy

The deep *Psuedomonas aeruginosa* species swabbed at necropsy in the first pig was confirmed with an aerobic bacterial culture of a deep soft tissue sample. There was no presence of deep tissue pathogens indicated by the aerobic bacterial culture in the second pig.

4.2.3 Assessment of Hypothesis

It was hypothesized that neither pig would develop infection by the 56 or 35 day endpoints, respectively. A superficial *Pseudomonas aeruginosa* species was found upon swabbing and confirmed at a deep location with a soft tissue biopsy in the first pig. A superficial *Enterococcus* species was found upon swabbing but unconfirmed with a deep soft tissue biopsy in the second animal. There was no clinical suspicion of infection (smell, excessive and unusual discharge, inflammation at the surgical site, or temperature spike) in either pig. As discussed in SA#1, the animals were receptive to palpation of the wound site and no spike in body temperature was noted. As will be discussed in SA#3, there was little inflammation or exudate in either animal. The superficial and deep *Pseudomonas aeruginosa* cultures are evidence of a deep tissue infection in the first animal. The superficial *Enterococcus* culture without clinical signs of infection is not evidence of an infection in the second animal. The hypothesis for SA#2 was unsupported as one of the two animals developed an infection.

4.3 Specific Aim #3: Wound Healing

4.3.1 Gross Observation

The surgical incisions and transcutaneous wounds healed at different rates. The incisions healed quicker, undergoing hemostasis and inflammatory phases that were characterized by clotting, swelling and warmth. The healing of the surgical incisions progressed to the proliferative phase by approximately day three. The tissues surrounding the incisions appeared pink as a result of newly formed capillaries. The surgical incisions granulated, contracted, and epithelialized at approximately two weeks. Scar tissue was observed at the study's endpoint as the incisions were still in the remodeling phase.

The transcutaneous wound healing progressed at a much slower rate (Figure 4.3, 4.4). Over their first respective weeks, no superficial wound healing could be seen in either pig. A pink ring surrounded the metal implants by the end of the second week. This was replaced by a purulent whitish/yellowish formation over the third week. Formation of pink granulation tissue occurred at approximately three weeks and surrounded the implants for the remainder of the study. There was little exudate visualized and little inflammation after the first week.

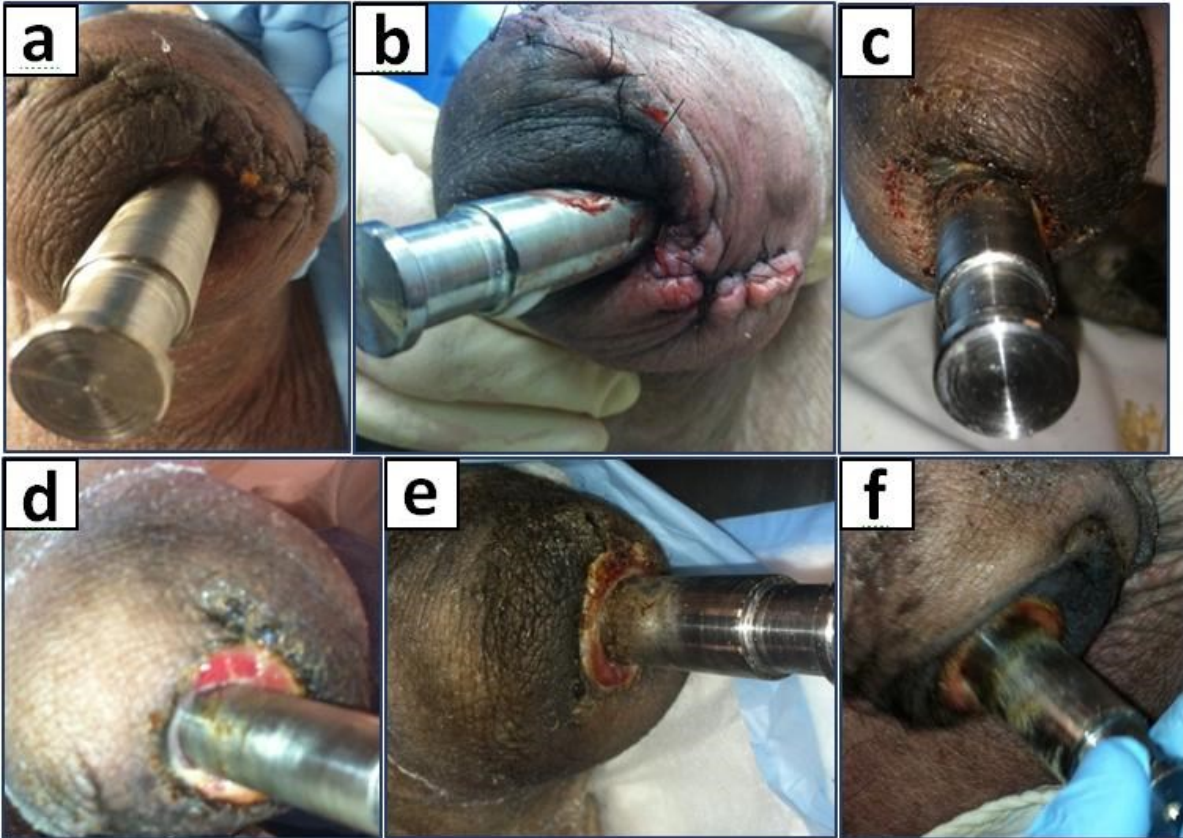


Figure 4.3: Transcutaneous wound healing. a) Post-surgery day two, b) Day 10, c) Day 18, d) Day 28, e) Day 35, f) Day 53. The transcutaneous wound can be seen progressing through the hemostasis phase over the first week which was characterized by the dark tissue surrounding the implant. The inflammatory phase was observed at the third week as seen by the yellowish exudate in 4.3c. The pink tissue observed after week four is evidence of the proliferative phase in which neovascularization develops. The remodeling phase was never reached.



Figure 4.4: Transcutaneous wound site at necropsy after implant removal. Note the progression of wound healing as traveling from healthy skin to bone.

4.3.2 Histological Evaluation

Processed slides were used to assess the extent of epidermal downgrowth, observe the inflammatory cells and neovasculature required for wound healing, and determine the cell types at the bone-skin-implant interface (Figure 4.5).

The mature skin was well defined in both pigs as indicated by the appearance of the epidermal (stratum corneum, stratum lucidum, stratum granulosum, stratum spinosum, stratum basale) and dermal layers when progressing superficial to deep. Epidermal downgrowth was evaluated after the termination of the mature skin layer. There was virtually no epidermal downgrowth observed in either animal. The developing skin trended away from the implant in the first pig but was seen migrating towards the transcutaneous implant in the second pig.

Progressing from deep to superficial at the transcutaneous site, wound healing was characterized by a new formation of scar tissue, granulation tissue, fibrin, basophilic material, and cell debris. Neovasculature was observed throughout the granulation tissue layer just deep to the superficial surface of the transcutaneous wound. Neutrophil granulocytes, which stain a neutral pink with H&E, and basophilic white blood cells, which stain a dark blue, can be seen populating the transcutaneous site as a response to the inflammatory phase of wound healing. There was no histological evidence of a seal at the bone-skin-implant interface in either animal.

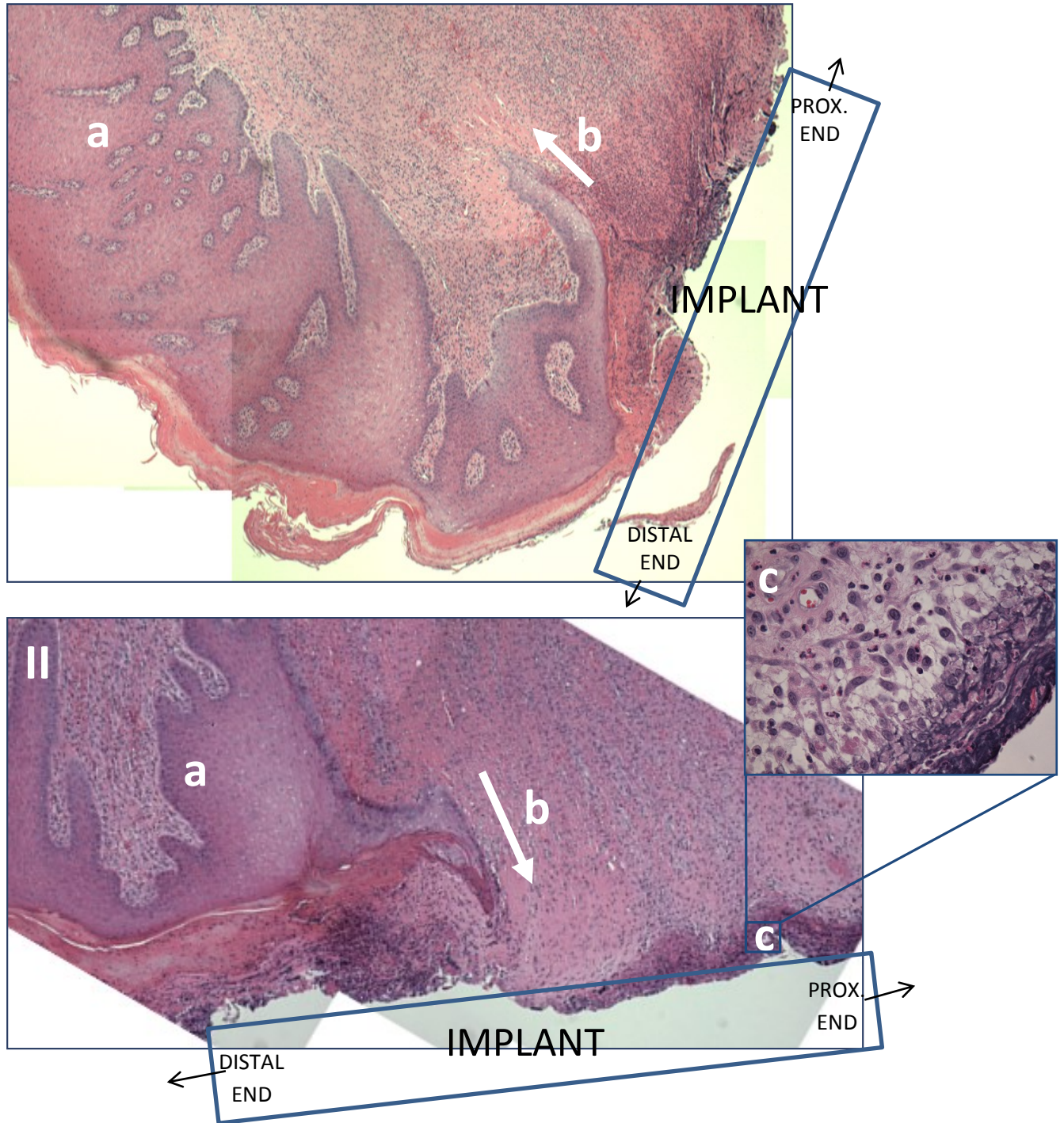


Figure 4.5: Histological evaluation of transcutaneous wound. I) 56 day animal, II) 35 day animal, 4x magnification of transcutaneous section after H&E stain. a) mature epithelial layer, b) developing epithelial layer, c) 40x magnification of transcutaneous site; new formation of scar tissue, granulation tissue, fibrin, basophilic material, and cell debris. Bone is not pictured in either image, but is located further proximally along the implant's surface.

4.3.3 Assessment of Hypothesis

It was hypothesized that the skin would not adhere to the smooth transcutaneous portion of the implant and that there would be a fully developed epidermal layer by the 56 day endpoint. Gross observation indicates that there was no skin-to-implant adherence. This observation was confirmed at necropsy when the implant was unthreaded from the bone. This portion of the initial hypothesis is supported by the results. Histological results indicate that the epidermal layer development was ongoing but incomplete. This portion of the initial hypothesis is not supported by the results.

Chapter 5: Discussion

5.1 Specific Aim #1: Pig Model

Pigs demonstrated incredible agility with an ability to ambulate on three legs for the immediate post-operative period. This was crucial for adjustment to the absence of a hind limb and balance training. Moreover, the implant without an attached exo-prosthesis limited the length of the moment arm during the initial two day recovery. Both pigs were receptive to human interaction and were non-reactive if pressure was applied to their amputated leg. Human-animal interaction was critical, making it possible to evaluate the operative leg on a daily basis. Further, it was observed that the pigs were able to quickly adjust to changes in the exo-prosthetic design. Within minutes of attaching a new prosthesis, the animals adjusted their gait to compensate for exo-prosthesis design variations. In the human model, the recovery steps through a number of prosthetic designs by extending prosthetic length and increasing the percentage weight bearing. The pigs' suppleness made mimicking this staged recovery possible, further depicting the human condition. Overall the pigs seemed to be in very minimal pain considering the invasiveness of the surgery and the pace of the recovery. By the second week, pig #2 was even voluntarily standing up on its hind legs while leaning on the top of the cage with its front legs (Figure 4.1.c). The staged recovery and tissue healing response demonstrated a physiological likeness to the human amputee.

Both pigs started to extend their leg behind them by day 14 and day 23, respectively. It is believed that this was due to the suturing of muscle and other soft tissues during surgery. The muscle layers may have retracted during the first couple weeks of recovery causing the leg extension. Attempts to retain even more soft tissue will be made in future animal surgeries to improve the overall elasticity of the muscle layers. Such a finding could not be documented in previous weight-bearing animal models because the level of the amputation was too far distal [41, 52, 53]. In those models there was an insufficient amount of soft tissue coverage at the transcutaneous site to fully understand the soft tissue response to a transcutaneous OI prosthetic. At necropsy, calcification of the tendons in the posterior side of the residual stump was also noted. This is a hardening of the tendons thought to occur in areas of reduced blood flow where calcium is wrongly developed by local cells. In humans, resulting impingement can

be a cause of prosthetic pain. Common sites of socket pain due to tendon calcification are the tibial tubercle, frontal tibia, fibular side of the knee, and hamstring tendons [87]. Given the seemingly human physiological soft tissue response of both the muscle retraction and tendon calcification, it is believed the pig model gives a more accurate portrayal of soft tissue healing around weight-bearing, transcutaneous implants than previously reported animal models.

For pig #2, the threaded, flanged implant held securely throughout the five week study and was unscrewed without issue at necropsy. Threading is the same method of bone fixation utilized by the OPRA implant. Porous in-growth implant surfaces have also demonstrated successful fixation. This is the method of fixation for the ILP and ITAP transcutaneous implants as well as typical hip and knee replacement stems. Ease of implant removal will be a critical and necessary feature of transcutaneous OI implants developed for human clinical trials in the USA in case of infection.

5.2 Specific Aim #2: Infection

The hydrogen peroxide solution was effective at keeping the wounds clean as demonstrated by the lack of bacterial cultivation for the first 44 days in the first pig. There was concern that it may be hindering colonization of normal flora as well, thus inhibiting the wound healing process. As such, the wound cleaning solution was switched to a 50% mild detergent soap for the remainder of the study. In the first pig, this may have caused an onset of superficial *Pseudomonas aeruginosa* species and *Enterococcus* species by failing to cleanse the wound of debilitating pathogens.

The day two spike in *Staphylococcus* species and *Enterococcus* species for the second pig was likely due to contamination. During the first post-operative night, the sling bandage had fallen off and been removed by the animal. The open wound was exposed to a contaminated pen environment. The wound was cleaned and rewrapped within hours of this happening, but non-sterile wood shavings had already infiltrated the wound site. The antibiotic effectively eliminated the *Staphylococcus* species bacterium over the three day regiment, but did not kill the *Enterococcus* species. The wound remained wrapped between cleanings for the remainder of the study. Neither superficial *Staphylococcus aureus* nor *Pseudomonas aeruginosa* were

isolated again, but the *Enterococcus* species colonized superficially at moderate levels. Unlike in the first pig, switching the cleaning solution from hydrogen peroxide to soap and water did not cause a resurgence of pathogens. This is a promising result for human users who generally prefer a milder cleaning solution.

The most common bacteria found in the pig model were *Enterococcus* species, *Staphylococcus* species, and *pseudomonas aeruginosa* species. This is consistent with human studies which have shown the most common bacteria found in the superficial and deep cultures around transcutaneous wound sites to be *Staphylococcus aureus* and coagulase-negative *staphylococci* [27].

5.3 Specific Aim #3: Wound Healing

Based on gross observation, the wound appeared to be healing over the course of the study. Although prolonged by the non-physiologic nature of the transcutaneous implant, the wound progressed through the four stages of traditional healing: hemostasis, inflammation, proliferation, and remodeling. The hemostasis phase is characterized by vasoconstriction and platelet aggregation leading to clot formation. Occurring immediately after surgery, this physiological process was evidenced by gross observation of dark tissue surrounding the implant. The inflammatory phase is characterized by the release of mediators, recruitment of cells, and leukocyte infiltration. Over the first weeks, the yellowish exudate observed at this time was perceived to be a byproduct of this response. The proliferative phase results in fibroblast propagation and secretion of type III collagen. The increase in structural tissues allowed for neovascularization and the formation of granulation tissue. For the remainder of the study, this phase was clinically characterized by the pinkish coloration and tissue hypertrophy. The later stages of the proliferative phase were never fully realized. In this stage, the fibroblasts comprising the granulation tissues further differentiate and secrete type I collagen. This process is called epithelialization, resulting in tissue that appears more like normal skin. The remodeling phase follows and is characterized by further cellular differentiation and organization. This process can take up to two years after injury to complete.

A longer study would be required to observe the full spectrum of epithelialization, remodeling and maturation of new skin.

Lacking the clinical observation of new skin maturation, histological techniques were used to assess whether a definitive skin seal existed at the skin-bone-implant interface. While there was no histological evidence of a definitive skin seal in either animal, there was evidence of migration of the epithelial layer towards the transcutaneous site in the second animal. The formation of new skin is a time-dependent phenomena, known to occur at approximately one millimeter per day in a healthy wound [88]. Assuming the skin continued to trend towards the implant, a skin seal may have tried to form. A longer study and more animals would be required to see if the migratory pattern observed in the second pig was naturally occurring. This desired healing response is imperative as transcutaneous implants intended for permanent fixation to a host tissue are entirely dependent on an impermeable junction to the outside environment [89].

Confounding the assessment of the skin seal was the somewhat unsuitable histological preparation and cutting protocol. Embedding in paraffin wax required that the transcutaneous titanium post be first unthreaded from the bone. Although the implant was removed uneventfully, the delicate nature of the tissue-implant interface may have eradicated the existence of a skin seal. Previous studies have embedded the specimen and transcutaneous metal implant in polymethyl methacrylate (PMMA) [41, 90]. Doing so enables the specimen to be sliced with a diamond wire saw and subsequently stained. Such a procedure results in better visualization of transcutaneous wound healing and epithelium-implant interaction. A useful PMMA embedding protocol has been published but was not used for this study because the required equipment was not available [91].

The porcine model of transcutaneous wound healing also sought to assess the modality of skin adhesion. As discussed in Chapter 1.3.4 and 1.3.6, transcutaneous implant design has been altered to encourage a skin seal in both human and animal studies. Bloebaum et al. were effective in preventing superficial and deep infection in 14 out of 14 sheep by using a porous metal transcutaneous collar [90]. Bachus et al. used a rabbit model to show that porous

structures displayed tissue in-growth into the implant while the smooth surfaces induced a thick, organized fibrotic capsule unattached to the implant [67]. While these animal studies indicate successful outcomes for transcutaneous implants using porous metals, it may be biomechanically advantageous to discourage an implant-skin interface. The elastic modulus of skin (along fibers), bone and titanium are approximately <1GPa, 18GPa, 115GPa, respectively [92, 93]. Compatible material properties help to sustain a two material interface, especially in cases of repeated loading such as walking. Inducing skin adherence to a material that has an elastic modulus one order of magnitude larger (e.g. bone) as opposed to two (e.g. titanium) generates a less strained interface at the attachment site.

Computational models, animal studies and human clinical trials have studied altered implant geometries in an attempt to promote an intact skin barrier. Kuiken et al. used a finite element model to verify that a larger surface area for skin adhesion reduces stresses at the skin-implant interface. Results indicated a substantial reduction in stress given a broader bone base. Bloebaum et al. used the POP implant in a sheep model to demonstrate that skin immobilization decreases skin regression around transcutaneous implants [35]. This is the same methodology behind the ITAP implant system which consists of a flanged base to immobilize the skin. While expanding the adhesion area seems to reduce skin regression, there is still the concern of attaching skin to a non-biologic surface. The ITAP system positions the HA-coated flange below the surface epidermal layer. While the flange is perforated to allow biological incorporation, short- and long-term vascularization must be maintained to keep the dermal tissues from retraction and necrosis. A finite element model of a weight-bearing transcutaneous OI prosthesis is being developed at the University of Kansas Medical Center to validate the relationship between soft tissue retention and resultant strain (detailed in Chapter 6, 'Computational Model Development').

An alternative surgical method encourages a seal to form directly to the bone as opposed to the implant. Both the OPRA and ILP implant systems directly attach the skin to the residual bone [27]. These implant systems utilize a smooth transcutaneous collar to ensure that there is no skin-implant incorporation. This smooth transcutaneous surface method has been better represented in human clinical trials as approximately 240 out of the 250 European

amputees with transcutaneous OI weight-bearing prosthesis have either the OPRA or ILP implants. Despite the success of the human clinical trials, there has been very little animal research using a smooth transcutaneous portion. Therefore, a smooth transcutaneous portion of the implant was chosen for the pig model. By preventing the skin from incorporating with the implant, it was theorized that the epidermal layer would grow down and heal at the level of the bone.

As previously discussed, the pig is an appropriate animal model for transcutaneous wound healing. Bloebaum et al. acknowledge that human skin may heal in different migratory patterns from those seen in the sheep model [90]. Therefore, implant design alterations should be investigated in a porcine model which is more physiologically-similar to the human condition. Reiterating the need for an appropriate animal model were contradictory assessments of a nylon velour transcutaneous coating. Hall et al. concluded an effective skin seal for up to 14 months using a goat model while Fernie et al. concluded complete skin retraction at 10 weeks using a pig model [51, 54]. While the pig model was weight-bearing and the goat model non weight-bearing, the animal models both assessed nylon velour transcutaneous materials with completely contradictory outcomes. Before conclusions are translated to human studies, they should first be shown effective in a pig model.

5.4 Statistical Limitations

The author acknowledges that this study only examined the wound healing and infection associated with two animals. No statistically significant data was meant to be derived from this study. Instead, this was a pilot study intended to assess the use of pigs as a model for human transcutaneous wound healing. Techniques for evaluating infection and wound healing were reported for suggested use in future studies.

5.5 Future Directions

5.5.1 Future Endo-prosthesis Design

After completing the two animal pilot study, a modified house of quality was made to aid in future implant design iterations (Appendix 11). The rubric scored immediate fixation, permanent fixation, in-house manufacturability, axial stability, and torsional stability, and skin incorporation as the most important design qualities. The modified house of quality rubric can be used in conjunction with the results from the animal study to design future iterations of the pig endo-prosthetic. The next iteration of implant design must consider the bone-implant interface and the skin-implant interface.

Anterior/posterior (A/P) and medial/lateral (M/L) radiographs were taken post-mortem of the operative leg of both animals (Figure 5.1). The radiographs show evidence of heterotopic ossification (HO) on the posterior shaft of the tibia. HO is the presence of bone in areas where soft tissue normally exists. Traumatic amputation can be the cause of HO in humans. The surgical technique used in this study could have contributed to the HO noted in the pigs.

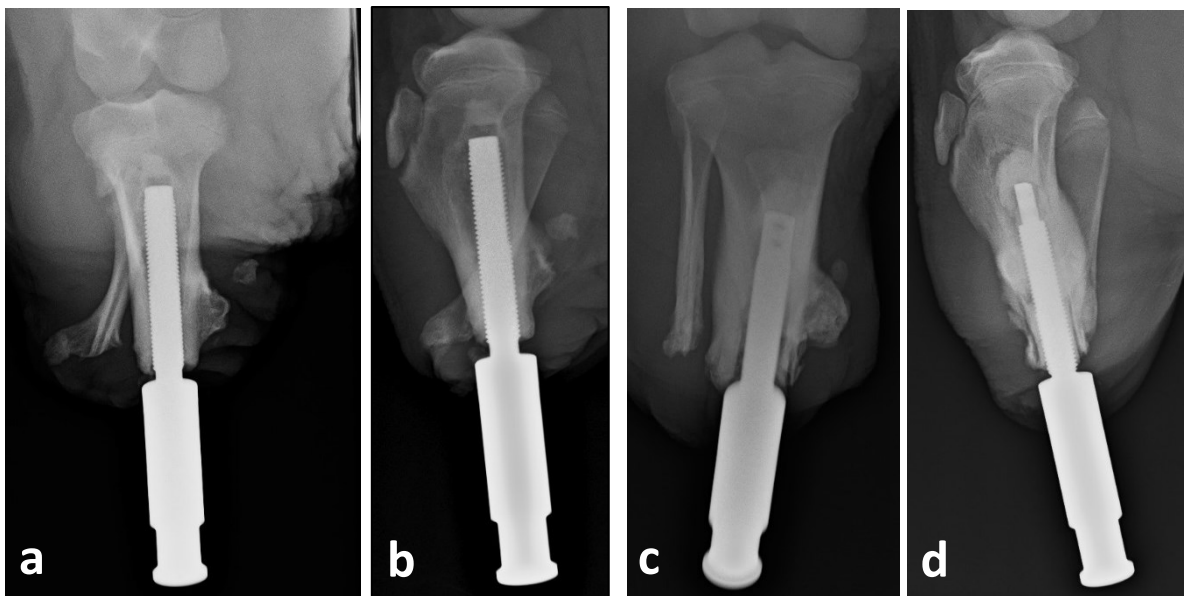


Figure 5.1: Post-mortem radiographs. a) Pig #1 A/P view, b) Pig #1 M/L view, c) Pig #2 A/P view, d) Pig #2 M/L view. Note the HO formation on the posterior shaft of the tibia in both animals. Bone cement can be visualized as the white ball proximal to the implant's tip. The implant unthreaded in the first animal as evidenced by the gap between the bone and implant. The implant in the second animal did not unthread but was not inserted completely during surgery.

In terms of the bone-implant interface, the implant should retain the self-tapping cutting flutes. The fluted implant was advantageous for threading the implant in by hand during the operation. However, the flute layout could be altered. Screws with more than two flutes have been shown to ease insertion and did not cause cortical bone damage [94]. Furthermore, three short cutting flutes have been shown to outperform two long cutting flutes in pull out strength [95]. Therefore a three 50 percent length cutting flute design should be used in an effort to ease insertion while optimizing pull out strength.

Threading the implant allowed for high levels of initial bone-implant stability in the animal model. This result was consistent with other studies which have shown that threaded implants improve initial mechanical interlock with bone more than porous-surfaced implants [96]. However, after approximately six months, a fibrous connective tissue has been previously shown to develop around threaded implants. As a result, the threaded implants lose mechanical fixation. A fibrous capsule was not a factor in these animals due to the brevity of the pilot study. However, if future porcine studies investigate transcaneous OI devices over a longer time period, porous-surfaced implants are known to stabilize with time through bone ingrowth.

Permanent fixation was not achieved in the first animal as the implant began loosening at day 21. The radiographic images from Figure 5.1 have been cropped and enlarged to show the bone-implant interface (Figure 5.2). The threads remained engaged with the bone for the 56 day animal, especially near the distal end of the bone (Figure 5.2a/b). However, the implant loosened due to a lack of torsional stability. The implant remained stable for the second animal throughout the 35 day study. However, the A/P radiograph suggests that the bone surrounding the distal implant resorbed (Figure 5.2c). This was likely the result of stress shielding as is often seen around total hip stems. The denser implant transfers the loads that the bone would normally see, effectively shielding the bone from stresses. According the Wolff's Law, bone material was resorbed by the body due to lack of loading. Over longer periods of time, stress shielding can lead to implant loosening. The M/L radiograph suggests less bone resorption (Figure 5.2d). The threads appear fully engaged along the implant-bone interface. The gap between the distal bone and implant that can be seen on the radiographs was due to the

implant not being fully threaded into the bone during the surgery. Future animal surgeries should ensure that the threads are inserted all the way into the medullary cavity during surgery so it is flush with the distal end of the amputated bone. The soft tissue makes visualization of this challenging so this could be better accomplished with intraoperative fluoroscopy if available. Due to the high importance of immediate fixation according to the modified house of quality, and the thread engagement observed in the post-mortem radiographs, threading remains the best choice for achieving mechanical fixation in the pig model.

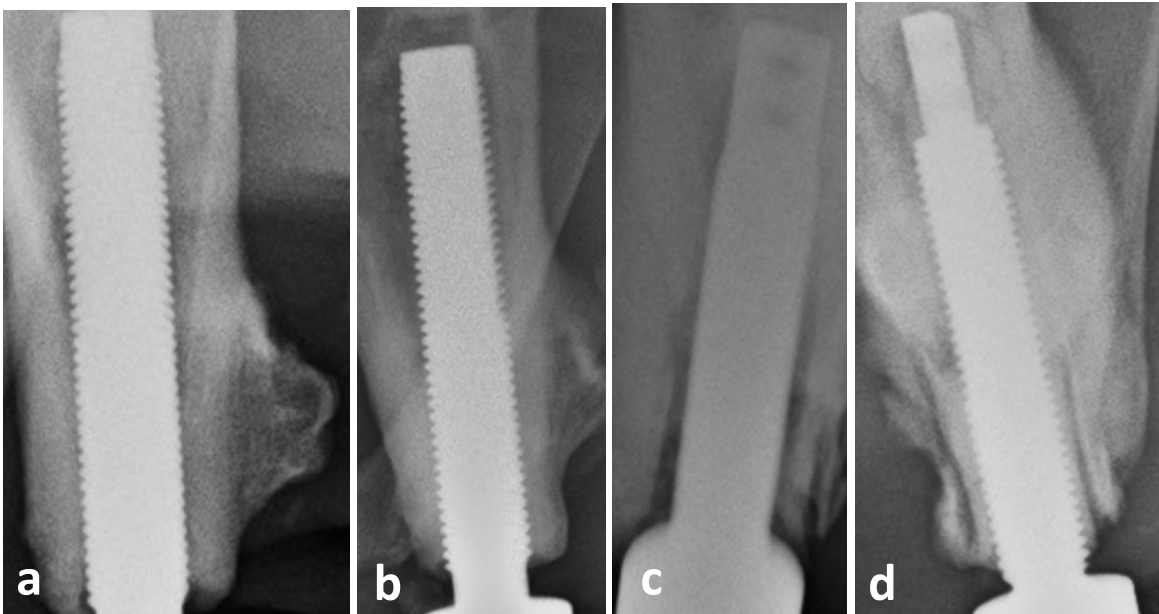


Figure 5.2: Post-Mortem Radiographs, close-up of the bone-implant interface. a) Pig #1 A/P view, b) Pig #1 M/L view, c) Pig #2 A/P view, d) Pig #2 M/L view. Note thread engagement in first animal but lack of bone cement and implant incorporation, resulting in lack of torsional stability. Potential bone resorption around distal threads for the second animal but improved torsional stability due to the bone cement engaging the flat at the proximal implant.

The cylindrical shape of the implant performed suitably as neither bone fractured during surgery or post-operatively. The point of greatest stress in the implant-bone construct was likely the cortical wall just beyond the tip of the implant. Stress risers likely occurred at this point because the load was transferred through the implant up to this point but was then distributed through the bone cement to the tibia. A tapered implant would better transfer loads through the implant to the bone, but the shape of the pig's tibia is not suited for a conical

implant. The cylinder allowed for a greater bone-implant contact area and will therefore be used in future implant iterations.

The implant design could be altered to better incorporate the bone cement. The bone cement appeared to be pushed by the end of the implant and ball up at the proximal diaphysis (Figure 5.1a). Due to the position of the cement and the non-incorporative design of the first implant, the cement used in the first pig was never useful for torsional stability. Similarly, the bone cement can be seen at the proximal diaphysis in the second animal (Figure 5.1d). However, the flat at the proximal end helped incorporate the cement and stabilize the implant. The implant could be further improved by changing the flat or cannulating the implant. First, the holes might be removed from the flat. The holes remove surface area that would otherwise resist implant rotation. Cannulating the implant would allow injection of bone cement after the implant had been inserted. Post-implantation injection would allow better incorporation of the cement so that the ball is not formed and pushed to the end of the cavity. Further, cannulated holes could be included on the sides of the proximal half of the implant so that additional fixation could be achieved where the shape of the bone opens up.

The implants used in the pilot animal study were designed with a smooth transcutaneous section that was meant to discourage skin-implant incorporation. It was hypothesized that epithelial downgrowth would allow for a biologic seal to be established at the skin-bone interface by the study's endpoint. Results from the porcine model indicated that a skin seal was not fully established but that the epithelial layer was migrating towards the transcutaneous surface in the second animal. Future design iterations should investigate incorporating a porous metal coating at the proximal end of the transcutaneous section of the implant. This may allow the skin layer to grow along the implant and provide a scaffold-like environment at the skin-bone-implant interface for tissue incorporation.

5.5.2 Future Exo-prosthesis Design

After completing the pilot study, a modified house of quality was made to aid in future exo-prosthetic design iterations (Appendix 12). The rubric indicated that strength, adjustability, in-house manufacturability, and interchangeability of parts were the most important design

qualities. The final exo-prosthesis for the second animal remained stable over the course of the 35 day study (Figure 5.3a). There was wear on the threading of the fiberglass all-thread, thus it should be replaced with aluminum all thread in future studies. Although this would slightly increase the weight of the prosthetic, the strength has been determined to be more important. The angled clamping bracket used for the second animal allowed the leg to be spun and clamped at any angle. The angle at which the bracket was clamped affected the positioning of the foot for the animal. Overall, the effect on the pig's gait was minimal and the animal continued to load the limb. The final hard foam material choice for the foot was also adequate. From observation, the pliability of the material simulated that of the natural foot. Future studies could continue to use a similar static prosthetic design if a simple manufacturing process is desired. However, to simulate the flexibility and energy storage of a natural ankle, a carbon-fibre-reinforced polymer blade could be used (Figure 5.3b). Although the carbon-fibre blades have demonstrated great success in human application with conventional prosthetic suspension, they have shown mixed results in veterinary applications for use with osseointegrated limbs. In one dog, the carbon-fibre blades caused excessive stress on the distal bone resulting in fracture [41]. Pig gait would need to be further analyzed before this design should be suggested for use with the porcine model.

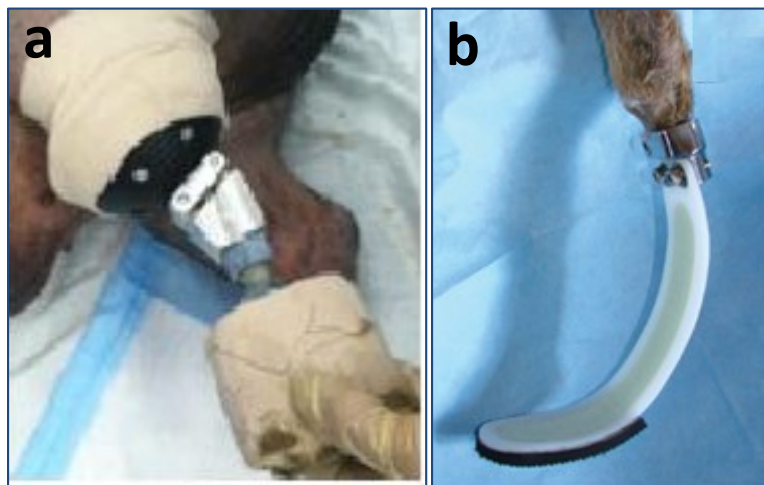


Figure 5.3: a) Final exo-prosthesis used on the second pig, b) Carbon-fibre blade used on transcutaneous osseointegrated canine model. Potential for use of similar blade in porcine model but was shown to cause excessive stress to the distal bone resulting in bone fracture in the canine model. *Image 5.3b reproduced from Fitzpatrick et al. (2010) [41].*

5.5.3 Study Execution

In regards to study execution, there are a few changes that would enable more transparency in the results. First, a more consistent approach should be taken with the wound cleaning solution to standardize the care protocol. It is difficult to draw definitive conclusions from this study regarding infection because the cleaning protocol was changed during the course of the study. Switching the solution from hydrogen peroxide to mild soap water may have affected the colonization of debilitating pathogens such as superficial *Pseudomonas aeruginosa* in the first pig. Because this switch was made on both pigs without a control, pinpointing the cause of the influx in pathogens is difficult. A future study could compare methods of wound care as this is of great importance to the human application. Second, future studies should consider use of the PMMA embedding protocol described by Bloebaum et al [91]. While embedding in paraffin simplified the cutting process, it was difficult to evaluate the bone-skin-implant interface histologically. More convincing histological results of the soft-tissue seal are obtainable if the transcutaneous implant is left undisrupted, embedded in PMMA, and cut with a diamond wire saw. Third, future animal studies should consider additional staining protocols to strengthen interpretation of histological results. A gram stain would enable bacterial species to be identified. This would be advantageous in the assessment of the transcutaneous section where bacterium was likely present. A cytokeratin 5/6 or 34 beta stain would have highlighted cytokeratin which is a molecular feature of epithelial cells. This may be valuable to verify the extent of epidermal downgrowth by staining the epithelial layer. A trichrome stain would stain collagen a blue color, fibron a red, and nuclei a dark brown. This may be useful for demonstrating the presence of certain cells at the transcutaneous section. Finally a CD-31 immunostain was considered to demonstrate endothelial cells that line blood vessels. This would be useful for quantifying neovasculature.

5.5.4 Direction of the Porcine Model

With respect to the future direction of the pig model, studies should consider different methods of decreasing the stress present in the tissues around the transcutaneous portion of the implant via material and surface topography changes to improve the skin-implant seal. It is well understood that lessening interfacial stress minimizes soft tissue breakdown, thus

increasing the likelihood of an intact skin barrier. Results from future animal studies could be coupled with computational models to lead in the development of an infection-free transcutaneous prosthetic option for humans.

Further, this pig model has the potential to become an assessment tool of transcutaneous OI devices for the diabetic population. Surgeons are hesitant to attempt the operation in diabetic amputees because of poor bone quality and vascularization to the extremities. This is a patient population which constitutes 864,000 of the 1.6 million amputees in the USA and is going to continue to grow. Current trends suggest an increasing number of obese Americans [97]. Given the known relationship between obesity and diabetes, the number of people with diabetes is expected to nearly double by the year 2030 [98]. That being said, the number of amputations secondary to dysvascular conditions is predictable. Due to the aging population and increase in number of people living with diabetes, limb loss is expected to more than double by 2050, from 1.6 million to 3.6 million. Diabetes mellitus and dysvascular disease affect the body's vasculature, especially in the extremities. Therefore, in order to study transcutaneous wound healing for the diabetic population, a translatable animal model is necessary. In 2000, Jansen et al. used an alloxan induced diabetic rabbit model to evaluate percutaneous devices [99]. Results indicated that there is a delayed tissue response in diabetic animals. Diabetes impairs the maturity and neovascularization of connective tissue, leading to diminished wound healing and greater rates of infection. In a related study, the group evaluated percutaneous OI devices in diabetic rabbits by comparing associated soft and hard tissue using clinical, histologic, and histomorphometric techniques [100]. In contrast to their previous study, results indicated that diabetes does not have negative effects on the soft tissue surrounding the implants. Further, while they observed lower cortical bone density in experimental animals, there was no indication of implant-bone loosening. A diabetic pig model has been previously developed for wound healing studies with limited success [101]. The model induced the diabetic condition using streptozotocin injections in Yorkshire pigs. Future studies could use a diabetic pig model to evaluate potential weight-bearing transcutaneous OI prosthetic device applications for the diabetic patient population. Findings could be compared to the Jansen rabbit model before human diabetic amputees are deemed unsuitable for the

prosthetic option. Transcutaneous OI devices have the potential to revolutionize the quality of life for these patients if the complications of bone quality and vasculature could be overcome. Diabetics are a patient population that are often times wheelchair bound after amputation because they have even more skin problems associated with their conventional prosthetic suspension.

Transcutaneous wound healing could also be a potential application for Negative Pressure Wound Therapy (NPWT). NPWT has been shown effective in closing wounds, inducing growth of granulation tissue, and increasing blood flow to the wound [102-104]. NPWT may also prove beneficial by ridding the wound site of inflammatory fluids (exudate), pulling the skin in tension, stabilizing the surrounding tissues, and creating an environment that is less ideal for bacterial expansion. Once the transcutaneous prosthetic option is available, NPWT could be coupled to immediately help amputees. The combined techniques would need to be proven safe through animal modeling and could be developed in the pig model.

Chapter 6: Development of a Computational Model

6.1 Introduction

To build upon the results of the animal model, a finite element (FE) model is being developed at the University of Kansas Medical Center. Few previous computational models have attempted to investigate the skin-implant seal, specifically the effects of skin seal disruption induced by prosthetic loading. Yerneni et al. hypothesized that a greater fixation area between the skin and bone at the distal end of the femur would reduce skin-implant stresses [92]. Shear and normal stresses induced by ambulation can create concentrations around the transcutaneous OI implant. Results indicated a 90% decrease in interfacial stress by increasing the distal cortical bone base thickness from two to eight millimeters. The study concluded that lessening the differential movement at the tissue-implant interface minimizes soft tissue breakdown, thus increasing the likelihood of an intact skin barrier. The results reiterate clinical findings that interfacial movement is detrimental to the formation of an effective tissue-implant seal. Implant design and surgical technique can be altered to reduce stresses and subsequent soft tissue breakdown at the transcutaneous site.

The model being developed at the University of Kansas Medical Center aims to investigate the strain in the soft tissue surrounding a transcutaneous OI implant. Strain, as opposed to stress, was measured because avulsion was considered as the primary mechanical failure modality. Avulsion occurs when surrounding soft tissues tear away from a transcutaneous implant due to externally applied mechanical forces. Therefore, a normalized measure of deformation in the surrounding soft tissues is more useful for predicting mechanical failure between the soft tissue and implant than a measure of force per unit area. We hypothesize that retaining a greater amount of soft tissue during surgery to surround the implant will result in a reduced distribution of strain at the transcutaneous interface. The hypothesis is being investigated with the development of a series of three-dimensional FE models of transcutaneous OI implants.

6.2 Methods

Two models were developed that include an implant, a distal femur, a region of subcutaneous soft tissue, and skin. The models were created and analyzed using FEA software

(ABAQUS/CAE 6.11-2 Dassault Systèmes, Waltham, MA). Models varied in the amount of soft tissue that was left at the distal end of the limb to surround the transcutaneous site. Model A represents a case in which minimal soft tissue is retained during surgery while model B represents a case in which a greater amount of soft tissue is retained during surgery. The amount of soft tissue retained affects how the strain was distributed through the model and transmitted to the interface. The geometry of skin-bone attachment also differed between model A and model B. In model A, a perpendicular skin-implant interface is established, meaning that the skin met the implant at a 90 degree angle (Figure 6.1a). In model B, a tangential skin interface is created, meaning that the skin encountered the implant at a 180 degree angle (Figure 6.1b).

Normal and shear loads of 50kPa were applied to an approximately 100 cm² rectangular area at the skin surface located on the posterior side of the limb. These loads were chosen to simulate the loads imposed on the soft tissue by a 75 kg male rising from a chair and applying pressure to the posterior proximal end of the limb. This activity induces stretching of the skin on the operative leg. The entire implant was constrained from translation and rotation using ABAQUS encastre constraints. The model was meshed using hex elements with a global average size of 5.0mm. The hex mesh in the analysis region and surrounding boundary regions was refined to an average size of 1.0mm. Material properties were assigned to each of the four part geometries (Table 6.1).

Table 6.1: Material properties for computational model.

Part	Behavior	Material Property Coefficients
Titanium Implant [105]	Newtonian	E = 115 GPa, ν = 0.3
Femur [105]	Newtonian	E = 18 GPa, ν = 0.3
Muscle [106]	Hyperelastic Mooney-Rivlin	C10 = 30 kPa, C01 = 10 kPa, K = 60 kPa
Skin [107]	Simplified Neo-Hookean	C10 = 1.11 MPa, K = 29.6 MPa

6.3 Preliminary Results

Preliminary results indicate that the amount of soft tissue retained appears to have some effect on the strain distribution around the transcutaneous implant. With the skin attached to both the implant and bone, Model A produced greater strain in the critical skin-bone-implant interface compared to model B (Figure 6.1). Strain values of 21% and 9% were demonstrated at the same relative location in the analysis region for model A and B, respectively. It is well established that micromotion at the transcutaneous site induces tissue avulsion and ultimately soft tissue breakdown. Strain levels of 5-20% have been shown to promote cellular proliferation, but those over 20% may be detrimental to the skin-bone-implant interface [108]. This model suggests that greater tissue retention reduces strain at the skin-bone-implant interface thus increasing the likelihood of maintaining an intact skin barrier.

The models assume a full surface tie attachment between the skin layer and the implant and bone. This may or may not be clinically achievable and should be further investigated. Such investigation could occur with histological analysis in future iterations of the porcine model that has been described in the previous thesis chapters. Future finite element studies will implement dynamic loading conditions, such as impulses from walking and running gait cycles, to better simulate the physiological loadings by amputees. The computational model and porcine model are clinically relevant and will be used in conjunction to optimize weight-bearing transcutaneous OI prosthetic implant design and associated surgical techniques.

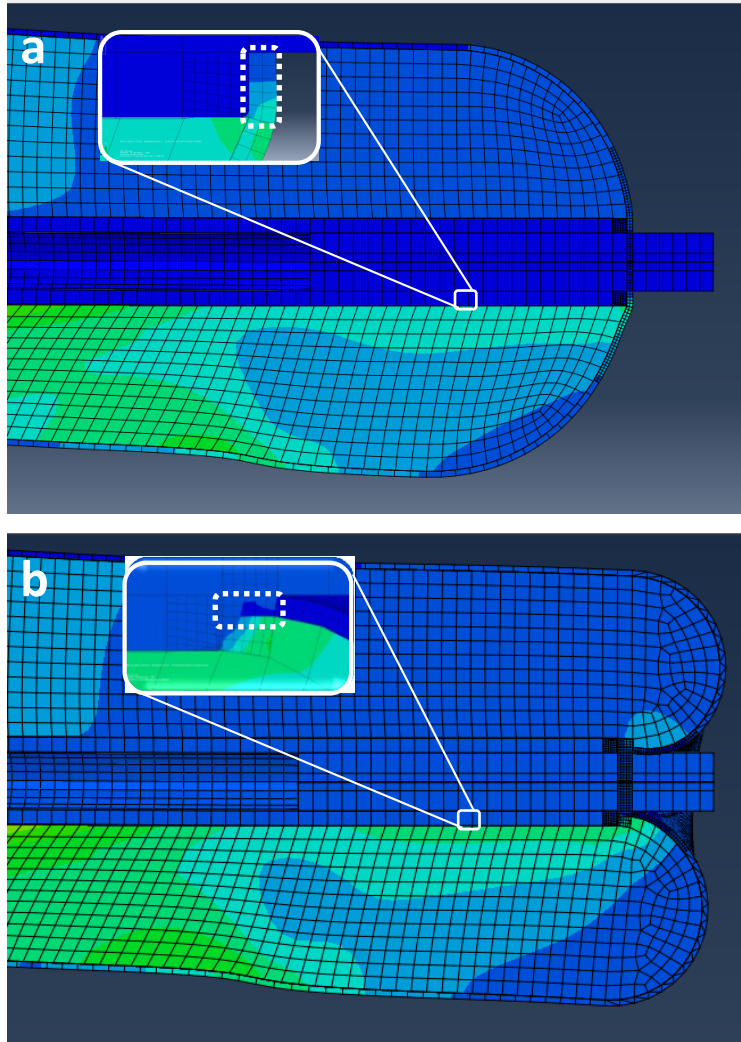


Figure 6.1: Strain surrounding the transcutaneous OI implant, a) perpendicular skin-implant interface, b) tangential skin-implant interface. The analysis region containing the skin-bone-implant interface is noted by the dotted white line. Maximum strain values in the analysis region were calculated to be 21% and 9% for the models pictured in 'a' and 'b', respectively.

Chapter 7: Conclusions

7.1 Conclusions

This pilot animal study establishes the use of porcine models to evaluate the wound healing and infection associated with weight-bearing transcutaneous osseointegrated prostheses. The animals used in this study achieved 70% and 67% pre-operative weight-bearing. The transcutaneous wounds progressed through the hemostasis and inflammatory stages of wound healing by the animal's 35 and 56 day endpoints. The proliferative phase of wound healing was not complete and the remodeling stage was never reached. Histological evaluation indicated migration of the epithelial layer towards the implant in one animal. However, there was no evidence of a definitive seal at the skin-bone-implant interface in either animal. Bacterial cultures indicated a likely deep tissue infection in one of the two animals. Preliminary results from the computational model suggest that strain can be reduced in the critical skin-bone-implant interface by retaining soft tissue during transcutaneous OI surgery.

Previous large animal models fail to demonstrate physiological similarity but have attempted to translate conclusions to the human transcutaneous wound healing condition. The porcine model outlined in the previous chapters should replace previous models and become the standard for implementing and testing future iterations of weight-bearing transcutaneous OI prosthetic devices. Future studies will address the transcutaneous implant's material, surface topography, and biological coatings for eventual translation to human amputees. The animal and computational models will continue to be used in conjunction to optimize implant design and associated surgical techniques. Efforts to improve the tissue-implant seal and thereby prevent bacterial infection must continue. The ability to regulate infection must be demonstrated before transcutaneous OI prostheses will be clinically implemented in the USA.

References

1. Ziegler-Graham, K., E.J. MacKenzie, P.L. Ephraim, T.G. Trivison, and R. Brookmeyer, *Estimating the prevalence of limb loss in the United States: 2005 to 2050*. Arch Phys Med Rehabil, 2008. 89(3): p. 422-9.
2. Isaacson, B.M., J.G. Stinstra, R.S. MacLeod, J.B. Webster, J.P. Beck, and R.D. Bloebaum, *Bioelectric analyses of an osseointegrated intelligent implant design system for amputees*. J Vis Exp, 2009(29): p. 1-6.
3. *Amputations of upper and lower extremities, active and reserve components, U.S. Armed Forces, 2000-2011*. MSMR, 2012. 19(6): p. 2-6.
4. Fischer, H., *U.S. Military Casualty Statistics: Operation New Dawn, Operation Iraqi Freedom, and Operation Enduring Freedom*, C.R. Service, Editor. 2013.
5. Thurston, A.J., *Pare and prosthetics: the early history of artificial limbs*. ANZ J Surg, 2007. 77(12): p. 1114-9.
6. Kapp, S., *Suspension systems for prostheses*. Clin Orthop Relat Res, 1999(361): p. 55-62.
7. Bader, D.L., *The recovery characteristics of soft tissues following repeated loading*. J Rehabil Res Dev, 1990. 27(2): p. 141-50.
8. Levy, S.W., *Amputees: skin problems and prostheses*. Cutis, 1995. 55(5): p. 297-301.
9. Highsmith, J.T. and M.J. Highsmith, *Common skin pathology in LE prosthesis users*. JAAPA, 2007. 20(11): p. 33-6, 47.
10. Hagberg, K. and R. Branemark, *Consequences of non-vascular trans-femoral amputation: a survey of quality of life, prosthetic use and problems*. Prosthet Orthot Int, 2001. 25(3): p. 186-94.
11. Lyon, C.C., J. Kulkarni, E. Zimerson, E. Van Ross, and M.H. Beck, *Skin disorders in amputees*. J Am Acad Dermatol, 2000. 42(3): p. 501-7.
12. Meulenbelt, H.E., J.H. Geertzen, M.F. Jonkman, and P.U. Dijkstra, *Skin problems of the stump in lower limb amputees: 1. A clinical study*. Acta Derm Venereol, 2011. 91(2): p. 173-7.
13. Dudek, N.L., M.B. Marks, S.C. Marshall, and J.P. Chardon, *Dermatologic conditions associated with use of a lower-extremity prosthesis*. Arch Phys Med Rehabil, 2005. 86(4): p. 659-63.
14. Berke, G.M., J. Ferguson, J.R. Milani, J. Hattingh, M. McDowell, V. Nguyen, and G.E. Reiber, *Comparison of satisfaction with current prosthetic care in veterans and servicemembers from Vietnam and OIF/OEF conflicts with major traumatic limb loss*. J Rehabil Res Dev, 2010. 47(4): p. 361-71.
15. Koc, E., M. Tunca, A. Akar, A.H. Erbil, B. Demiralp, and E. Arca, *Skin problems in amputees: a descriptive study*. Int J Dermatol, 2008. 47(5): p. 463-6.
16. Branemark, R., P.-I. Branemark, B. Rydevik, and R. Myers, *Osseointegration in skeletal reconstruction and rehabilitation*. Journal of Rehabilitation & Development, 2001. 38(2): p. 175-181.
17. Branemark, P.I., B.O. Hansson, R. Adell, U. Breine, J. Lindstrom, O. Hallen, and A. Ohman, *Osseointegrated implants in the treatment of the edentulous jaw. Experience from a 10-year period*. Scand J Plast Reconstr Surg Suppl, 1977. 16: p. 1-132.
18. Hagberg, K., Haggstrom, E., Jonsson, S., Rydevik, B., Branemark, R. , *Osseoperception and Osseointegrated Prosthetic Limbs*, in *Psychoprosthetics*. 2008, Springer London. p. 131-140.
19. Adell, R., B. Eriksson, U. Lekholm, P.I. Branemark, and T. Jemt, *Long-term follow-up study of osseointegrated implants in the treatment of totally edentulous jaws*. Int J Oral Maxillofac Implants, 1990. 5(4): p. 347-59.

20. Hagberg, K., ed. *Physiotherapy for patients having a trans-femoral amputation*. The Osseointegration Book: From Calvarium to Calcaneus., ed. P.-I. Branemark. 2005, Quintessence: Berlin, Chicago. 477-487.
21. Hagberg, K. and R. Branemark, *One hundred patients treated with osseointegrated transfemoral amputation prostheses--rehabilitation perspective*. J Rehabil Res Dev, 2009. 46(3): p. 331-44.
22. Hagberg, K., R. Branemark, B. Gunterberg, and B. Rydevik, *Osseointegrated trans-femoral amputation prostheses: Prospective results of general and condition-specific quality of life in 18 patients at 2-year follow-up*. Prosthetics and Orthotics International, 2008. 32(1): p. 29-41.
23. Hagberg, K., E. Haggstrom, M. Uden, and R. Branemark, *Socket versus bone-anchored trans-femoral prostheses: hip range of motion and sitting comfort*. Prosthet Orthot Int, 2005. 29(2): p. 153-63.
24. Hall, C.W., *A future prosthetic limb device*. J Rehabil Res Dev, 1985. 22(3): p. 99-102.
25. Frossard, L., Hagberg, K., Haggstrom, E., Gow, DL., Branemark R., Percy, M., *Functional Outcome of Transfemoral Amputees Fitted With an Osseointegrated Fixation: Temporal Gait Characteristics*. Journal of Prosthetics & Orthotics, 2010. 22(1): p. 11-20.
26. von Recum, A.F., *Applications and failure modes of percutaneous devices: a review*. J Biomed Mater Res, 1984. 18(4): p. 323-36.
27. Tillander, J., K. Hagberg, L. Hagberg, and R. Branemark, *Osseointegrated titanium implants for limb prostheses attachments: infectious complications*. Clin Orthop Relat Res, 2010. 468(10): p. 2781-8.
28. Sullivan, J., M. Uden, K.P. Robinson, and S. Sooriakumaran, *Rehabilitation of the trans-femoral amputee with an osseointegrated prosthesis: the United Kingdom experience*. Prosthet Orthot Int, 2003. 27(2): p. 114-20.
29. Michael, J., *ICAP Highlight: Osseointegration*. 2000.
30. Adell, R., U. Lekholm, B. Rockler, and P.I. Branemark, *A 15-year study of osseointegrated implants in the treatment of the edentulous jaw*. Int J Oral Surg, 1981. 10(6): p. 387-416.
31. Nebergall, A., C. Bragdon, A. Antonellis, J. Karrholm, R. Branemark, and H. Malchau, *Stable fixation of an osseointegrated implant system for above-the-knee amputees: titel RSA and radiographic evaluation of migration and bone remodeling in 55 cases*. Acta Orthop, 2012. 83(2): p. 121-8.
32. Xu, W. and K. Robinson, *X-ray image review of the bone remodeling around an osseointegrated trans-femoral implant and a finite element simulation case study*. Ann Biomed Eng, 2008. 36(3): p. 435-43.
33. Frossard, L., N. Stevenson, J. Smeathers, E. Haggstrom, K. Hagberg, J. Sullivan, D. Ewins, D.L. Gow, S. Gray, and R. Branemark, *Monitoring of the load regime applied on the osseointegrated fixation of a trans-femoral amputee: a tool for evidence-based practice*. Prosthet Orthot Int, 2008. 32(1): p. 68-78.
34. Lee, W.C., L.A. Frossard, K. Hagberg, E. Haggstrom, D.L. Gow, S. Gray, and R. Branemark, *Magnitude and variability of loading on the osseointegrated implant of transfemoral amputees during walking*. Med Eng Phys, 2008. 30(7): p. 825-33.
35. Holt, B.M., K.N. Bachus, J.P. Beck, R.D. Bloebaum, and S. Jeyapalina, *Immediate post-implantation skin immobilization decreases skin regression around percutaneous osseointegrated prosthetic implant systems*. J Biomed Mater Res A, 2012.
36. Pendegrass, C.J., A.E. Goodship, and G.W. Blunn, *Development of a soft tissue seal around bone-anchored transcutaneous amputation prostheses*. Biomaterials, 2006. 27(23): p. 4183-91.
37. Pendegrass, C.J., A.E. Goodship, J.S. Price, and G.W. Blunn, *Nature's answer to breaching the skin barrier: an innovative development for amputees*. J Anat, 2006. 209(1): p. 59-67.

38. Tomaszewski, P.K., N. Verdonshot, S.K. Bulstra, and G.J. Verkerke, *A comparative finite-element analysis of bone failure and load transfer of osseointegrated prostheses fixations*. *Ann Biomed Eng*, 2010. 38(7): p. 2418-27.
39. *What is the OPRA Implant System?* 2013; Available from: <http://www.sahlgrenskaic.com/medical-care/treatments/opra-implant-system/treatment-success/>.
40. *Better Quality, Better Life*, in *Endo-Exo Prosthesis DVD*, U. Henssge, Editor, ESKA America: Braselton, GA.
41. Fitzpatrick, N., T.J. Smith, C.J. Pendegrass, R. Yeadon, M. Ring, A.E. Goodship, and G.W. Blunn, *Intraosseous transcutaneous amputation prosthesis (ITAP) for limb salvage in 4 dogs*. *Vet Surg*, 2010. 40(8): p. 909-25.
42. Jeyapalina, S., Bachus, K.N., Beck, J.P., Bloebaum, R.D., *An Amputation Model for Evaluating the Efficacy of a Porous Coated Subdermal Barrier to Create Skin-Seal in Load Bearing Osseointegrated Implants*. 2012.
43. Aschoff, H.H., A. Clausen, K. Tsoumpris, and T. Hoffmeister, *[Implantation of the endo-exo femur prosthesis to improve the mobility of amputees]*. *Oper Orthop Traumatol*, 2011. 23(5): p. 462-72.
44. Daroiche, R., *Device-Associated Infections: A Macroproblem that Starts with Microadherence*. *Clin Infect Dis*, 2001. 33(9): p. 1567-1572.
45. Hobson, J.C., A.J. Roper, R. Andrew, M.P. Rothera, P. Hill, and K.M. Green, *Complications of bone-anchored hearing aid implantation*. *J Laryngol Otol*, 2010. 124(2): p. 132-6.
46. Webster, J.B., Chou, T., Kenly, M., English, M., Roberts, T., Bloebaum, R., *Perceptions and Acceptance of Osseointegration Among Individuals With Lower Limb Amputations: A Prospective Survey Study*. *Journal of Prosthetics & Orthotics*, 2009. 21(4): p. 215-222.
47. Hagberg, E., O.K. Berlin, and P. Renstrom, *Function after through-knee compared with below-knee and above-knee amputation*. *Prosthet Orthot Int*, 1992. 16(3): p. 168-73.
48. Kegel, B., M.L. Carpenter, and E.M. Burgess, *Functional capabilities of lower extremity amputees*. *Arch Phys Med Rehabil*, 1978. 59(3): p. 109-20.
49. Lundberg, M., K. Hagberg, and J. Bullington, *My prosthesis as a part of me: a qualitative analysis of living with an osseointegrated prosthetic limb*. *Prosthet Orthot Int*, 2011. 35(2): p. 207-14.
50. *Amputee Adventures*: United Kingdom.
51. Fernie, G.R., J.P. Kostuik, and R.J. Lobb, *A percutaneous implant using a porous metal surface coating for adhesion to bone and a velour covering for soft tissue attachment: results of trials in pigs*. *J Biomed Mater Res*, 1977. 11(6): p. 883-91.
52. Drygas, K., R. Taylor, C. Sidebotham, R. Hugate, and H. McAlexander, *Transcutaneous Tibial Implants: A Surgical Procedure for Restoring Ambulation After Amputation of the Distal Aspect of the Tibia in a Dog*. *Veterinary Surgery*, 2008. 37: p. 322-327.
53. Shelton, T.J., J.P. Beck, R.D. Bloebaum, and K.N. Bachus, *Percutaneous osseointegrated prostheses for amputees: Limb compensation in a 12-month ovine model*. *J Biomech*, 2011. 44(15): p. 2601-6.
54. Hall, C.W., *Developing a permanently attached artificial limb*. *Bull Prosthet Res*, 1974: p. 144-57.
55. Gangjee, T., R. Colaizzo, and A.F. von Recum, *Species-related differences in percutaneous wound healing*. *Ann Biomed Eng*, 1985. 13(5): p. 451-67.
56. Jansen, J.A., J.P. van der Waerden, H.B. van der Lubbe, and K. de Groot, *Tissue response to percutaneous implants in rabbits*. *J Biomed Mater Res*, 1990. 24(3): p. 295-307.
57. Mooney, V., S.A. Schwartz, A.M. Roth, and M.J. Gorniewsky, *Percutaneous implant devices*. *Ann Biomed Eng*, 1977. 5(1): p. 34-46.
58. Tagusari, O., K. Yamazaki, P. Litwak, A. Kojima, E.C. Klein, J.F. Antaki, M. Watach, L.M. Gordon, K. Kono, T. Mori, H. Koyanagi, B.P. Griffith, and R.L. Kormos, *Fine trabecularized carbon: ideal*

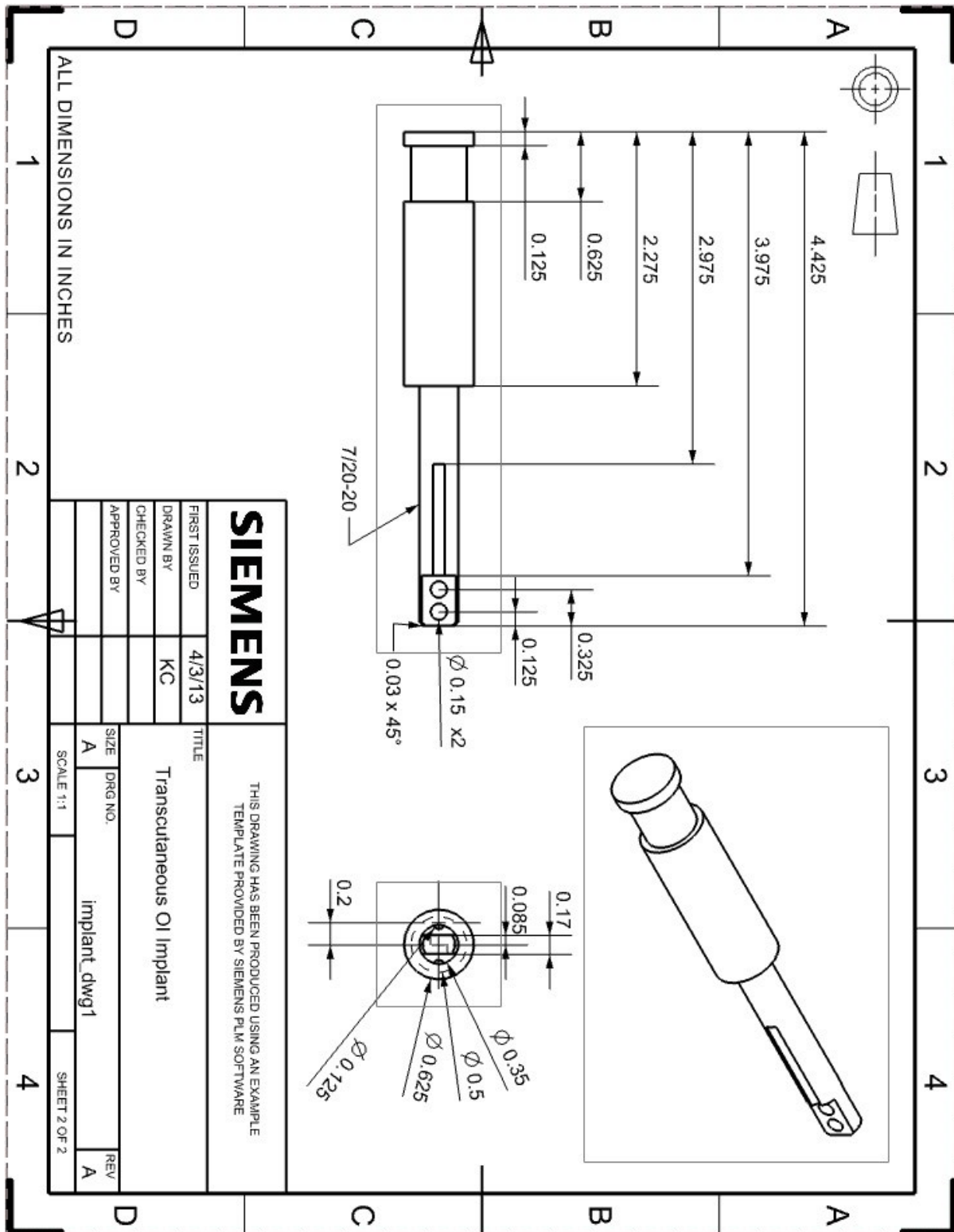
- material and texture for percutaneous device system of permanent left ventricular assist device.* Artif Organs, 1998. 22(6): p. 481-7.
59. Chou, T.G., C.A. Petti, J. Szakacs, and R.D. Bloebaum, *Evaluating antimicrobials and implant materials for infection prevention around transcatheter osseointegrated implants in a rabbit model.* J Biomed Mater Res A, 2009. 92(3): p. 942-52.
 60. Winter, G.D., *Transcutaneous implants: reactions of the skin-implant interface.* J Biomed Mater Res, 1974. 8(3): p. 99-113.
 61. Squier, C.A. and P. Collins, *The relationship between soft tissue attachment, epithelial downgrowth and surface porosity.* J Periodontal Res, 1981. 16(4): p. 434-40.
 62. Grosse-Siestrup, C. and K. Affeld, *Design criteria for percutaneous devices.* J Biomed Mater Res, 1984. 18(4): p. 357-82.
 63. Chehroudi, B., T.R. Gould, and D.M. Brunette, *A light and electron microscopic study of the effects of surface topography on the behavior of cells attached to titanium-coated percutaneous implants.* J Biomed Mater Res, 1991. 25(3): p. 387-405.
 64. Chehroudi, B. and D.M. Brunette, *Subcutaneous microfabricated surfaces inhibit epithelial recession and promote long-term survival of percutaneous implants.* Biomaterials, 2002. 23(1): p. 229-37.
 65. Walboomers, X.F. and J.A. Jansen, *Effect of microtextured surfaces on the performance of percutaneous devices.* J Biomed Mater Res A, 2005. 74(3): p. 381-7.
 66. Pendegrass, C.J., D. Gordon, C.A. Middleton, S.N.M. Sun, and G.W. Blunn, *Sealing the skin barrier around transcutaneous implants.* The Journal of Bone and Joint Surgery, 2007. 90(B): p. 114-121.
 67. Isackson, D., L.D. McGill, and K.N. Bachus, *Percutaneous implants with porous titanium dermal barriers: an in vivo evaluation of infection risk.* Med Eng Phys, 2011. 33(4): p. 418-26.
 68. Chimutengwende-Gordon, M., C. Pendegrass, and G. Blunn, *Enhancing the soft tissue seal around intraosseous transcutaneous amputation prostheses using silanized fibronectin titanium alloy.* Biomed Mater, 2011. 6(2): p. 025008.
 69. Affeld, K., J. Grosshauser, K. Reiter, C. Grosse-Siestrup, and U. Kertzscher, *How can we achieve infection-resistant percutaneous energy transfer?* Artif Organs, 2011. 35(8): p. 800-6.
 70. Jansen, J.A. and K. de Groot, *Guinea pig and rabbit model for the histological evaluation of permanent percutaneous implants.* Biomaterials, 1988. 9(3): p. 268-72.
 71. Smith, T.J., A. Galm, S. Chatterjee, R. Wells, S. Pedersen, A.M. Parizi, A.E. Goodship, and G.W. Blunn, *Modulation of the soft tissue reactions to percutaneous orthopaedic implants.* J Orthop Res, 2006. 24(7): p. 1377-83.
 72. Perry, E.L., J.P. Beck, D.L. Williams, and R.D. Bloebaum, *Assessing peri-implant tissue infection prevention in a percutaneous model.* J Biomed Mater Res B Appl Biomater, 2010. 92(2): p. 397-408.
 73. Williams, D.L., R.D. Bloebaum, J.P. Beck, and C.A. Petti, *Characterization of bacterial isolates collected from a sheep model of osseointegration.* Curr Microbiol, 2010. 61(6): p. 574-83.
 74. Isackson D, C.K., McGill LD, Bachus KN, *Mesenchymal Stem Cells Increase Collagen Infiltration and Improve Wound Healing Response to Porous Titanium Percutaneous Implants.* Medical Engineering and Physics, Under Review, 2011.
 75. Isackson D, C.K., McGill LD, Bachus KN, *Mesenchymal Stem Cell Therapeutics Improve Tissue Integration with Porous Metal Percutaneous Implants and Decrease Infection Risk.* Journal of Tissue Engineering and Regenerative Medicine, Under Review, 2011.
 76. Jansen, J.A., J.P. van der Waerden, and K. de Groot, *Tissue reaction to bone-anchored percutaneous implants in rabbits.* J Invest Surg, 1992. 5(1): p. 35-44.

77. Paquay, Y.C., A.E. De Ruijter, J.P. van der Waerden, and J.A. Jansen, *A one stage versus two stage surgical technique. Tissue reaction to a percutaneous device provided with titanium fiber mesh applicable for peritoneal dialysis*. ASAIO J, 1996. 42(6): p. 961-7.
78. Paquay, Y.C., J.E. de Ruijter, J.P. van der Waerden, and J.A. Jansen, *Wound healing phenomena in titanium fibre mesh: the influence of the length of implantation*. Biomaterials, 1997. 18(2): p. 161-6.
79. MacKenzie, E.J., A.S. Jones, M.J. Bosse, R.C. Castillo, A.N. Pollak, L.X. Webb, M.F. Swiontkowski, J.F. Kellam, D.G. Smith, R.W. Sanders, A.L. Jones, A.J. Starr, M.P. McAndrew, B.M. Patterson, and A.R. Burgess, *Health-care costs associated with amputation or reconstruction of a limb-threatening injury*. J Bone Joint Surg Am, 2007. 89(8): p. 1685-92.
80. Mertz, P.M.W.E.S.D.P., *The pig as a model for human wound healing*. Wound Repair and Regeneration, 2001. 9(2): p. 66-76.
81. Wang, J.F., M.E. Olson, C.R. Reno, J.B. Wright, and D.A. Hart, *The pig as a model for excisional skin wound healing: characterization of the molecular and cellular biology, and bacteriology of the healing process*. Comp Med, 2001. 51(4): p. 341-8.
82. Ordman, L.J. and T. Gillman, *Studies in the healing of cutaneous wounds. I. The healing of incisions through the skin of pigs*. Arch Surg, 1966. 93(6): p. 857-82.
83. Singer, A.J. and S.A. McClain, *Development of a porcine excisional wound model*. Acad Emerg Med, 2003. 10(10): p. 1029-33.
84. Chvapil, M., T.A. Chvapil, ed. *Wound healing models in the miniature Yucatan pig*. Swine in Biomedical Research, ed. M.M. In Swindle. 1992, Iowa State University Press: Ames. 265-288.
85. Orsini, E., G. Giavaresi, A. Trire, V. Ottani, and S. Salgarello, *Dental implant thread pitch and its influence on the osseointegration process: an in vivo comparison study*. Int J Oral Maxillofac Implants, 2012. 27(2): p. 383-92.
86. Schropp, K., *Personal Correspondence*. 2012.
87. *The Rehabilitation of People with Amputations*. 2004, World Health Organization.
88. Bhavsar, D., *Personal Correspondence*. 2013.
89. Gillaspay, A.F., S.G. Hickmon, R.A. Skinner, J.R. Thomas, C.L. Nelson, and M.S. Smeltzer, *Role of the accessory gene regulator (agr) in pathogenesis of staphylococcal osteomyelitis*. Infect Immun, 1995. 63(9): p. 3373-80.
90. Jeyapalina, S., J.P. Beck, K.N. Bachus, D.L. Williams, and R.D. Bloebaum, *Efficacy of a porous-structured titanium subdermal barrier for preventing infection in percutaneous osseointegrated prostheses*. J Orthop Res, 2012. 30(8): p. 1304-11.
91. Emmanuel, J., C. Hornbeck, and R.D. Bloebaum, *A polymethyl methacrylate method for large specimens of mineralized bone with implants*. Stain Technol, 1987. 62(6): p. 401-10.
92. Yerneni, S., Y. Dhaher, and T.A. Kuiken, *A computational model for stress reduction at the skin-implant interface of osseointegrated prostheses*. J Biomed Mater Res A, 2012. 100(4): p. 911-7.
93. Fung, Y.-c., ed. *Biomechanics: Mechanical Properties of Living Tissues*. Vol. 10. 1993, Springer-Verlag.
94. Yerby, S., C.C. Scott, N.J. Evans, K.L. Messing, and D.R. Carter, *Effect of cutting flute design on cortical bone screw insertion torque and pullout strength*. J Orthop Trauma, 2001. 15(3): p. 216-21.
95. Rubel, I., Fornari, E., Miller, B., Hayes, W., *Are all Self Tapping Screws Similar? A Biomechanical Study*. J Bone Joint Surg Br, 2006. 88-B(30).
96. Maniatopoulos, C., R.M. Pilliar, and D.C. Smith, *Threaded versus porous-surfaced designs for implant stabilization in bone-endodontic implant model*. J Biomed Mater Res, 1986. 20(9): p. 1309-33.

97. Flegal, K.M., M.D. Carroll, C.L. Ogden, and C.L. Johnson, *Prevalence and trends in obesity among US adults, 1999-2000*. JAMA, 2002. 288(14): p. 1723-7.
98. Mokdad, A.H., B.A. Bowman, E.S. Ford, F. Vinicor, J.S. Marks, and J.P. Koplan, *The continuing epidemics of obesity and diabetes in the United States*. JAMA, 2001. 286(10): p. 1195-200.
99. Gerritsen, M., J.A. Lutterman, and J.A. Jansen, *The influence of impaired wound healing on the tissue reaction to percutaneous devices using titanium fiber mesh anchorage*. J Biomed Mater Res, 2000. 52(1): p. 135-41.
100. Gerritsen, M., J.A. Lutterman, and J.A. Jansen, *Wound healing around bone-anchored percutaneous devices in experimental diabetes mellitus*. J Biomed Mater Res, 2000. 53(6): p. 702-9.
101. Velandar, P., C. Theopold, T. Hirsch, O. Bleiziffer, B. Zuhaili, M. Fossum, D. Hoeller, R. Gheerardyn, M. Chen, S. Visovatti, H. Svensson, F. Yao, and E. Eriksson, *Impaired wound healing in an acute diabetic pig model and the effects of local hyperglycemia*. Wound Repair Regen, 2008. 16(2): p. 288-93.
102. Meeker, J., P. Weinhold, and L. Dahners, *Negative Pressure Therapy on Primarily Closed Wounds Improves Wound Healing Parameters at 3 Days in a Porcine Model*. J Orthop Trauma, 2011.
103. Demaria, M., B.J. Stanley, J.G. Hauptman, B.A. Steficek, M.C. Fritz, J.M. Ryan, N.A. Lam, T.W. Moore, and H.S. Hadley, *Effects of negative pressure wound therapy on healing of open wounds in dogs*. Vet Surg, 2011. 40(6): p. 658-69.
104. Morykwas, M.J., L.C. Argenta, E.I. Shelton-Brown, and W. McGuirt, *Vacuum-assisted closure: a new method for wound control and treatment: animal studies and basic foundation*. Ann Plast Surg, 1997. 38(6): p. 553-62.
105. Xu, W., A.D. Crocombe, and S.C. Hughes, *Finite element analysis of bone stress and strain around a distal osseointegrated implant for prosthetic limb attachment*. Proc Inst Mech Eng H, 2000. 214(6): p. 595-602.
106. Teran, J., E. Sifakis, S.S. Blemker, V. Ng-Thow-Hing, C. Lau, and R. Fedkiw, *Creating and simulating skeletal muscle from the visible human data set*. IEEE Trans Vis Comput Graph, 2005. 11(3): p. 317-28.
107. Tran, H.V., F. Charleux, M. Rachik, A. Ehrlacher, and M.C. Ho Ba Tho, *In vivo characterization of the mechanical properties of human skin derived from MRI and indentation techniques*. Comput Methods Biomech Biomed Engin, 2007. 10(6): p. 401-7.
108. Saxena, V., C.W. Hwang, S. Huang, Q. Eichbaum, D. Ingber, and D.P. Orgill, *Vacuum-assisted closure: microdeformations of wounds and cell proliferation*. Plast Reconstr Surg, 2004. 114(5): p. 1086-96; discussion 1097-8.

Appendices

Appendix 1: Engineering Drawing for Transcutaneous OI Implant



Appendix 2: List of Medication

Drug	Species	Class of drug	Hazardous (yes/no)	Dose	Route	Duration of treatment
cephazoline	Porcine	Antibiotic	no	15 - 25 mg/kg	IV	Preop once
atropine	Porcine	Anticholinergic Tranquilizer Sedative	no	0.02 – 0.05 mg/kg	IM	Preop once
ketamine	Porcine	Dissociative agent (Schedule III)	no	15 - 25 mg/kg	IM	Preop and at x-ray
xylazine	Porcine	Analgesic Sedative	no	2.0 mg/kg	IM	Preop (optional)
isoflurane	Porcine	Anesthetic	no	1 – 2%	Inhalation	Intraop 1 to 1.5 hours
flunixin meglumine	Porcine	Analgesic NSAID	no	1 - 2.2 mg/kg	IM (neck)	1 to 5 days (every 24 hours)
fentanyl	Porcine	Opioid Analgesic (Schedule II)	no	50 - 100 µg/hr	Transdermal patch	Up to 5 days (or more if needed)
midazolam	Porcine	Sedative	no	100 - 500 mcg/kg	IM or IV	Daily: As required for procedural handling
Beuthanasia-D	Porcine	Barbiturate mixture (Schedule III)	no	5ml/kg150 mg/kg (.4 mL/kg)	IP	Once

Lidocaine	Porcine	local anesthetics	no	4.4 mg/kg	epidural	Once (optional)
Bupivacaine	Porcine	local anesthetics	no	4.4 mg/kg	epidural	Once (optional)
Morphine (preservative free)	Porcine	Local Anesthesia	No	.1 mg/kg	Epidural	Once (optional)
Buprenorphine	Porcine	Opioid Analgesic	No	.005-.01 mg/kg	SQ, IM	1-5 days, twice daily (Optional)
Carorifen	Porcine	NSAID Analgesic	No	2-4 mg/kg	PO, IM, SQ	1-5 days, twice daily (optional)
Omeprazole	Porcine	Proton pump inhibitor – treatment for gastric ulceration	No	.7 mg/kg	PO	Once daily, as needed
Famotadine	Porcine	H2 receptor antagonist – treatment for gastric ulceration	No	.5 mg/kg	IM	1-2 times per day, as needed

Appendix 3: List of Surgical Supplies

From the Orthopedic Research Center		Tools for the Operation - Sterilized LAR	
Sterile Marker	1	Towel clips	3
Sterile Chucks	8	Needle Driver	2
4 x 4 Gauze Pads	10	Rat Tooth Forceps	1
DuraPrep surgical solution	1	Adson Forceps (for skin)	1
Sterile Drapes	4	Metzenbaum Scissors	1
Ioban	2	No. 15 Scalpel Handle	2
Surgical Blades (#15)	Box	No. 20 Scalpel Handle	2
Surgical Blades (#20)	Box	No. 15 Scalpel Blades	Box
3-0 Vicryl	Box	No. 20 Scalpel Blades	Box
3-0 Ethylon	Box	Blunt Hohmann Retractor	2
Silk Ties w/o needle	1	Rasp (file fibula)	1
Skin Prep Tray	1	Curved Clamps, hemostats	6
Tegaderm Patch	1	Cobb	1
Irrigation Syringe	1	Micro-Air Surgical saw	1
Cautery Pen	1	Bone saw tool	2
Cautery Ground	1	Micro-Air Hand Drill	1
Sterile Gloves	Box	Micro-Air hose	1
Sterile Gowns	4	K-wire driver	1
Non-Sterile Gowns	4	K-wire	1
Face masks	Box	Larger Hand Drill (non-sterile)	1
Foot Covers	Box	.275" surgical drill bit	1
Hairnets	Box	.315" surgical drill bit	1
Non-sterile latex gloves	Box	.354" surgical drill bit	1
Pantepinto Sling	1	.394" surgical drill bit	1
Coban wrap	1	Bone Cement	1
Lap Sponges	4	Mixing Cup	1
Non-Sterile Towels	8	Bone Cement Mixing Tower	1
Sterile Towels	6	60 mL Syringe for Bone Cement	1
Hair Clippers	1	Bone Cement Pusher	1
Mayo Stand Covers	2	SS Skin Punch	1
Tourniquet	1	Racked opp. scissors	2
Video Camera	1	Bone clamps	2
Lab Notebooks	2	Metal Implant	2
Surgical Calipers	1	Prosthetic Bracket	1
Light Covers	2	¼"-20 SS Screws	1
Saline	Bottle	¼" SS Allen Wrench	1
Suction Hose	1	Implant Tightening Rod (Screw Driver)	1
Suction Poole Handle	1	Irrigation Bowls	3
Micro-Air machine and plug (non-sterile)	1	Ruler	1
		Drill Guides	4
		Bone Taker Clamps	1
		Suction tool handle	1

Appendix 4: Surgical Protocol

SETUP

1. Prepare skin area approximately 2x size of expected surgical field.
2. Shave and remove all hair from incision area.
3. Position the pig on back in dorsal recumbency.
4. Sterilely prep skin area with Betadine or chlorhexidine scrub followed by alcohol rinse (3 times).
5. Dry with sterile gauze sponges.
6. Apply a tourniquet to the thigh.

APPROACH

Latero-Anterior Compartment

7. Mark skin laterally with marker at the anterior tibiotarsal joint.
8. Mark skin with a fish mouth incision .60" proximal to the joint mark (posterior-medial flap includes the heel pad and is longer than the anterior-lateral flap).
9. Cut skin along incision line.
10. Clear the fascia and subcutaneous tissue in line with the fish mouth incision.
11. Tie the large saphenous vein on lateral anterior side of the tibia with 0 Silk tie.
12. Cut 3 tendon groups on anterior side as distal as possible (just below the rentinaculum).
13. Dissect down to the bone at the tibiotarsal joint.
14. Retract all soft tissue including tendons proximally up the bone.

Posterior Approach

15. Create the heel flap by clearing the soft tissue (gastrocnemius and soleus attachments) off the calcaneus on the posterior bone (sharp dissection with No.15 scalpel).
16. Expose the *common calcanean tendon*. Use Cobb to peel all soft tissue off the calcaneal bone, Remove only the calcaneus bone leaving a substantial heel pad flap.
17. Strip the connective tissue bluntly using a Cobb from the posterior tibia.
18. Retract all soft tissues 1.0" proximally to the anticipated bone cut.
19. Cut through the tibia from an anterior approach (at a pre-specified height) with a bone saw.
20. Cut the fibula as proximal as possible without destroying soft tissue.
21. Remove the hock.

IMPLANT

22. Initial ream with 7mm diameter bit. Clear cortical bone up 2.1".
23. Ream until 9mm diameter bit. Clear cortical bone up 2.1"

WOUND CLOSURE

24. Check fit of the implant by tightening into medullary cavity 3 full turns to get threads started.
25. Suture subcutaneous muscle and soft tissue with 3/0 Ethylon for subcutaneous layers. Close from posterior-medial to anterior-lateral, drawing the suture line as far away from the face of the distal tibia as possible.
26. Pull the skin medial to lateral, suture the skin with 3-0 Nylon as far lateral as possible to clear for skin punch.
27. Use k-wire to send through the skin and into the bone's medullary cavity to line up the skin punch.
28. Use a 3/4" diameter skin punch. Punch through the most distal aspect of the limb in line with the implant. Remove the soft tissue leaving a circular hole exposing the implant.
29. Hand screw in the implant, up through the IM canal, for permanent fixation. (tighten with prosthetic attachment).
30. Do not suture the wound at the soft tissue/ implant interface. Want soft tissue to attach at the level of the bone. Wrap the wound, don't form a seal.

Appendix 5: Wound Cleaning Protocol

Preparing

1. Uwrap wound.
2. Unscrew exo-prosthetic bracket.
3. Remove prosthetic leg.
4. Remove retention cup.
5. Swab transcutaneous wound.

Cleaning

1. Remove all dried blood and exudates.
2. Wash with solution.
3. Dry with gauze.
4. Apply triple antibiotic ointment using cotton swab.

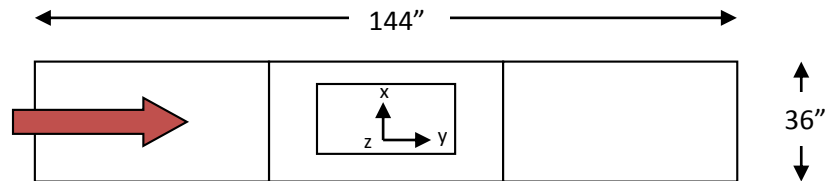
Covering

1. Cut slit in middle of 4x4" gauze pads. Slide over the end of the implant (can use 2x2" after first month of wound healing).
2. Slide retention cup over the implant to hold on the gauze.
3. Fasten retention cup to the skin using coflex bandaging.
4. Tighten exo-prosthetic back to the implant using the bracket.
5. Wrap coflex bandaging over the implant.

Appendix 6: Force Plate Analysis

Data Collection:

1. Orient the platforms and force plate as shown below.



2. Ensure force plate is stable and level.
3. Walk pig across platform at a steady state. Record the force in the z direction on trials in which the operative leg cleanly strikes the force plate.

Data Analysis:

1. Take the mean of the force in the z direction across trials for each day of data analysis.
2. Report as a percentage of animal body weight.

Appendix 7: Histology Preparation Protocol

Objectives: This protocol outlines the steps and processes that will be utilized to evaluate specified measures of soft tissues for the transcutaneous OI pig study. The primary evaluation is divided into two histological procedures: the first is a classic H&E method and the second is a decalcified bone H&E method. The primary objectives and related measures are detailed in the following table.

Objective	Potential Measures	H&E Method
Assess adherence of skin to implant	Area (% of total possible)	1
Determine extent of epithelial growth on implant	Length (mm) of proximal skin migration	1
Evaluate any deep tissue infection	Presence of small, gram positive rods	1
Quantify inflammatory cells	Count in predefined area (#/mm ²)	1
Quantify neovasculature		1
Determine the types of cells at the bone/implant/skin interface		2

The measures in the above table will be attempted to be determined from histology slides generated by the following harvesting and prep procedures.

Harvesting: The following procedure outlines the process of tissue harvesting from the euthanized animal. This process will be repeated for both animals included in this study and will be performed on the same day, directly after euthanasia. The harvesting process will yield two tissue specimens, one for each of the two H&E methods to be used.

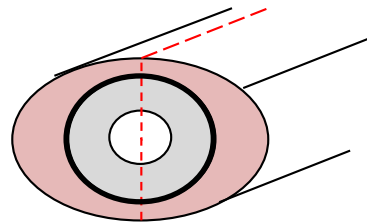
1. Harvest non-operative hind leg using scalpel, disarticulating at the knee. Immediately store specimen in -80°C freezer.
2. Harvest amputated (operative) leg using a scalpel. Disarticulate the leg at the knee, ensuring that the soft tissue surrounding the implant and tibia are intact.



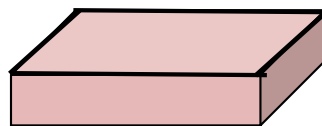
3. Make an anterior longitudinal incision along the length of the specimen. Take incision all the way down the bone proximal of the implant-bone interface (distal most portion of tibia).



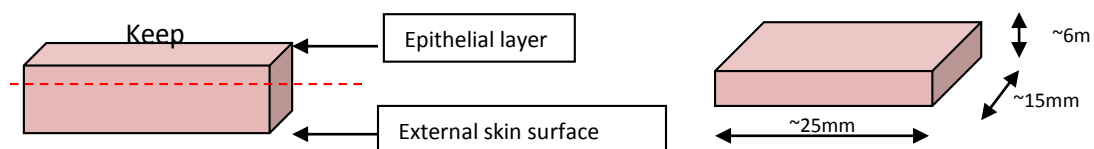
4. Being careful not to disrupt any soft tissue at implant-tibia interface, carefully unthread and remove implant from tibia. Hold proximal most portion of tibia in a clamp to help stabilize during implant removal.
5. Mark a vertical line over the end of the leg, splitting the leg in half.



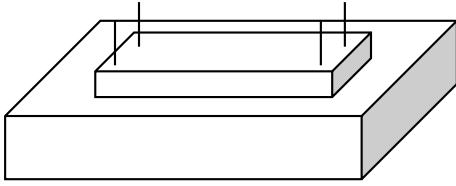
6. On the medial side, using a scalpel, carefully resect tissue off the implant and bone moving circumferentially, from anterior to posterior, trying to maintain a consistent, unbroken piece of removed tissue. Orient the epithelial layer face up.



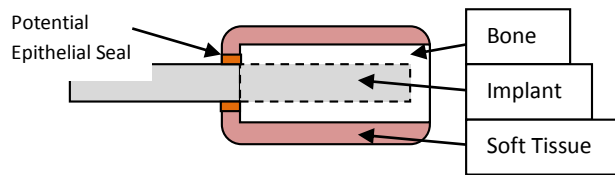
7. Lay the resected distal tissue from step 4 with the epithelial (inner most) layer facing up. Using a horizontal incision, resect the top 6mm of the specimen in a single sheet (removing the epithelial layer with a thin layer of muscle/extra tissue on its back side). Freeze remaining extra tissue for possible future use/analysis (-80C freezer).



8. Pin resected sheet facing up (epithelial layer up) on a paraffin block as flat as possible.



9. Fix the pinned sheet in formalin for 48hrs. This specimen will be used for the first H&E method.
10. On the lateral side of the specimen (see step 5), remove all soft tissue from tibia starting that is not 20mm from the distal end of the bone. Try to minimize any disruption of soft tissue on the distal end of the tibia.



11. Using a fine-toothed hacksaw, transversely cut the tibia ~10mm from the distal end.
12. Pin the distal-most portion of bone and soft tissue specimen to a paraffin block. Soak in formalin for 48hrs. This ~10mm thick specimen with the remaining soft tissue will be used for the second H&E method.
13. Freeze all bone/soft tissue not used in steps 9 or 12 for possible future use/analysis (-80C freezer).

Appendix 8: Histology Processing and Embedding Protocol

Solution	Time	Temperature	Notes
Neutral Buffered 10% Formalin	48 hours	Room	
70% Alcohol Solution	24 hours	Room	Not necessary
RBD Decalcifying Solution	1 hour	Room	Using stir plate. Skip this step if specimen does not contain bone.
Running Tap Water Rinse	10 minutes	Room	
70% Alcohol	3 hours	Room	Vacuum and Pressure
95% Alcohol	3 hours	Room	Vacuum and Pressure
100% Alcohol	3 hours	Room	Vacuum and Pressure
Xylene	3 hours	Room	Vacuum and Pressure
Paraffin Liquid	4.5 hours	Room	Vacuum and Pressure

Appendix 9: Histology Cutting and Staining Protocol

Step	Time
Cut to 4-5 micron thickness	
Air dry	12 hours
Bake at 65°C	30 minutes
Deparaffinize	
Hematoxylin and Eosin Phloxine Stain	Routine Manner
Permanently Mount	

Appendix 10: Gait Progress and Monitoring

0 = not used at all

1 = supported incidentally

2 = loaded in a standing position and incidentally while walking

3 = loaded in a standing position and while walking but with a limp

4 = normal walking and standing pattern

Animal #: 4172

Date of Surgery: 11/12/12

Days post op	Gait	Notes
1	0 1 2 3 4	Occasionally gets up
2	0 1 2 3 4	Will get up
3	0 1 2 3 4	
4	0 1 2 3 4	
5	0 1 2 3 4	
6	0 1 2 3 4	
7	0 1 2 3 4	
8	0 1 2 3 4	
9	0 1 2 3 4	
10	0 1 2 3 4	
11	0 1 2 3 4	
12	0 1 2 3 4	
13	0 1 2 3 4	
14	0 1 2 3 4	
15	0 1 2 3 4	
16	0 1 2 3 4	Stretching leg
17	0 1 2 3 4	
18	0 1 2 3 4	
19	0 1 2 3 4	
20	0 1 2 3 4	Exo-Prosthesis Change
21	0 1 2 3 4	
22	0 1 2 3 4	Exo-Prosthesis Change
23	0 1 2 3 4	
24	0 1 2 3 4	Exo-Prosthesis Change
25	0 1 2 3 4	
26	0 1 2 3 4	
27	0 1 2 3 4	
28	0 1 2 3 4	
29	0 1 2 3 4	
30	0 1 2 3 4	
31	0 1 2 3 4	
32	0 1 2 3 4	

33	0	1	2	3	4	
34	0	1	2	3	4	
35	0	1	2	3	4	
36	0	1	2	3	4	
37	0	1	2	3	4	
38	0	1	2	3	4	
39	0	1	2	3	4	
40	0	1	2	3	4	
41	0	1	2	3	4	
42	0	1	2	3	4	
43	0	1	2	3	4	
44	0	1	2	3	4	
45	0	1	2	3	4	
46	0	1	2	3	4	
47	0	1	2	3	4	
48	0	1	2	3	4	
49	0	1	2	3	4	
50	0	1	2	3	4	
51	0	1	2	3	4	
52	0	1	2	3	4	
53	0	1	2	3	4	
54	0	1	2	3	4	
55	0	1	2	3	4	
56	0	1	2	3	4	

Animal Number: 4178

Date of Surgery: 12/3/12

Days post op	Gait					Notes
1	0	1	2	3	4	Loads Incidentally
2	0	1	2	3	4	Three leg walking
3	0	1	2	3	4	Exo-Prosthesis attached
4	0	1	2	3	4	Weight Bearing
5	0	1	2	3	4	
6	0	1	2	3	4	
7	0	1	2	3	4	
8	0	1	2	3	4	
9	0	1	2	3	4	Slight limp
10	0	1	2	3	4	
11	0	1	2	3	4	
12	0	1	2	3	4	
13	0	1	2	3	4	
14	0	1	2	3	4	

15	0	1	2	3	4	Got up on back legs
16	0	1	2	3	4	
17	0	1	2	3	4	
18	0	1	2	3	4	
19	0	1	2	3	4	
20	0	1	2	3	4	Healthy gait
21	0	1	2	3	4	
22	0	1	2	3	4	
23	0	1	2	3	4	Extending leg, stretch
24	0	1	2	3	4	
25	0	1	2	3	4	
26	0	1	2	3	4	
27	0	1	2	3	4	
28	0	1	2	3	4	
29	0	1	2	3	4	
30	0	1	2	3	4	
31	0	1	2	3	4	
32	0	1	2	3	4	
33	0	1	2	3	4	
34	0	1	2	3	4	Some hobbling
35	0	1	2	3	4	

Appendix 11: Modified house of quality for endo-prosthesis and implant-bone interface

Legend: ▲ = 1 point, ○ = 2 points, ⊖ = 3 points

Direction of Improvement		▼	▼	▼	▲	▼	▼	▼		
Functional Requirements	Weight/Importance	▼	▼	▼	▲	▼	▼	▼	Score	Weight x Score
		Implant cost (\$)	Manufacturing Time (hrs)	Surgeon familiarity (operations)	Fatigue life (cycles)	Weight (g)	Number of parts (number)	Bone cement required (cc)		
Demanded Qualities										
Immediate fixation upon implantation	10	⊖	⊖	▲	▲			⊖	11	110
Permanent fixation throughout the study	10	○	○		⊖			⊖	10	100
Surface cleanable with hydrogen peroxide and soap/water solution	6						▲		1	6
Autoclavable	8						▲		1	8
Biocompatible	8	○							2	16
Facilitates skin incorporation to bone or implant	10	○	○						4	40
Manual insertion technique	7				○			○	2	28
Removable if infection confirmed	6			○			⊖	⊖	8	32
Withstand axial forces up to 356N (2.0 FoS)	9				⊖			⊖	6	54
Withstand torques up to 60 N-m (2.0 FoS)	9				⊖			⊖	6	54
Scalable to fit any porcine medullary cavity	7						▲		1	7
Manufacturable in the Orthopedic Research Lab's machine shop	9	⊖	⊖			▲	○		9	81
Target Value		100	10	2	300k	200	1	6		

Appendix 12: Modified house of quality for exo-prosthesis (including the brackets, prosthetic leg, prosthetic foot, and all hardware).

Legend: ▲ = 1 point, ○ = 2 points, ⊖ = 3 points

Direction of Improvement		▼	▼	▲	▼	▼	▼		
Functional Requirements	Weight/Importance	Prosthetic cost (\$)	Manufacturing Time (hrs)	Point of Failure (N)	Weight (g)	Donning/Doffing Time (sec)	Number of parts (number)	Score	Weight x Score
Demanded Qualities									
Adjustable angle	7		⊖	⊖		▲	○	9	63
Adjustable length	7		⊖	⊖		▲	○	9	63
Attach endo-prosthesis in less than 30 seconds	5					⊖	○	5	25
Detach endo-prosthesis in less than 15 seconds	5					⊖	○	5	25
Able to be withstand dirt, moisture, excrement, urine	7				▲			1	7
All components rated to axial 356N (2.0 FoS)	9	○		⊖	○		○	9	81
All components rated to torsional 60N-m (2.0 FoS)	9	○		⊖	○		○	9	81
Brackets under 38mm in height	6			▲	○			3	18
Replaceable parts including prosthetic feet	6	○	○			○	▲	7	42
Simulate natural point of contact for foot	7			○				2	14
Simulate natural contact material and surface	7			○	▲			3	21
Manufacturable in the Orthopedic Research Lab's machine shop	9	○	⊖				○	7	63
Target Value		50	8	356	1500	30	15		